

**Physiological, Anatomical, and Behavioral Investigations  
on the Bed Nucleus of the Stria Terminalis**

by

Olga E. Rodríguez-Sierra

A dissertation submitted to the

Graduate School – Newark

Rutgers, The State University of New Jersey

in partial fulfillment of the requirements

for the degree of

Doctor of Philosophy

Graduate Program in Behavioral and Neural Sciences

written under the direction of

Professor Denis Paré

and approved by

---

---

---

---

---

Newark, New Jersey

January, 2014

© 2014

Olga E Rodríguez-Sierra

ALL RIGHTS RESERVED

## **ABSTRACT OF THE DISSERTATION**

Physiological, anatomical and behavioral investigations on the bed nucleus of the stria terminalis.

By Olga E Rodríguez Sierra

Dissertation Director: Prof. Denis Paré

The anterior part of the bed nucleus of the stria terminalis (BNST-A) has emerged as a critical structure mediating fear and anxiety-like behavior. It is strategically situated to integrate information from limbic forebrain regions such as the amygdala, prefrontal cortex and hippocampus; and influence major fear and stress output effectors. Previous pharmacobehavioral studies have assumed that the BNST is a homogeneous structure despite the fact that anatomical studies contradict this assumption. The work presented in this thesis aimed to systematically examine the functional organization of BNST-A and its relation to anxiety-like behavior. In the first chapter, I examined the electroresponsive and morphological properties of BNST-A neurons. I showed that there are two dominant BNST-A cell types intermingled with at least other three less numerous cell types. In the second chapter, I investigated the intrinsic connections of BNST-A with the use of glutamate uncaging (GU). Overall, GU usually elicited inhibitory postsynaptic potentials and the incidence of intraregional connections was higher than interregional links. Lastly, I investigated the physiological properties of BNST-A neurons in a rat model of post-traumatic stress disorder. I show that neurons in BNST-A regions exhibit opposing alterations in synaptic

responsiveness, supporting the idea that BNST-A is physiologically heterogeneous, with some regions exerting anxiolytic and others anxiogenic influences.

## Acknowledgements and Dedication

My sincere gratitude to my thesis advisor Denis Paré for being my role model of commitment and hard work in science. I would also like to thank the members of my thesis committee, Bart Krekelberg, Catherine Myers, Jorge Golowasch, and Jom Hammack; the director of the BNS program, Ian Creese; all CMBN faculty members; administrative staff; RAF staff; postdocs; technicians; students; friends; family; and specially the rats.

In retrospective, now I see the process of getting a PhD as a journey full of experiences. There were times when I perceived it as an endurance test. Therefore, I started running long distances. I was surrounded by wonderful models of discipline (yes, the 4.30 am morning PI and the bamboo bike builder), that frequently made me feel inadequate with my levels of discipline. I thought that by running long distances I could train myself such qualities. So I did, and I trained hard, but the prime race never took place. My dear husband pointed out that although the goal was important, it was more important all what I did prior to the race. What a wonderful analogy for the completion of a PhD! I am probably not able to capture the richness, vastness, and uniqueness of all my experiences during graduate school. Having limited space and time, I resignify my graduate school journey through this cascade of words dedicated to all the important and relevant persons/experiences during these years, specially to my little *Κόσμος*.

*Courses, tests, quals, beer, rats, silicone probes, oscillations, multicultural, NYC, Princeton, NJ Transit, Newark, QNS, martinis, Israel, Germany, geek, sunshine, Poland, Olga Da Polga, Kenya, embodied cognition, consciousness, 1984, newspapers, politics, social movements, rose, cooking, vegetarian, cozy time, hair, thumb, Taiwan, UNOW, photography, fish, sustainable, organic, Puebla, UNAM, Romania, Japan, back-propagation, patch-clamp, clogged pipettes, noise, frustration, NPR, perfusion, behavior, PTSD, predator threat, statistics, collaboration, dumplings, Savannah, USPS, Butler, seasons, snowtorious, Rt 1, shopping, hipster, moron, tattoo, quetzal, bicycle, flowers, Europe, running, toe-path, Amis, 6:00 a.m., 4.30 a.m., 50, diligence, deliverance, food, scallops, gardening, ethics, philosophy of science, self-organized, emergence, nurture, nature, Argentina, mate, knitting, mushrooms, hugs, nostalgia, zombies, volcano, Bacalar, Chacchoben, permaculture, Chiapas, nature, climate change, collapse, thinking fast and slow, cognitive bias, illusions, delusions, Turkey, henna, proposal, stress, fear, talk, Brazil, India, shanna, swimming, reproductive rights, Netherlands, pirate, depression, love, yoga, fountain, reunions, BBQ, 7/11, mezcal, mazateca, Hierve el Agua, Chicago, San Diego, SfN, Gordon, hangover, compadre, José José, morris, Mexico City, tacos, chile, Canada, gamma, Ironbound, pão de queijo, running, mimosa, elections, arguing, fb, contra la reacción, media, propaganda, virtual, innovation, anxiety, doubts, weddings, babies, CCLC, New Orleans, sci-fi, distress, randomness, probability, empathy, flamma, sicalipsis, epistolary, audiobooks, runner high, NYRR, Central Park, Game of life, Philly, cigarettes, MOOCs, logics, history, theory of mind, sleeping, kimchee, Guyana, Doha, lab, gym, skydiving, pink, friendship, Sierra Gorda, jokes, ajo, motherhood, feminism, sorority, normative, construct, savage, subversion, human rights, wicked, enjoy the silence, solitude, Nexus 10, music, obsessions, notes, thesis, bonfire autism, sensorimotor integration, good dad, marmosets, soccer, chess, family, love again, intense, me.*

## **Preface**

The work in Chapter III and IV are the result of a collaboration between myself and Hjalmar K. Turesson (currently at Brain Institute, Universidade Federal do Rio Grande do Norte, Brazil). These studies have been published in the Journal of Neurophysiology (Turesson et al., 2013; Rodríguez-Sierra et al., 2013). Chapter V describes work that is currently under preparation for publication.

# Table of Contents

Abstract	ii
Acknowledgements and dedication	iv
Preface	vi
Table of contents	vii
List of tables	xii
List of figures	xiii
List of abbreviations	xv
<b>Chapter I: Introduction</b>	<b>1</b>
1.1    Background and significance	2
1.1.1.    Mechanisms underlying the expression and acquisition of fear/defensive responses	2
1.1.2.    The role of BNST in fear	4
1.2    Anatomical organization of the BNST-A	6
1.2.1.    BNST-A nuclei	6
1.2.2.    Afferents and efferents of BNST-A	7
1.2.3.    Transmitters used by BNST-A neurons	10
1.3    Intrinsic connections of BNST-A	10
1.4    Physiological properties of BNST-AL neurons	11
1.5    Understanding anxiety disorders: the case of PTSD	14

1.5.1.	Definition of PTSD	15
1.5.2.	Neurobiology of PTSD	15
1.5.3.	Genotypic and phenotypic alterations in PTSD	18
1.6	Towards an animal model of PTSD	22
1.7	Objectives of this thesis	26
<b>Chapter II: General Methods</b>		<b>28</b>
2.1	In vitro techniques	29
2.1.1	Slice preparation	29
2.1.2	Electrophysiological recordings	30
2.1.3	Data analysis	31
2.2	Histological Techniques	32
2.2.1	Biocytin revelation	32
2.3	Nomenclature used for different BNST-A subregions	33
2.4	Behavioral paradigm	33
2.4.1	Predator threat	33
2.4.2	Elevated Plus maze	34
2.4.3	Behavioral cut-off criteria	34
<b>Chapter III: Physiological Cell Types in Different Regions of the Bed Nucleus of the Stria Terminalis</b>		<b>36</b>
3.1	Rationale	37

3.2	Brief overview of methods	38
3.3	Results	39
3.3.1	Regular spiking (RS) cells (Type-I)	40
3.3.2	Low-threshold bursting cells (Type II)	42
3.3.3	Rare cell types	46
3.3.4	Passive properties and spike characteristics in different BNST-A regions	51
3.3.5	Morphological correlates	53
3.3.6	Other approaches to classification	58
3.3.7	Summary of results	59

#### **Chapter IV: Intrinsic Connections in the Anterior Part of the**

#### **Bed Nucleus of the Stria Terminalis 61**

4.1	Rationale	62
4.2	Brief overview of methods	63
4.3	Results	65
4.3.1	Spatial specificity of glutamate uncaging	65
4.3.2	Distinguishing GABAergic and glutamatergic PSPs elicited by glutamate uncaging	70
4.3.3	Mapping of intrinsic BNST-A connections with glutamate uncaging	71
4.3.4	Intrinsic BNST-A connections	75

4.3.5	Heterogeneous directionality and polarity of intrinsic BNST connections	79
4.3.6	Morphological correlates	80
4.4	Summary of results	83

## **Chapter V: Altered synaptic responsiveness of BNST-A**

### **neurons in resilient and PTSD-like rats 84**

5.1	Rationale	85
5.2	Brief overview of methods	86
5.3	Results	87
5.3.1	Incidence, passive properties, and spike characteristics of BNST-A neurons in resilient vs. PTSD-like rats	90
5.3.2	Synaptic responsiveness of BNST-A neurons in resilient vs. PTSD-like rats	91
5.3.3	BNST-AL neurons	92
5.3.4	BNST-AM neurons	93
5.3.5	BNST-AV neurons	95
5.3.6	Mechanisms underlying phenotype-related differences in synaptic responsiveness	97
5.4	Summary of results	98

<b>Chapter VI: General Discussion</b>	<b>100</b>
6.1    Physiological properties of BNST-A neurons	101
6.1.1    Prior studies on the cellular physiology of BNST-A neurons	102
6.1.2    Similarities and differences in the physiological properties of neurons in BNST-A	103
6.1.3    Morphological correlates	105
6.2    Intrinsic BNST-A connections	108
6.2.1    Nature of the synaptic connections	109
6.2.2    Overall pattern of intrinsic BNST-A connections	111
6.2.3    Functional implications of the intrinsic pattern of connectivity in BNST-A	114
6.3    Altered synaptic responsiveness of BNST-A neurons in a rat model of PTSD	116
6.3.1    Limitations of the ex vivo approach	116
6.3.2    Functional organization of BNST-A	117
6.3.3    Nature and origin of the altered neuronal responsiveness	119
<b>References</b>	<b>121</b>
<b>Vita</b>	<b>148</b>

## List of Tables

Table 3.1	Physiological properties of BNST-A neurons by cell type	40
Table 3.2	Physiological properties of RS (type-I) neurons by region	41
Table 3.3	Physiological properties of LTB (type-II) neurons by region	46
Table 3.4	Physiological properties of BNST-A neurons by region	46
Table 3.5	Morphological properties of BNST-A neurons	58
Table 5.1	Incidence of BNST-A cell types in resilient and PTSD-like rats	91
Table 5.2	Physiological Properties of RS cells in BNST-AL	93
Table 5.3	Physiological Properties of LTB cells in BNST-AL	94
Table 5.4	Physiological Properties of RS cells in BNST-AM	94
Table 5.5	Physiological Properties of LTB cells in BNST-AM	94
Table 5.6	Physiological Properties of RS cells in BNST-AV	96
Table 5.7	Physiological Properties of LTB cells in BNST-AV	96

## List of Illustrations

Figure 3.1.	Anatomical subdivisions and recording configuration	39
Figure 3.2	Regular spiking (RS; Type I) BNST-A neurons	42
Figure 3.3	Low-threshold bursting (LTB; Type II) BNST-A neurons	44
Figure 3.4	Cells generating rebound single spikes	45
Figure 3.5	Type-III (fIR) and late-firing (LF) neurons	48
Figure 3.6	Spontaneously active (SA) neuron recorded in BNST-AV	50
Figure 3.7	Incidence and spatial distribution of various physiological cell types in different sectors of BNST-A	51
Figure 3.8	Morphological properties of aspiny BNST-A neurons	54
Figure 3.9	Morphological properties of BNST-A neurons	55
Figure 4.1	Approach used to study intrinsic BNST-A projections	64
Figure 4.2	Spatial selectivity of glutamate uncaging	67
Figure 4.3	Distinguishing responses to uncaged glutamate vs. synaptically released transmitters	69
Figure 4.4	Examples of response patterns observed in BNST-AL, AM, and AV	72
Figure 4.5	Plots of intra-BNST connections evidenced with glutamate uncaging	74

Figure 4.6	Relative incidence of inhibitory and excitatory connections within BNST-A	76
Figure 4.7	Properties of intrinsic BNST connections	77
Figure 4.8	Properties of IPSPs and EPSPs elicited by GU	79
Figure 4.9	Morphological correlates of intrinsic connectivity	82
Figure 5.1	Experimental paradigm and recording sites	89
Figure 5.2	Synaptic responsiveness of BNST-AL neurons to ST stimuli in resilient and PTSD-like rats	93
Figure 5.3	Synaptic responsiveness of BNST-AM neurons to ST stimuli in resilient and PTSD-like rats	95
Figure 5.4	Synaptic responsiveness of BNST-AV neurons to ST stimuli in resilient and PTSD-like rats	96
Figure 5.5	Properties of paired-pulse facilitation at glutamatergic inputs to BNST-AM and AV neurons	98
Figure 6.1	Overall pattern of intrinsic BNST-A connections	112

## List of Abbreviations

AC	Anterior commissure
aCSF	Artificial cerebrospinal fluid
ACTH	adrenocorticotrophic hormone
ANS	Autonomic nervous system
BA	Basal nucleus of the amygdala
BLA	Basolateral complex of the amygdala
BLAp	Posterior BLA
BM	Basomedial nucleus of the amygdala
BNST	Bed nucleus of the stria terminalis
BNST-A	Anterior portion of the bed nucleus of the stria terminalis
BNST-AL	Anterolateral BNST
BNST-AM	Anteromedial BNST
BNST-AV	Anteroventral BNST
BNST-P	Posterior portion of the bed nucleus of the stria terminalis
CeA	Central nucleus of the amygdala
CeL	Centro-lateral nucleus of the amygdala
CeM	Centro-medial nucleus of the amygdala
CNQX	6-cyano -7-nitroquinoxaline-2,3-dione
CS	Conditioned stimulus
CSF	Cerebrospinal fluid
CRF	Corticotropin-releasing factor

DMV	Dorsal valgal nucleus
EPM	Elevated plus maze
EPSC	Excitatory postsynaptic current
EPSP	Excitatory postsynaptic potential
fIR	Fast inward rectification cell type
GABA	Gamma-aminobutyric acid
GU	Glutamate uncaging
HPA	Hypothalamic-pituitary-adrenocortical axis
IC	Internal capsule
IL	Infralimbic component of the medial prefrontal cortex
IPSP	Inhibitory postsynaptic potential
IsPSPi	Inter-spontaneous PSP interval
ITC	Intercalated cell masses of the amygdala
LA	Lateral nucleus of the amygdala
LC	Locus coeruleus
LF	Late firing cell type
LH	Lateral hypothalamus
LTB	Low-threshold bursting cell type
MeA	Medial nucleus of the amygdala
NMDA	N-methyl-D-aspartate
NST	Nucleus of the solitary tract
mPFC	Medial prefrontal cortex
PACAP	Pituitary adenylate cyclase-activating polypeptides

PAG	Periaqueductal gray
PB	Parabrachial nucleus
PHAL	<i>Phaseolus vulgaris</i> - leucoagglutinin
PPF	Paired-pulse facilitation
PSPs	Postsynaptic potentials
PTSD	Post-traumatic stress disorder
PVN	Paraventricular nucleus of the hypothalamus
$R_{in}$	Input resistance
RS	Regular spiking cell type
RT-PCR	reverse transcription polymerase chain reaction
SA	Spontaneous active cell type
ST	Stria terminalis
Str	Striatum
US	Unconditioned stimulus
UV	Ultraviolet
VLM	Ventral lateral medulla
$V_r$	Resting potential
VTA	Ventral tegmental area

# **CHAPTER I**

## **Introduction**

## 1.1. Background and significance

This thesis focuses on the functional organization of a poorly understood brain structure: the bed nucleus of the stria terminalis (BNST). My experiments aimed to shed light on the intrinsic connectivity of BNST neurons, their electroresponsive properties, and their potential contribution to anxiety disorders. Anxiety disorders are the most common type of psychiatric disorders, accounting for 30 to 50% of reported cases. They are more common than any other affective disorder or substance abuse disorder (Kessler et al., 2005). As a result, anxiety disorders are the object of intense scrutiny in the scientific literature. A key component of anxiety disorders is excessive fear. Thus a large portion of the experimental work has examined the neurocircuitry underlying fear responses. As reviewed below, two densely interconnected brain structures have been implicated in the expression and learning of fear/defensive responses: the amygdala and the BNST. Yet, the amygdala and the BNST appear to play different roles in fear. Below, I first review this evidence. Next, I will review the anatomical organization of BNST, prior work about the electroresponsive properties of BNST neurons, as well as evidence implicating BNST and related structures in anxiety disorders.

### 1.1.1. Mechanisms underlying the expression and acquisition of fear/defensive responses

The most common behavioral paradigm to study fear learning is Pavlovian fear conditioning (LeDoux, 2000). In fear conditioning, a neutral stimulus or a

context is paired with a noxious unconditioned stimulus (US). The neutral stimulus initially does not elicit any emotional reaction, but after a few pairings with the US, the neutral stimulus or context becomes a conditioned stimulus (CS) signaling imminent US onset. After learning the contingency, the sole presence of the CS can trigger fear responses even in the absence of the US. Through multiple repetitions of the CS without the US, conditioned fear responses gradually diminish, a process termed extinction. In other words, one can learn that the CS no longer predicts the US. This form of learning is very robust and widely conserved across species. As a consequence, fear conditioning is a widely used model in laboratory settings.

The neuronal circuit underlying auditory fear conditioning is particularly well characterized. A large body of evidence indicates that sensory information about the CS and US is relayed from the thalamus and cortex to lateral amygdala (LA) neurons. The convergence of CS and US inputs results in an increased efficacy of the synapses carrying CS information (reviewed in LeDoux 2000; Blair et al., 2001; Maren, 2001). The change in synaptic efficacy is reflected in larger CS-evoked responses in LA neurons after fear conditioning (Quirk et al., 1995; Collins and Paré 2000; Repa et al., 2001). LA then relays CS information to the central medial amygdala (CeM), the major source of amygdala projections to fear effector neurons in the brainstem and hypothalamus (Hopkins and Holstege, 1978; LeDoux, 2000; Davis, 2000).

The last decade has witnessed major progress in our understanding of amygdala microcircuits involved in fear expression. For example, it is now widely

accepted that LA projects indirectly to CeM (Paré et al., 2004) via the lateral portion of the central amygdala (CeL), intercalated (ITC) cells and the basal amygdala subnuclei (BA) (Krettek and Price, 1978a; Smith and Paré, 1994; Paré et al., 1995, Pitkanen et al., 1997). Also, it has been shown that there are two mechanisms for transferring CS information from LA to CeM: a) through excitation of CeM cells via glutamatergic BA neurons (Amano et al., 2011), and b) through disinhibition of CeM neurons from GABAergic inputs arising in CeL (Ciocchi et al., 2010; Haubensak et al., 2010; Duvarci et al., 2011) and ITC cells at the BA-CeM border (Amir et al., 2011).

Lesions of areas receiving inputs from the central amygdala (CeA) disrupt the expression of conditioned fear responses. For instance, lesioning the lateral hypothalamus (LH) reduces blood pressure but not freezing responses, whereas lesions to the periaqueductal gray (PAG) abolish freezing but not blood pressure responses (LeDoux et al., 1988).

#### 1.1.2. The role of BNST in fear

Despite the fact that the CeA and the BNST have similar anatomical, neurochemical, and cytoarchitectural properties, these two structures appear to play different roles in the genesis of conditioned fear (Hopkins and Holstege, 1978; Holstege et al., 1985; Gray and Magnusson, 1987; Alheid et al., 1995; Dong et al., 2001a). Initially, lesion experiments suggested that BNST was not required for the acquisition or expression of conditioned fear responses to discrete sensory cues (LeDoux et al., 1988; Hitchcock and Davis, 1991; Gewirtz

et al., 1998; Sullivan et al., 2004). Instead, it was reported that lesions of BNST disrupted corticosterone and freezing responses to contextual stimuli that had been associated with adverse outcomes (Sullivan et al., 2004). Moreover, it was noted that BNST lesions block the gradual elevation in baseline startle responses that develops over the course of training (Gewirtz et al., 1998). Further, inactivation of BNST was found to abolish light-enhanced startle (Walker and Davis, 1997) and freezing responses during predator stress (Fendt et al., 2003). Consequently, it was initially proposed that BNST mediates *unconditioned fear responses* whereas CeA mediates *conditioned fear responses* (Walker and Davis, 1997). However, this hypothesis was inconsistent with the effect of BNST lesions in contextual fear conditioning (Gray et al., 1993; Sullivan et al., 2004, Duvarci et al., 2009). As a result, it was later proposed that BNST mediates *long-duration, sustained, anxiety-like fear responses* to diffuse environmental contingencies as opposed to CeA which mediates *short-duration, phasic, fear responses* to discrete threatening stimuli (Walker et al., 2003).

However, studies in our laboratory also suggest that BNST shape inter-individual variations in the expression of fear and anxiety. Indeed, animals with BNST lesions exhibit higher discriminative abilities in differential cued fear conditioning paradigms (Duvarci et al., 2009). Thus, the possibility remains that CeA and BNST functions are intertwined and that BNST contributes to generalize cued fear in time and to different (safe) stimuli.

## **1.2. Anatomical organization of the bed nucleus of the stria terminalis**

### 1.2.1. BNST-A nuclei

In contrast to the amygdala, our understanding of the BNST is limited. Contrary to what its name implies, the BNST is in fact a collection of nuclei that lies ventral to the lateral septal nucleus, dorsal to the preoptic region of the hypothalamus, and surrounds the anterior commissure (AC). BNST has similar developmental origin, cytoarchitecture, chemoarchitecture, and pattern of connectivity as the CeA. Also, it is reciprocally connected to the CeA and the medial nucleus of the amygdala (MeA). This has led some authors to suggest that together, the MeA, the substantia innominata, CeA, and BNST form an integrated functional unit called the “extended amygdala” (de Olmos and Heimer, 1999).

At a macroscopic level, the BNST can be divided into anterior (BNST-A) and posterior (BNST-P) regions. The latter is a sexually dimorphic region involved in reproductive and defensive behaviors (Simerly, 2002). My research focused on BNST-A since is most often implicated in the regulation of anxiety and contextual fear (Davis et al., 2010). There is little consensus regarding the number and location of BNST subnuclei. For instance, Ju and Swanson (1989a, 1989b) recognized 18 subnuclei based on cyto- and chemoarchitecture. In contrast, Saper and colleagues (Moga et al., 1989) described 13 subnuclei. Also, the most commonly used stereotaxic atlas of rat brain (Paxinos and Watson, 2007) identifies 10 subnuclei (De Olmos et al., 1985). This lack of consensus is not limited to the boundaries and number of subdivisions, but also includes the

nomenclature used. Moreover, these subdivisions cannot be identified with precision in unstained, living tissue.

For my research, I adopted a simpler subdivision based on the position of major fiber bundles that can be easily identified in trans-illuminated slices: the AC, dividing the BNST-A into dorsal and ventral (BNST-AV) sectors, and the intra-BNST component of the stria terminalis, subdividing the dorsal portion into medial (BNST-AM) and lateral (BNST-AL) regions. The correspondence between my subdivisions and the subnuclei identified by Swanson and colleagues is as follows: the BNST-AV corresponds to Swanson's anteroventral, fusiform, parastrial and dorsomedial subnuclei plus the subcommisural zone; the BNST-AL corresponds to Swanson's oval, juxtacapsular, and anterolateral subnuclei; and the BNST-AM corresponds to Swanson's anterodorsal subnucleus. In the following paragraphs, I will review the contrasting pattern of afferent and efferent connections in BNST-A according to this simpler subdivision.

### 1.2.2. Afferent and efferent BNST-A connections

BNST-A is in a key position to integrate inputs from limbic forebrain regions and influence the output to fear and stress effector systems. From numerous anatomical and, more recently, optogenetic experiments, it is clear that different BNST regions form contrasting connections. For instance, excitatory inputs from the ventral subiculum and medial prefrontal cortex (mPFC), particularly its infralimbic region (IL), target BNST-AM and BNST-AV but not BNST-AL (Cullinan et al., 1993; McDonald et al., 1999b; Shin et al., 2008;

Bienkowski and Rinaman, 2013). In contrast, the insular cortex has the opposite pattern of projections (McDonald et al., 1999a). Inputs from the basomedial nucleus of the amygdala (BM) primarily send projections to BNST-AM and medial AV whereas the Ce sends a strong GABAergic projection to BNST-AL and lateral AV (Sun and Cassell, 1993; Dong et al., 2001a). Further, the posterior region of the basolateral amygdala (BLAp) contacts the most caudal part of BNST-AL and AM (Dong et al., 2001a; Kim et al., 2013). It is important to note that whereas the connections between BNST-A and the BM and BLAp are largely unidirectional, the BNST-A and CeA connections are reciprocal (Sun and Cassell, 1993; Dong et al., 2001a).

Additionally, the BNST receives differentiated inputs from all major neuromodulatory pathways (Phelix et al., 1992). For instance, a strong noradrenergic input from the nucleus of the solitary tract (NST – A2 cell group); and the ventral lateral medulla (VLM- A1 cell group) innervates primarily BNST-AV (Sofroniew, 1983; Forray and Gysling, 2004; Myers et al., 2005). Additionally, a weaker noradrenergic projection arising from the locus coeruleus (LC- A6 cell group) also targets the BNST-AV (Aston-Jones et al., 1999; Park et al., 2009). In contrast, serotonergic inputs from the dorsal raphe nucleus terminate mostly dorsal to the AC, more prominently in AM than AL (Vertes, 1991; Phelix et al., 1992). Dopaminergic inputs from the ventral tegmental areas (VTA), PAG, and the retrorubral field preferentially target BNST-AL (Hasue and Shammah-Lagnado, 2002; Meloni et al., 2006; Krawczyk et al., 2011a).

Similarly, tracing studies have reported that different sectors of BNST-A

contribute with contrasting projections. Briefly, BNST-AM and AV preferentially project to neuroendocrine output systems in the hypothalamus (Prewitt and Herman, 1998; Dong et al., 2001b; Dong and Swanson, 2006a) whereas BNST-AL cells preferentially projects to brainstem structures such as the NTS, parabrachial nucleus (PB), and the dorsal vagal nucleus (DMV) (Sofroniew et al., 1983; Holstege et al., 1985; Moga et al., 1989; Sun and Cassell, 1993). Anatomical studies indicate that a population of GABAergic cells located in BNST-AM and AV innervate the parvocellular subregion of the paraventricular nucleus of the hypothalamus (PVN) (Cullinan et al., 1993; Cullinan et al., 2008; Radley and Sawchenko, 2011). Additionally, BNST-AM and -AV send both primarily GABAergic but also glutamatergic projections to the VTA, an area implicated in the reward and motivation (Cullinan et al., 1993; Georges and Aston-Jones, 2001, 2002; Jalabert et al., 2009; Kudo et al., 2012; Jennings et al., 2013). Further, the BNST-AL sends a substantial projection to the LH, a brain area critical for autonomic responses, drug-seeking and avoidance behavior (Dong et al., 2001b; Dong and Swanson, 2004b, 2006b; Kim et al., 2013). Finally, the PAG, an area implicated in central autonomic control, is innervated by most BNST-A regions (Dong and Swanson, 2004, 2006a, 2006b). In summary, BNST-A is a critical relay station between limbic forebrain cortical regions and neuroendocrine as well as autonomic effector structures (Ulrich-Lai and Herman, 2009).

### 1.2.3. Transmitters used by BNST-A neurons

Most BNST-A cells are GABAergic cells. However, BNST-A also contains a small population of glutamatergic cells, mostly concentrated in close proximity to the AC (Sun and Cassell, 1993; Day et al., 1999; Georges and Aston-Jones, 2001, 2002; Hur and Zaborsky, 2005; Larriva-Sahd, 2006; Poulin et al., 2009; Kudo et al., 2012). A very rich set of neuropeptides is differentially expressed in BNST-A regions. Among them, corticotropin releasing factor (CRF), neurotensin, somatostatin, and pituitary adenylate cyclase-activating polypeptides (PACAP) are expressed by different subsets of BNST-AL neurons (Gray and Magnuson, 1992; Hannibal, 2002; Hammack et al., 2010). Also, opioid peptides, such as enkephalin and dynorphin, are found primarily in BNST-AL and the lateral portion of BNST-AV (Poulin et al., 2009). In contrast, neuropeptide Y (NPY) is expressed diffusely across all BNST-A regions (Pleil et al., 2012).

### **1.3. Intrinsic connections of BNST-A**

While the heterogeneous connectivity reviewed in the previous section suggests a degree of functional specialization within BNST-A, a seminal series of tracing studies by Swanson and colleagues (Dong and Swanson, 2003, 2004, 2006a, 2006b, 2006c) suggest that different BNST-A regions do not act as independent processing channels, but that they interact via inter-nuclear connections. For instance, they reported that components of BNST-AL, particularly, the oval nucleus, strongly projects to parts of BNST-AV, such as the fusiform nucleus (Dong and Swanson, 2004). However, the interpretation of

these findings is complicated by the fact that the distance between different BNST regions is relative small to the considerable extent of dendritic trees in the BNST (McDonald, 1983; Larriva-Sahd, 2006). Moreover, this problem is compounded by tracer diffusion from the injection site in the small volume of BNST, particularly along the tract of the pipettes used to inject the tracers.

#### **1.4. Physiological properties of BNST-AL Neurons**

The electroresponsive properties of BNST neurons have received little attention so far. Indeed, most electrophysiological studies have focused on other aspects of BNST physiology such as the influence of various peptides/transmitters (Grueter and Winder, 2005; McElligott and Winder, 2008; Shields et al., 2009; Puente et al., 2010; Krawczyk et al., 2011a; Nobis et al., 2011; Li et al., 2012; Lungwitz et al., 2012), particularly CRF (Kash and Winder, 2006; Gafford et al., 2012; Oberlander and Henderson, 2012; Ide et al., 2013; Silberman et al., 2013), mechanisms of addiction and relapse to drug seeking (Dumont and Williams, 2004; Dumont et al., 2005, 2008; Davis et al., 2008; Grueter et al., 2008; Kash et al., 2008a, 2008b, 2009; Krawczyk et al., 2011b; Conrad et al., 2012), synaptic plasticity (Weitlauf et al., 2005), and the impact of stress (Conrad et al., 2011).

Although a few studies compared the passive properties of neurons in different BNST-A sectors (e.g. Egli and Winder, 2003), most did not examine the temporal dynamics of current-evoked spiking. To our knowledge, a systematic physiological characterization of BNST-A neurons has only been performed in

the AL region in general (Rainnie, 1999; Hammack et al., 2007; Guo et al., 2009, 2012; Hazra et al., 2011, 2012) and its juxtacapsular sector in particular (Francesconi et al., 2009; Szucs et al., 2010).

Rainnie and colleagues distinguished three cell types in BNST-AL. *Type I neurons* display a regular firing pattern in response to depolarizing current injection and a depolarizing sag in response to membrane hyperpolarization. *Type II neurons* also exhibit a depolarizing sag in response to hyperpolarizing current injection but burst firing in response to depolarizing current injection, due to the activation of the low-threshold calcium current  $I_T$ . This type of cell, the most frequently encountered in BNST-AL, could putatively switch between tonic and burst firing modes, depending on membrane potential. *Type III neurons* do not exhibit a depolarizing sag in response to hyperpolarizing current injection, but instead exhibit a fast time-independent inward rectification, indicative of the activation of an inwardly rectifying potassium current  $I_{K(IR)}$ . Type III neurons exhibit a regular firing pattern in response to depolarizing current. Also, Type III neurons are the least excitable due to a more hyperpolarized resting membrane potential and a higher threshold for action potential generation (Hammack et al., 2007, Hazra et al., 2011).

This tripartite classification of BNST-AL neurons found support in a single-cell reverse transcription polymerase chain reaction (RT-PCR) study where the alpha sub-unit expression profile of key ionic channels correlated with the electrophysiological classification (Hazra et al., 2011). Moreover, another study revealed that serotonergic receptor subtypes were differentially expressed in

three cell types. For instance, 5HT-2C receptors were almost exclusively expressed by Type-III neurons whereas 5HT-7 receptors were commonly expressed by Type-I and II neurons but not Type-III cells (Guo et al., 2009; Hazra et al., 2012).

To summarize, the three BNST-A subregions have contrasting afferents and efferents connections to brain structures involved in fear/defensive behaviors. They might also be interconnected by GABAergic and/or glutamatergic axons. Further, major neuromodulatory pathways differentially innervate BNST-A. This suggests that BNST-A has a heterogeneous modular structure, not a uniform organization as many studies have assumed. Indeed, the lesion and pharmacological studies reviewed above did not have the spatial resolution to selectively target the different subnuclei identified by anatomical studies. As a result, it is difficult to interpret them.

To understand the operations carried out by BNST-A, it will be necessary to investigate the intrinsic membrane properties of its constitutive elements and the synaptic network in which they are embedded. Presently, with the exception of BNST-AL, we lack a systematic description of the properties of BNST-A neurons. In addition, little data is available on the intrinsic connections linking different BNST-A subregions and its local circuit. To address this, I will expand the work of Hammack and colleagues and investigate the electroresponsive properties of BNST-AM and BNST-AV neurons (Chapter III). In Chapter IV, I will examine the intrinsic connections within and between different BNST-A regions using patch recordings and ultraviolet (UV) uncaging of glutamate (GU) in vitro.

Finally in Chapter V, I will investigate the potential contribution of BNST-A neurons to anxiety disorders. Thus, the next section provides background information on the mechanisms underlying normal and pathological anxiety.

### **1.5. Understanding anxiety disorders: the case of PTSD**

Fear and anxiety are conceptualized as two different behavioral states. The most common framework conceives *fear* as being triggered by unambiguous cues signaling imminent threat, and giving rise to intense but short-lasting defensive behaviors. In contrast, *anxiety* is elicited by more diffuse, distal or unpredictable threats that produce longer-lasting defensive responses and risk assessment behaviors (Grupe and Nitschke, 2013). A major scientific challenge is to operationalize these two constructs so that they can be studied in an experimental setting. One approach is to identify cases where extreme manifestations of related behaviors occur naturally. Commonly, the study of psychopathology offers broad avenues for this kind of research. Because similar networks underlie fear learning and expression in animals and humans (Phelps and LeDoux, 2005), animal models of anxiety disorders constitute a promising path toward understanding these debilitating conditions. Accordingly, in Chapter V, I will describe experiments aiming to shed light on the potential participation of BNST-A neurons to a particular anxiety disorder: post-traumatic stress disorder (PTSD). Therefore, the following section provides a quick overview of the manifestations and causes of PTSD.

### 1.5.1. Definition of PTSD

To receive a PTSD diagnosis, individuals must experience or witness an actual or threatened trauma, or learn that a close acquaintance was exposed to trauma, or experience indirect exposure to aversive details of a trauma (DSM 5; APA, 2013). Individuals must strongly express each of four symptom clusters: intrusion, avoidance, negative alterations in mood/ cognition, and alterations in arousal and activity. Symptoms must occur for >1 month and cause significant impairment in functioning.

### 1.5.2. Neurobiology of PTSD

Given that PTSD is precipitated by a traumatic event, it is important to consider how the body reacts and adapts to environmental challenges. Any event that disrupts homeostasis produces an adaptive response known as the stress response (Selye, 1978). Stressors can be physical or psychological in nature; they can originate from peripheral receptors or the brain itself. Similarly, the kind of trauma that precipitates PTSD can be both, physical or/and psychological, but it must be strong enough to threaten, at least potentially, the physical integrity of the person. The stress response is mediated by the autonomic nervous system (ANS) and the hypothalamic-pituitary-adrenocortical (HPA) axis (Dayas et al., 2001).

The ANS controls visceral functions through its sympathetic and parasympathetic arms; it can cause rapid alterations in physiological states such as increases in heart rate, blood pressure, and respiration rate, though these are

short-lived responses. In case of imminent danger, this fast response increases glucose availability to skeletal muscles and prepares the organism to face the threat or to escape (Ulrich-Lai and Herman, 2009).

In contrast, the HPA axis mediates longer lasting responses that develop more slowly. As its name implies, it involves the hypothalamus, the pituitary, and the adrenal glands, and it generates the neuroendocrine responses to stress. Upon stressor exposure, neurons in the PVN secrete CRF and vasopressin in the median eminence. These hormones act on the anterior pituitary and stimulate the secretion of adrenocorticotrophic hormone (ACTH) into the blood stream. ACTH acts on the adrenal cortex by promoting the synthesis and release of glucocorticoid hormones (for example, corticosterone in rats and cortisol in humans) (Herman et al., 2003). Glucocorticoids affect metabolism, immune function, and a variety of brain areas such as the hypothalamus, hippocampus, amygdala, mPFC, lateral septum and brainstem monoaminergic nuclei (Yehuda, 2002; Joëls and Baram, 2009; Ulrich-Lai and Herman, 2009). A feedback exists between different areas of the brain and the HPA axis. For instance, the hippocampus and mPFC can inhibit the HPA axis (Diorio et al., 1993; Figueiredo et al., 2003; Herman and Mueller, 2006; Radley et al., 2006), whereas the amygdala and monoaminergic brainstem nuclei stimulate the activity of PVN CRF neurons (Plotsky et al., 1989; Dayas et al., 2001; Lowry, 2002; Herman et al., 2003).

PTSD symptoms are commonly believed to reflect an inadequate adaptation of the neurobiological systems that process stressors. Accordingly,

high reactivity to the environment is thought to reflect an autonomic dysregulation leading to symptoms of hyperarousal. PTSD patients tend to show high heart rates, elevated electrodermal arousal, and profound cardiac vagal withdrawal (Blechert et al., 2007). Additionally, it was reported that PTSD patients have a dysregulated HPA axis. However, much controversy surrounds this claim (Heim and Nemeroff, 2009). For instance, some PTSD studies have found decreased basal levels of cortisol (Yehuda et al., 1990, 1994, 1996) while others failed to reproduce this finding (Young and Breslau, 2004a, 2004b). Some authors have proposed that hypocortisolism is a preexisting condition and a predisposing factor for developing PTSD (Resnick et al., 1995; Yehuda et al., 1998). A meta-analysis of studies on cortisol levels in PTSD concluded that low levels of cortisol are only found under certain conditions (e.g. females, certain type of trauma, afternoon samples) (Meewisse et al., 2007) and thereby more research needs to be done on this topic. Paradoxically, it was reported that PTSD subjects have higher levels of CRF in the cerebrospinal fluid (CSF) (Bremner et al., 1997a; Baker et al., 1999), and that they display blunted ACTH responses to CRF (Yehuda et al., 2004; Ströhle et al., 2008).

A more promising approach to study HPA axis dysregulation uses pharmacological and non-pharmacological challenge paradigms. In non-pharmacological challenges, patients are exposed to cognitive stress or trauma reminders to provoke a stress response (Liberzon et al 1999; Bremner et al., 2003; Elzinga et al., 2003). Pharmacological challenges includes the administration of dexamethasone, ACTH, CRH and naloxone followed by cortisol

measurements. A meta-analysis of the literature revealed that subjects with PTSD have enhanced salivary cortisol levels in response to cognitive challenge and enhanced plasma cortisol suppression after administration of dexamethasone (see review, de Kloet et al., 2006).

Additionally, PTSD is associated with an imbalance in various neurotransmitter systems. For instance, PTSD patients show increased urinary excretion and CSF concentration of noradrenaline, adrenaline and dopamine (Yehuda et al., 1992; Hamner and Diamond, 1993; Lemieux and Coe, 1995; Geraciotti et al., 2001). Indirect evidence for the involvement of serotonin in PTSD comes from pharmacological interventions since serotonin reuptake inhibitors seem to be partially effective at alleviating certain PTSD symptoms (Davidson et al., 2002).

### 1.5.3. Genotypic and phenotypic alterations in PTSD

Approximately 50 - 60% of Americans are exposed to at least one traumatic event during their lifetime (Kessler et al., 1995). Yet only 1.4% to 11.2% of them develop PTSD (Afifi et al., 2010). Identifying the factors that make individuals susceptible to trauma could help design preventive interventions for the general population. Epidemiological studies have started to identify risk factors that make individuals more likely to develop PTSD following trauma. The available evidence suggests that the etiology of PTSD is multi-factorial; since the interplay between genetic and environmental factors determines the expression and severity of the pathology (Gillespie et al., 2009). Studies with monozygotic

and dizygotic twins (with and without PTSD) attempt to tease apart the nurture and nature elements of the disease (Gillespie et al., 2009).

Bidirectional gene-environment interactions not only imply that the individual's personality can influence the selection of his or her environment, but also that environmental factors can affect how particular genes are expressed. The emerging field of epigenetics illustrates the dramatic influence of these interactions (for review, see Zhang and Meaney, 2010). For instance, a history of childhood abuse by itself is a good predictor of PTSD (Bernard-Bonnin et al., 2008; Kingston and Raghavan, 2009). Interestingly, genetic polymorphisms at the stress-related gene FKBP5 show significant interaction with history of childhood abuse (Binder et al., 2008). In rodents, maternal behavior has been shown to alter DNA methylation of the glucocorticoid receptor gene promoter in the hippocampus and thereby modulates the offspring's stress response (Weaver et al., 2004). Recently, it was proposed that the altered immune responses seen in PTSD are linked to epigenetic modifications. Indeed, a significant positive correlation was found between the methylation levels of stress-related genes and immune function in PTSD patients (Uddin et al., 2010).

Several imaging studies have reported reduced hippocampal volume in PTSD (Bremner et al., 1995, 1997b; Schuff et al., 2001; Villarreal et al., 2002; Lindauer et al., 2004; Kitayama et al., 2005; Jatzko et al., 2006). Consistent with this, individuals with PTSD exhibit impaired performance on hippocampal-dependent tasks involving allocentric spatial processing (Gilbertson et al., 2007). Importantly, these morphological and functional abnormalities predate trauma

(Gilbertson et al., 2002, 2007): individuals with PTSD and their non-traumatized co-twin are impaired relative to non-PTSD control twins (Gilbertson et al., 2007). Together, these findings suggest that the hippocampal impairments seen in PTSD predate trauma.

Also, functional imaging studies generally report that PTSD subjects have a hyperactive amygdala in response to trauma reminders, emotional faces and/or threatening cues (Shin et al., 2004, 2005). In contrast, the mPFC, including the anterior cingulate cortex, is generally reported to be hypoactive in the same paradigms (Shin et al., 2001, 2004, 2005; Lanius et al., 2003; Britton et al., 2005).

At the cognitive level, it has been reported that PTSD patients have deficits in declarative and short-term memory (Bremner et al., 1993; Yehuda et al., 1995; Moore, 2009). In contrast, studies using aversive conditioning paradigms have found enhanced acquisition of conditioned fear responses as well as impaired ability to extinguish these aversive associations (Orr et al., 2000; Bremner et al., 2005; Blechert et al., 2007). Studies of identical and fraternal twins discordant for trauma exposure found that this extinction deficit does not predate trauma but develops after trauma (Milad et al., 2008). Thus, while the extinction deficit is not a predisposing factor, it might contribute to maintaining the disorder.

Based on the data reviewed in the previous section, most accounts of PTSD situate the amygdala, hippocampus, and mPFC as key mediators of the pathology. These models are also supported by animal studies investigating the

role of these structures in fear conditioning paradigms. In particular, animal studies indicate that the amygdala plays a critical role in the acquisition and expression of conditioned fear responses (Paré et al., 2004). Naturally, it is thought that a hyperactive amygdala will contribute to the maladaptive stress responses and exaggerated acquisition of fear associations seen in PTSD (Shin et al., 2004, 2005; Shin and Liberzon, 2010). Further, the hippocampus is required for contextual fear memory (Maren et al., 2013), therefore, an abnormal hippocampus is thought to explain not only the deficits in verbal and contextual memory but also the difficulties in discriminating between safe and unsafe contexts (Gilbertson et al., 2007). Finally, the IL component of mPFC plays a critical role in the extinction of conditioned fear (Quirk and Mueller, 2008). Therefore, the decreased mPFC function observed in PTSD patients is thought to reflect a reduced inhibitory control over the amygdala and thereby stress and fear responses.

Nevertheless, we are still lacking a general model that integrates neuroanatomical, neurochemical, neurophysiological, and neuroendocrinological findings in PTSD. Undoubtedly, human studies of PTSD have helped identify some of the key neurobiological alterations in the disorder. However, to develop a model that fully explains PTSD, better-controlled and more invasive experimental designs are required. Due to ethical limitations, human subjects cannot be used for such investigations. Therefore, researchers have developed simplified animal models of the disease aiming to understand not only the etiology and pathophysiology of PTSD but also to identify possible treatment targets.

Moreover, the contributions of structures that are too small for the resolution of current imaging techniques in humans (e. g. different subregions of the amygdala or BNST) can only be studied in animal models.

### **1.6. Towards an animal model of PTSD**

Assessment of animal models is usually done considering four dimensions: face, construct, predictive, and discriminant validity. At the phenomenological level, a model with face validity should resemble the disorder in etiology, physiology, and symptomatology. Different animal models of PTSD have successfully induced changes in autonomic and neuroendocrine responsiveness that reproduce PTSD symptoms such as increased heart rate, hyperarousal, hypervigilance, exaggerated fear responses, blunted HPA axis, etc. Construct validity refers to the theoretical rationale of the model. It assumes that if the animal model is homologous to the human condition, then it is possible to develop theories of the psychopathology. Predictive validation could be assessed through therapeutic treatments of the disorder. For example, one could test if PTSD-like symptoms in the animal model are alleviated by SSRIs or anxiolytics. Discriminant validity refers to the ability of the model to differentiate between those with and without the disorder (Willner, 1986; Siegmund and Wotjak, 2006; Goswami et al., 2013).

Fortunately, significant progress has been made in developing animal models of PTSD (see Adamec et al., 2006; Cohen et al., 2006a; Siegmund and Wotjak, 2006; Goswami et al., 2013). One approach focuses on the impact of

species-relevant threatening stimuli that reproduce the type of life-and-death circumstances known to precipitate PTSD. In rodents, it has been shown that a single 10 minutes presentation of a predator or predator smell, causes long-lasting behavioral changes akin to PTSD (Adamec and Shallow, 1993; Cohen et al., 2003, 2006a; Goswami et al., 2010). In the weeks following predator exposure, rats show decreased activity in the hole board, reduced time in light chamber, reduced latency to leave the light chamber in the light-dark box test, reduced social behavior as measured with the social interaction test, and deficits in spatial memory tasks (Adamec and Shallow, 1993; Adamec et al., 1998, 2001, 2003; Cohen et al., 2003). On the elevated plus maze (EPM), rats show reduced open arm exploration (Adamec and Shallow, 1993; Adamec et al., 1998; Cohen et al., 2003; Adamec et al., 2003, 2006a). Moreover, startle responses are persistently increased both in amplitude and habituation time (Adamec, 1997; Adamec et al., 2003). Importantly, these maladaptive responses remain unabated in some cases for at least 3 - 4 weeks (Adamec and Shallow, 1993; Cohen and Zohar, 2004).

A few studies have investigated individual variability in symptom expression after predator exposure. This is of tremendous interest because in humans not all the individuals exposed to a traumatic event develop PTSD. Cohen and colleagues proposed the use of a behavioral cut-off criteria for their predatory threat animal model, similar to the inclusion and exclusion criteria described in the DSM-IV (Cohen et al., 2006b). They reported that one day after predator threat, nearly all rats displayed signs of increased anxiety. However, one

week later, only 10-50% of the exposed rats remained hyper-anxious depending on the strain (Cohen and Zohar, 2004; Cohen et al., 2006b). Through the analysis of exploratory behavior in the EPM and of the acoustic startle response, they classified rats into those that display extreme behavioral manifestations of anxiety (or *PTSD-like* rats) and those with minimal levels of anxiety (or *Resilient* rats; Cohen et al., 2006b). A comparison between the Sprague Dawley, Fisher, and Lewis rat strains revealed different levels of propensity to develop persistent anxiety after predator exposure with prevalence of 25%, 10% and 50%, respectively (Cohen et al., 2006b). The high prevalence of the PTSD-like phenotype in Lewis rats is very convenient in a laboratory setting because it allows investigators to rapidly obtain equal samples of Resilient and PTSD-like rats.

Several lines of evidence indicate that the Lewis rat model of PTSD has face validity. Indeed, Lewis rats have a dysregulated HPA axis and abnormal immune responses, abnormalities that have high incidence in humans with PTSD (Shurin et al., 1995; Stöhr et al., 1999; Cohen et al., 2006b; Uddin et al., 2010). Control studies comparing naïve rats and rats subjected to predator threat show that exploratory behavior in the EPM is highly compromised in a proportion of rats that underwent predator threat but not in naïve rats. Also, PTSD-like but not Resilient rats are deficient at extinguishing conditioned fear responses *after*, but not *before* predatory threat, matching the results obtained in human PTSD (Goswami et al., 2010). Further, Lewis rats have been tested in three types of recognition memory tasks that vary in their hippocampal dependence (Goswami

et al., 2012). Paralleling human observations, rats that show impairment in the hippocampal dependent task prior predator threat are more likely to develop PTSD-like symptoms (Goswami et al., 2013). Therefore, the predator threat paradigm in Lewis rats constitutes an attractive model to investigate the biological basis of PTSD. It reproduces a natural life-threatening situation that makes rats react with an intense fear response (criterion 1 in DSM-IV). Rodents display behavioral symptoms of extreme avoidance in the EPM (criterion 3), arousal, exaggerated startle response (criterion 4), and the symptoms persist, relative to the rat's life-span, for a long time.

Analysis of brain activation through *c-fos* immunoreactivity after predatory threat revealed activation of the medial amygdala, ventromedial and dorsomedial hypothalamus, periaqueductal gray, premammillary nucleus, BNST, and cuneiform nucleus (Dielenberg and McGregor, 2001; Dielenberg et al., 2001; Takahashi et al., 2005). However, these studies examined brain activation immediately after predator exposure and do not provide information about the regions involved in sustaining the persistent anxiety. Putatively, the aforementioned results reflect the activation of brain areas involved in innate defensive responses. In contrast, electrophysiological studies have examined plasticity in relevant pathways a week or more after predator stress. Specifically, projections from the CeA to the lateral column of the PAG show a long-lasting potentiation. Similar results were obtained in the hippocampo-amygdala pathway via the ventral angular bundle (Adamec et al., 2001, 2003, 2005). Induction of plasticity in these pathways is dependent on NMDA receptor activation as

systemic administration of NMDA receptor antagonists 30 min prior predator threat prevents the long-lasting behavioral changes in the rats (Blundell et al., 2005).

Importantly, most of prior electrophysiological studies fail to take into account individual differences. Their experimental design considers only comparisons between the presence versus the absence of predator threat.

### **1.7. Objectives of this thesis**

In the previous section, I introduced the reader to the concepts of fear and anxiety and reviewed evidence that these two states mostly depend on the amygdala and BNST, respectively. The current definition is that fear is evoked to discrete cues signaling imminent danger. In contrast, anxiety is produced by more diffuse, unpredictable threats. The CeA and BNST are two candidate structures to regulate these two behavioral states. After reviewing BNST-A anatomical organization and pattern of connectivity, I argued that the BNST-A is a brain structure strategically positioned to integrate inputs from limbic forebrain regions and influence the output of autonomic and neuroendocrine effectors involved in long lasting anxiety responses. However, previous research on the functional organization of BNST-A considered BNST-A a homogeneous brain structure. My aim is to advance our knowledge on the role of BNST-A in anxiety disorders, by studying the electroresponsive properties of neurons in different BNST-A regions (Chapter III), and understanding how different BNST-A subregions are interconnected (Chapter IV). Finally, through the use of a well

characterized animal model of PTSD, I aim to investigate the long-lasting alterations associated to trauma exposure in BNST-A neurons (Chapter V).

## **CHAPTER II**

### **General Methods**

## 2.1. *In vitro* techniques

This chapter describes the general methods used in most experiments. Additional details on methods and techniques are included in the relevant data chapters.

Experiments were performed in accordance with the National Institutes of Health *Guide for the Care and Use of Laboratory Animals* and with the approval of the Institutional Animal Care and Use Committee of Rutgers University (Newark, NJ). We used adult (60-90 days) male Lewis rats (Charles River Laboratories, New Field, NJ) maintained on a 12 h light/dark cycle. The animals were housed three per cage with *ad libitum* access to food and water. Prior to the experiments, they were habituated to the animal facility and handling for one week.

### 2.1.1. Slice preparation

The rats were anesthetized with avertin (300 mg/kg, i.p.), followed by isoflurane. After abolition of all reflexes, they were perfused through the heart with a cold (4°C) modified artificial cerebrospinal fluid (aCSF) that contained (in mM): 248 sucrose, 2.5 KCl, 7 MgCl<sub>2</sub>, 23 NaHCO<sub>3</sub>, 1.2 NaH<sub>2</sub>PO<sub>4</sub>, 7 glucose. Their brains were then extracted and cut in 300 µm-thick coronal slices with a vibrating microtome while submerged in the same solution as above. After cutting, slices were transferred to an incubating chamber where they were allowed to recover for at least one hour at room temperature in a control aCSF with the following composition (in mM) 124 NaCl, 2.5 KCl, 1.25 NaH<sub>2</sub>PO<sub>4</sub>, 26 NaHCO<sub>3</sub>, 1 MgCl<sub>2</sub>,

2 CaCl<sub>2</sub>, 10 glucose. (pH 7.2, 300 mOsm). The temperature of the chamber was kept at 34°C for at least 20 min and then returned to room temperature. Slices were then transferred to a recording chamber perfused with oxygenated aCSF at 32°C (7 ml/min).

### 2.1.2. Electrophysiological recordings

Under visual guidance with differential interference contrast and infrared video-microscopy, we obtained whole-cell patch recordings of BNST neurons using pipettes (7-10 MΩ) pulled from borosilicate glass capillaries and filled with a solution containing (in mM): 130 K-gluconate, 10 N-2-hydroxyethylpiperazine-N'-2-ethanesulfonic acid, 10 KCl, 2 MgCl<sub>2</sub>, 2 ATP-Mg, and 0.2 GTP-tris(hydroxymethyl)aminomethane (pH 7.2, 280 mOsm). The liquid junction potential was 10 mV with this solution and the membrane potential was corrected accordingly. Current-clamp recordings were obtained with an Axoclamp 2B amplifier and digitized at 10 kHz with a Digidata 1200 interface (Axon Instruments, Foster City, CA).

To characterize the electroresponsive properties of recorded cells, graded series of depolarizing and hyperpolarizing current pulses (0.01 nA, 500 ms in duration) were applied from rest and other pre-pulse potentials, as pre-hyperpolarization of different magnitudes can greatly affect spike latency due to the interaction between A-Type and T-Type currents (Molineux et al., 2005). The input resistance ( $R_{in}$ ) of the cells was estimated in the linear portion of current-voltage plots.

To study the morphological properties of recorded neurons, 0.5% biocytin was added to the pipette solution in a subset of experiments. No special current injection protocol had to be used to label BNST cells with biocytin. It diffused into the cells as we studied their electroresponsive properties. At the conclusion of the recordings, the slices were removed from the chamber and fixed for 1 to 3 days in 0.1 M phosphate buffer saline (pH 7.4) containing 4% paraformaldehyde.

For the extracellular stimulation protocols, pairs of tungsten stimulating electrodes (inter-tip spacing of 100 $\mu$ m) were placed between 250 – 300 $\mu$ m dorsal to the recording site. Postsynaptic responses were investigated by stimulating fibers of passage with current pulses of 0.1 ms duration and intensities ranging between 0.1 - 0.8 mA in 0.1 mA increments. Reversal potentials were determined by evoking synaptic responses from different membrane potentials and plotting response amplitudes as a function of the membrane potential. The excitatory postsynaptic potentials (EPSPs) and the inhibitory postsynaptic potentials (IPSPs) were isolated by adding picrotoxin (100  $\mu$ M) or 6-cyano -7-nitroquinoxaline-2,3-dione (CNQX; 25  $\mu$ M) to the aCSF.

### 2.1.3. Data analysis

The evoked activity of all neurons was acquired through pClamp, digitized, and stored on a computer. The electrophysiological data was analyzed off-line using Clampfit 9.2 (Molecular Devices, Sunnyvale, CA), IGOR (Wavemetrics, Oregon), Stimfit (<http://www.stimfit.org/>) and custom written software using Numpy and Scipy (<http://www.scipy.org>). Additionally, a digital image of the

anatomical configuration of each recording was captured through a camera attached to the microscope and stored in the computer.

## **2.2. Histological techniques**

### 2.2.1. Biocytin revelation for morphological identification

At the conclusion of the recordings, the slices were removed from the chamber and fixed for 1 to 3 days in 0.1 M phosphate buffer saline (pH 7.4) containing 4% paraformaldehyde. Slices were then embedded in agar (3%) and sectioned on a vibrating microtome at a thickness of 100  $\mu\text{m}$ . Sections were washed several times in phosphate buffer (PB, 0.1 M, pH 7.4) and then transferred to a  $\text{H}_2\text{O}_2$  solution (0.5%) in PB for 15 min. After numerous washes in PB, sections were incubated for 12 h at 20°C in a solution containing 0.5% triton, 1% solutions A and B of an ABC kit (Vector, Burlingame, CA) in PB. The next day, they were washed in PB (5 x 10 min). Biocytin was visualized by incubating the sections in a 0.1 M PB solution that contained diaminobenzidine tetrahydrochloride (0.05%, Sigma), 2.5 mM nickel ammonium sulfate (Fisher) and  $\text{H}_2\text{O}_2$  (0.003%) for 5-10 min. Then, the sections were washed in PB (5 X 10 min), mounted on gelatin-coated slides, and air-dried. The sections were then counterstained with cresyl violet and coverslipped with permount for later reconstruction.

All visible processes of the labeled neurons were observed in a microscope using a 40X objective and photographed. Typically, their processes extended over several sections. To align the sections, we layered the

photographs in Photoshop (Adobe Systems Incorporated, CA) and used blood vessels or other obvious landmarks present in the various sections to align them. The layers were then collapsed and the entire neuron drawn.

### **2.3. Nomenclature used to designate different BNST subregions**

Individual BNST subnuclei cannot be identified with precision in unstained, living slices. Therefore, we subdivided BNST-A in three regions, based on the position of major fiber bundles that can be easily identified in trans-illuminated slices: the anterior commissure, dividing the BNST-A in dorsal and ventral (BNST-AV) sectors, and the intra-BNST component of the stria terminalis, subdividing the dorsal portion in medial (BNST-AM) and lateral (BNST-AL) regions. The correspondence between our subdivisions of the BNST-A and the subnuclei identified by Swanson and colleagues (Ju and Swanson 1989; Ju et al., 1989) is as follows. BNST-AV corresponds to Swanson's anteroventral, fusiform, parastrial, and dorsomedial subnuclei plus his subcommisural zone. BNST-AL corresponds to Swanson's oval, juxtacapsular, and anterolateral subnuclei. BNST-AM corresponds to Swanson's anterodorsal subnucleus. However, note that in more recent publications (Dong and Sawnsen 2006a), Swanson also termed the latter region BNST-AM.

### **2.4. Behavioral paradigm**

#### **2.4.1. Predator threat**

In order to simulate the type of life-and-death situation known to

precipitate PTSD in humans, rats were exposed to predator threat by placing them in a plastic cage containing soiled cat litter (48-h use period, sifted for stool) for 10 min and then returned to their home cage. Previous studies in our laboratory showed that soiled cat litter is efficient at inducing long-lasting manifestations of anxiety in a proportion of susceptible rats, presumably because it constitutes a compound olfactory stimulus that includes odors of cat skin/hair, urine, and feces (Goswami et al., 2010, 2012).

#### 2.4.2. Elevated plus maze

In order to distinguish Resilient vs. PTSD-like rats, one week after predatory threat, we examined their exploratory behavior in the EPM, a well established behavioral assay of anxiety in rodents (Pellow et al., 1985; Pellow and File, 1986). The EPM is a cross-shaped maze with two open arms (no walls and a white floor) and two closed arms (black floor and black walls 0.3 m high). The rationale is that anxious rats tend to avoid the open arms due to their innate aversion to open spaces, where the risk of predation is higher. Behavior in the EPM was recorded by a video camcorder and scored off-line by an observer who was blind to the electrophysiological data. Animals were tested in the EPM under red light illumination for 5 min. The trial started by placing the rat in the center of the EPM facing an open arm.

#### 2.4.3. Behavioral cut-off criteria

A cut-off behavioral criterion was used to classify rats into two distinct

behavioral phenotypes. Rats with extremely compromised exploratory behavior in the EPM, spending zero time in the open arms, were categorized as PTSD-like, while rats that spent some time in the open arms were classified as Resilient. The present cut-off criterion is consistent with previous reports (Cohen et al., 2006a; Goswami et al., 2010; 2012).

## **CHAPTER III**

### **Contrasting Distribution of Physiological Cell Types in Different Regions of the Bed Nucleus of the Stria Terminalis**

### 3.1. Rationale

The electroresponsive properties of neurons shape their spontaneous activity and synaptic responses, which in turn may give rise to distinctive neuronal discharge patterns (Llinás, 1988). Consequently, knowing the electroresponsive properties of different neuronal groups can become a tool to identify neurons recorded extracellularly in behaving animals. Therefore, a fundamental step toward understanding BNST is to study the physiological properties of BNST neurons.

So far, the best-characterized BNST neurons are those located in its anterolateral portion (BNST-AL). Rainnie and colleagues reported that there are three main cell types in the dorsal part of BNST-AL (Hammack et al., 2007). When depolarized, the two main types displayed a regular spiking (Type-I) or low-threshold bursting (Type-II) phenotype and both exhibited time-dependent inward rectification in the hyperpolarizing direction. A less common cell type (Type-III) lacked the latter property, instead displaying fast inward rectification in response to hyperpolarization and a regular firing pattern when depolarized. Importantly, this tripartite classification was validated using single-cell RT-PCR, revealing that the three cell types express mRNA transcripts for distinct complements of voltage-gated channels (Hazra et al., 2011) and serotonergic receptors (Hazra et al., 2012).

At present, it is unclear whether similar types of neurons are present in other sectors of BNST. Although there is much disagreement regarding the number and boundaries of BNST nuclei (De Olmos et al., 1985; Ju and Swanson

1989; Moga et al., 1989), it is clear that different BNST regions form contrasting connections. In the anterior portion of BNST (BNST-A) for instance, BNST-AL neurons contribute most BNST outputs to brainstem structures regulating fear expression (Sofroniew et al., 1983; Holstege et al., 1985; Sun and Cassell 1993). In contrast, neurons projecting to the PVN are concentrated in its ventral and medial portions (Prewitt and Herman 1998; Dong et al., 2001b; Dong and Swanson 2006a). Therefore, the experiments in this chapter aimed to characterize the electroresponsive properties of neurons in different BNST-A regions and to determine whether distinct physiological cell types exhibit contrasting morphological properties.

### **3.2. Brief overview of methods**

We studied the electroresponsive properties of neurons in different parts of the BNST-A using visually guided patch recordings in coronal slices kept in vitro (see section 2.1.1; Fig. 3.1). After 1 hr incubation, slices were then transferred one at the time to the recording chamber and perfused with oxygenated aCSF. Current-clamp recordings were obtained under visual guidance from BNST-AL, AM, and AV.

To study the morphological properties of recorded neurons, 0.5% biocytin was added to the pipette intracellular solution in a subset of experiments. Section 2.2.1 describes the histological procedures for biocytin revelation.

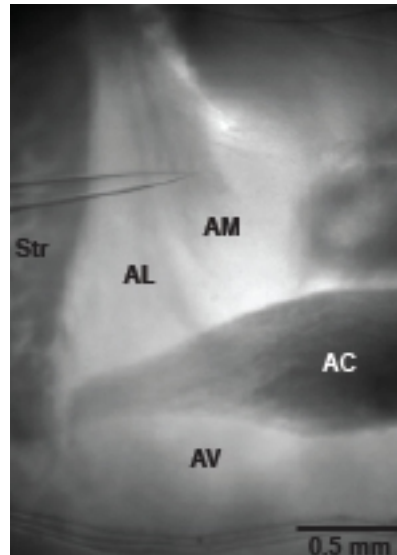


**Figure 3.1.** Anatomical subdivisions and recording configuration. A transilluminated slice as it appeared during our experiments. Abbreviations: AC, anterior commissure; AL, anterolateral; AM, anteromedial; AV, anteroventral; Str, striatum.

### 3.3. Results

We obtained stable recordings from 127 BNST-AL, 87 BNST-AM, and 83 BNST-AV neurons, some of which were morphologically identified with biocytin (n=60). The three cell types observed in BNST-AL by Rainnie and colleagues were also present in BNST-AM and AV, together accounting for >90% of neurons in these regions. However, there were significant regional variations in their electroresponsive properties. In addition, we encountered two previously unknown cell types. Below, we first describe the electroresponsive properties of these various types of neurons (Tables 3.1-3.4) and then consider their morphology (Table 3.5).

Table 3.1 *Physiological Properties of BNST-A neurons by cell type (values are means  $\pm$  SEM)*

Cell Type	n	(%)	Rest (mV)	Rin (M $\Omega$ )	Time Constant (ms)	Action Potential		
						Threshold (mV)	Amplitude (mV)	Duration (ms)
RS (type-1)	74	24.9	-70.6 $\pm$ 0.8	722 $\pm$ 45.6	31.5 $\pm$ 2.6	-40.8 $\pm$ 0.8	71.7 $\pm$ 1.4	1.22 $\pm$ 0.35
LTB (type-2)	162	54.5	-68.7 $\pm$ 0.6	686.4 $\pm$ 23.2	30.4 $\pm$ 1.2	-40.6 $\pm$ 0.5	71 $\pm$ 0.9	1.28 $\pm$ 0.02
fIR (type-3)	49	16.5	-76.9 $\pm$ 1.7	546.7 $\pm$ 27.8	38.6 $\pm$ 2.7	-40.1 $\pm$ 0.8	74.3 $\pm$ 1.5	1.32 $\pm$ 0.05
LF	5	1.7	-85.8 $\pm$ 1.5	452 $\pm$ 33.5	23.3 $\pm$ 1.8	-40.4 $\pm$ 1.9	71.9 $\pm$ 2.9	1.37 $\pm$ 0.13
SA	7	2.3	-63 $\pm$ 2.8	622.6 $\pm$ 122.5	48.4 $\pm$ 7.5	-45.3 $\pm$ 1.8	62.9 $\pm$ 3.7	0.77 $\pm$ 0.05

### 3.3.1. Regular spiking (RS) cells (Type-I)

A major cell type observed in all three BNST-A regions displayed a regular spiking (RS) phenotype (Fig. 3.2A-B; see Table 3.1 for passive properties and spike characteristics). They correspond to the Type-I cells of Rainnie and colleagues (Hammack et al., 2007). The incidence of RS cells did not vary significantly depending on the BNST-A region ( $\chi^2 = 0.44$ ,  $p = 0.8$ ; range 23-27% of the cells). In response to depolarizing current pulses, these neurons generated spike trains that displayed frequency adaptation (Fig. 3.2A-B, top). In response to hyperpolarization, most displayed time- and voltage-dependent inward rectification (Fig. 3.2A, bottom; Fig. 3.2C2 and C3). This phenomenon manifested itself by a depolarizing sag in the voltage response to negative current pulses (Fig. 3.2A, dashed line in lowest trace). In light of prior observations in BNST-AL (Hammack et al., 2007; Hazra et al., 2011) and other brain regions (Pape 1996),

this sag is likely due to the expression of the hyperpolarization-activated mixed cationic current  $I_H$ . Sag amplitude was generally higher in RS neurons of BNST-AL than AM or AV. Indeed, the proportion of RS cells with sag amplitudes  $> 2$  mV in the same testing conditions ( $-0.06$  nA current from  $-65$  mV) showed significant regional variations (Fig. 3.2C3;  $\chi^2 = 13.1$ ,  $p < 0.0014$ ). As depicted in the examples of figure 3.2 and discussed further below, the RS phenotype coincided with marked variations in other properties such as  $R_{in}$ , amplitude/shape of spike afterhyperpolarizations, and sag amplitude, with no preferential associations between them.

Table 3.2 *Physiological Properties of RS (Type-1) neurons by region* (values are means  $\pm$  SEM)

Region	n	Rest (mV)	$R_{in}$ (M $\Omega$ )	Time Constant (ms)	Action Potential		
					Threshold (mV)	Amplitude (mV)	Duration (ms)
BNST-AL	34	$-70.4 \pm 1$	$554.9 \pm 51.8$	$27.7 \pm 4.8$	$-42.3 \pm 1$	$73.4 \pm 2$	$1.3 \pm 0.04$
BNST-AM	21	$-70.7 \pm 2$	$876.9 \pm 102.3$	$34.6 \pm 3.9$	$-41.6 \pm 1.4$	$67.9 \pm 2.6$	$1.27 \pm 0.06$
BNST-AV	19	$-71.1 \pm 1.8$	$850.1 \pm 77.9$	$35 \pm 3$	$-37.1 \pm 1.5$	$67.5 \pm 3.7$	$1.01 \pm 0.06$

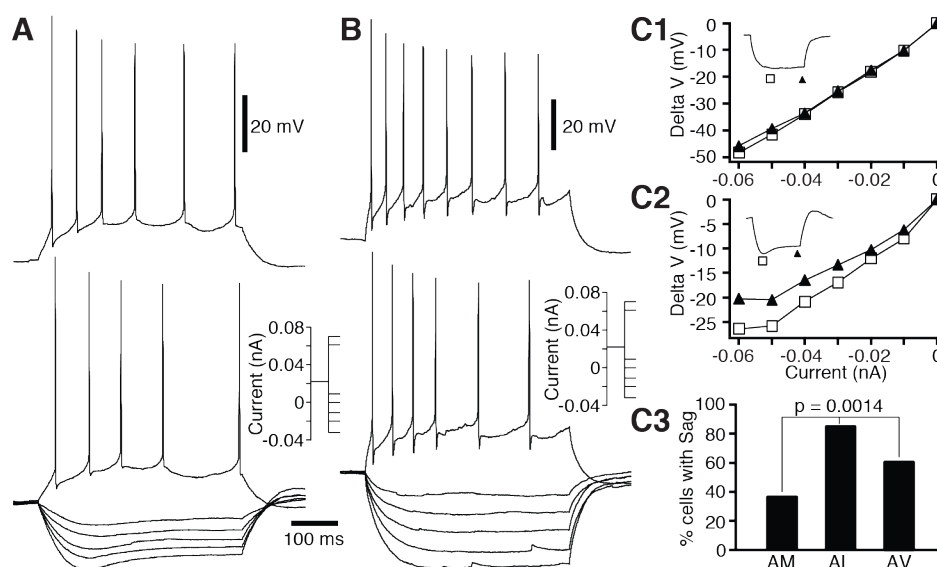


**Figure 3.2.** Regular spiking (RS; Type-I) BNST-A neurons. **(A-B)** Voltage responses of two different RS neurons (recorded in BNST-AL and AV, respectively) to gradually increasing pulses of positive or negative current applied from  $-65$  mV. Note that the top traces in panels A and B were offset graphically for clarity; the pre-pulse potential was  $-65$  mV, as for the traces just below. **(C1-2)** Amplitude of voltage responses (y-axis) to negative current pulses (x-axis) for cells shown in C and B, respectively. Voltage responses were measured at the beginning and end of the current pulses (symbols in insets). **(C3)** Percent RS cells (y-axis) with depolarizing sag  $> 2$  mV ( $-0.06$  nA current from  $-65$  mV) in the three BNST-A regions (x-axis).

### 3.3.2. Low-threshold bursting (LTB) cells (Type-II)

A second major cell type observed in the three BNST-A regions were neurons generating spike doublets or bursts at the onset of depolarizing pulses applied from membrane potentials negative to  $-70$  mV (Fig. 3.3A2, B2), but single spikes from more depolarized levels (Fig. 3.3A1, B1). At the end of hyperpolarizing current pulses applied from membrane potentials positive to  $-70$  mV, these low-threshold bursting (LTB) neurons generated spike bursts (Fig. 3.3A1) or doublets (Fig. 3.3B1) similar to those seen at the onset of depolarizing current pulses applied from membrane potentials negative to  $-70$  mV. These cells correspond to the Type-II neurons of Rainnie and colleagues (Hammack et al., 2007). The spikes bursts or doublets generated by LTB cells rode on a slower

depolarizing potential (arrows in Fig. 3.3A-B), hereafter termed low-threshold spike, which outlasted the rebound firing. On average, from a membrane potential of  $-80$  mV and with a current injection of  $0.04$  nA, these low-threshold spikes were  $12.4 \pm 0.5$  mV in amplitude and  $156.2 \pm 8.0$  ms in duration. Given prior findings in BNST-AL (Hammack et al., 2007; Hazra et al., 2011) and other brain regions (Huguenard 1996), these properties likely reflect the expression of a low-threshold  $\text{Ca}^{2+}$  conductance ( $I_T$ ).

Not only did the incidence of LTB cells vary significantly depending on the BNST-A region (Fig. 3.3C1;  $\chi^2 = 48.1$ ,  $p < 0.0001$ ), so did the number of spikes per rebound burst (Fig. 3.3C2, ANOVA,  $F = 4.84$ ,  $p = 0.009$ ) and the peak instantaneous firing rate reached during these bursts (Fig. 3.3C3, ANOVA,  $F = 4.42$ ,  $p = 0.01$ ). Bonferroni corrected post-hoc t-tests revealed that the latter two variables were significantly lower amongst BNST-AL than BNST-AV neurons ( $p$ 's  $\leq 0.012$ ). A similar trend was seen in AL to AM comparisons ( $p$ 's  $\leq 0.08$ ) and no differences were found between AM and AV neurons. As was seen in RS neurons, sag amplitude was generally higher in LTB neurons of BNST-AL than AM or AV. Figure 3.3C4 depicts the proportion of LTB cells with sag amplitudes  $> 2$  mV ( $-0.06$  nA current from  $-65$  mV) in the three regions.

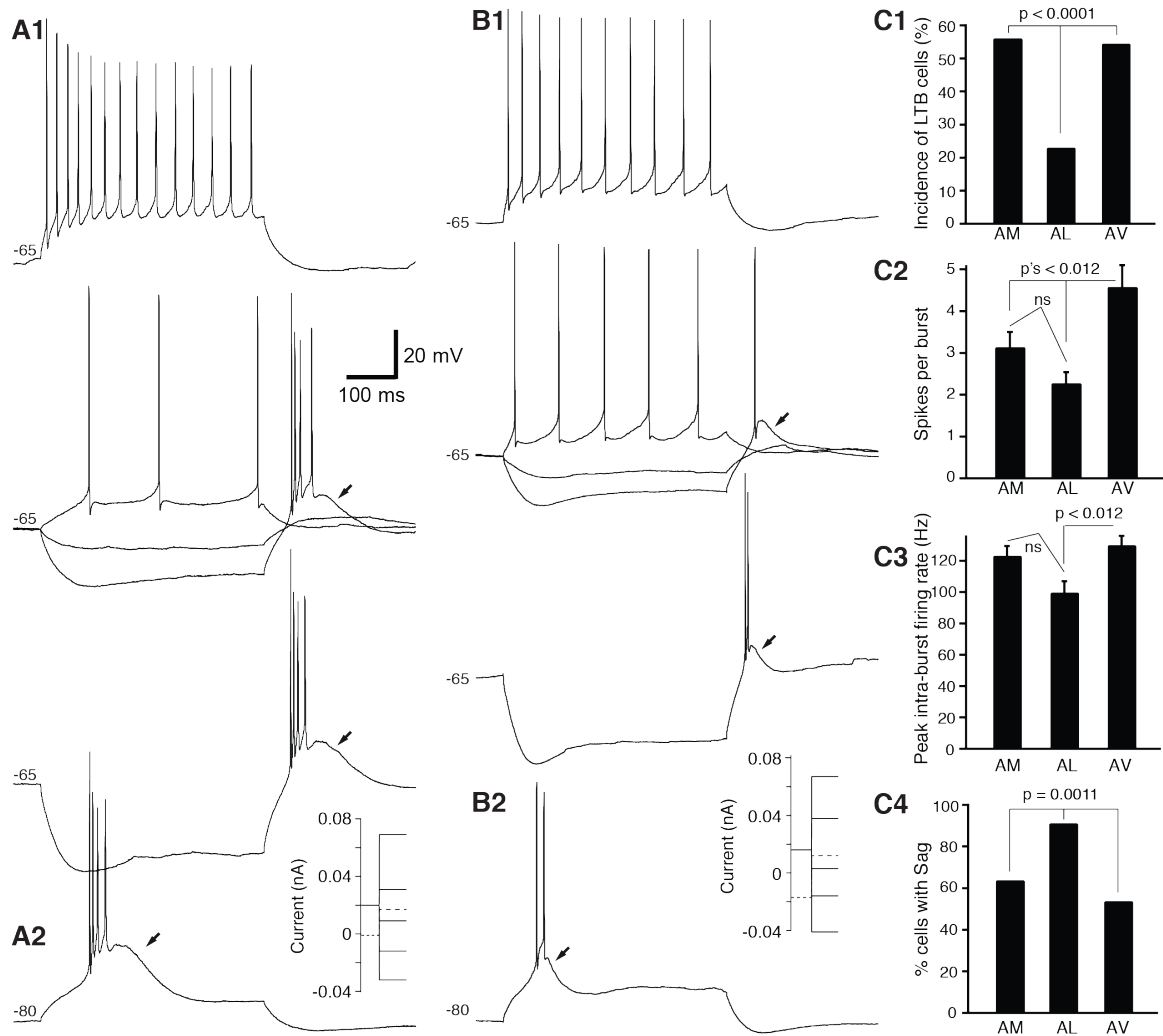


**Figure 3.3.** Low-threshold bursting (LTB; Type-II) BNST-A neurons. **(A-B)** Voltage responses of two different LTB neurons (recorded in BNST-AM and AL, respectively) to gradually increasing pulses of positive or negative current applied from -65 mV (**A1**, **B1**) or -80 mV (**A2**, **B2**). Arrows in A and B point to low-threshold spikes. Note that the top traces in panels A1 and B1 were offset graphically for clarity; the pre-pulse potential was -65 mV, as for the traces just below. **(C)** Graphs plotting the incidence of LTB cells (**C1**), the number of spikes per burst (**C2**), the peak instantaneous intra-burst spike frequency (**C3**), and the proportion of LTB cells with depolarizing sag > 2 mV (-0.06 nA current from -65 mV) (**C4**) in the three BNST regions.

In the three BNST-A regions, we also observed neurons identical in most respects to LTB cells with the exception that they did not generate spike bursts, yet did exhibit rebound firing (Fig. 3.4). As in LTB cells, rebound action potentials rode on a slower depolarizing potential (Fig. 3.4A, arrow), similar to the low-

threshold spikes discussed above. Moreover, in response to juxta-threshold depolarizing current pulses applied from negative to -70 mV, the same cells generated single action potentials that also rode on a conspicuous slow depolarization (Fig. 3.4B, arrow; 0.04 nA from a membrane potential of -80 mV,  $10.8 \pm 0.7$  mV and  $164.0 \pm 10.4$  ms). Consequently, for the remainder of this study, cells exhibiting these properties are pooled with LTB neurons.

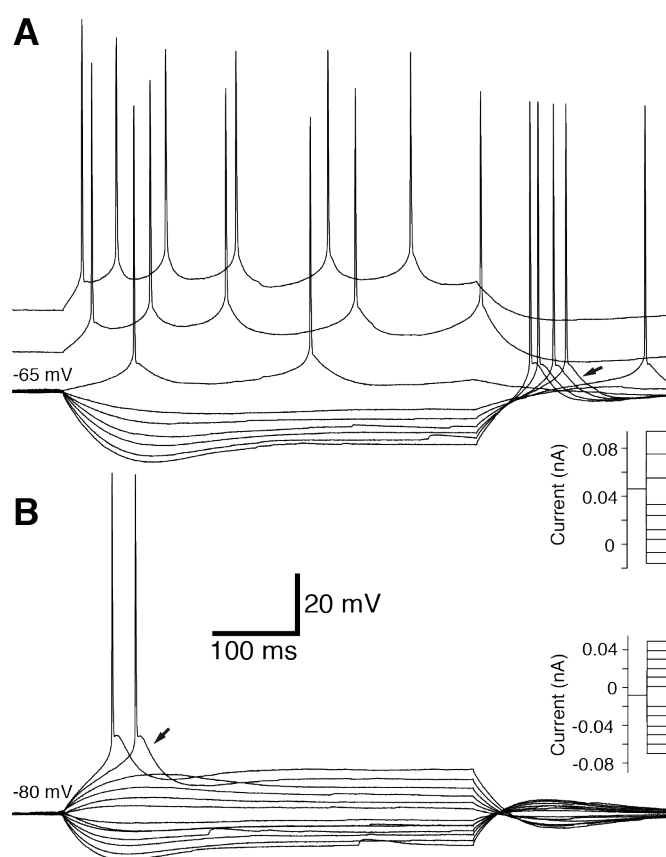


**Figure 3.4.** Cells generating rebound single spikes. Voltage responses of a BNST-AL neuron to gradually increasing pulses of positive or negative current applied from -65 mV (**A**) or -80 mV (**B**). Note that the top two traces in panel A were offset graphically for clarity; the pre-pulse potential was -65 mV, as for the traces just below.

Table 3.3 *Physiological Properties of LTB (Type-2) neurons by region (values are means  $\pm$  SEM)*

Region	n	Rest (mV)	R <sub>in</sub> (M $\Omega$ )	Time Constant (ms)	Action Potential		
					Threshold (mV)	Amplitude (mV)	Duration (ms)
BNST-AL	51	-67.8 $\pm$ 1	567.3 $\pm$ 31.1	29.4 $\pm$ 1.6	-41.8 $\pm$ 0.9	70.9 $\pm$ 1.7	1.33 $\pm$ 0.05
BNST-AM	59	-67.7 $\pm$ 1	690.5 $\pm$ 40.9	31.6 $\pm$ 1.9	-40.8 $\pm$ 0.7	71.2 $\pm$ 1.5	1.38 $\pm$ 0.05
BNST-AV	52	-70.7 $\pm$ 1	803.2 $\pm$ 41.1	34.2 $\pm$ 2.4	-39.3 $\pm$ 0.8	68.2 $\pm$ 1.6	1.12 $\pm$ 0.04

Table 3.4 *Physiological Properties of BNST-A neurons by region (values are means  $\pm$  SEM)*

Region	n	Rest (mV)	R <sub>in</sub> (M $\Omega$ )	Time Constant (ms)	Action Potential		
					Threshold (mV)	Amplitude (mV)	Duration (ms)
BNST-AL	127	-72.6 $\pm$ 0.8	539.1 $\pm$ 19.5	29.5 $\pm$ 1.7	-41.3 $\pm$ 0.5	73.3 $\pm$ 0.9	1.31 $\pm$ 0.02
BNST-AM	87	-69.1 $\pm$ 0.9	729 $\pm$ 38.6	32.7 $\pm$ 1.6	-41.1 $\pm$ 0.6	71.4 $\pm$ 1.2	1.37 $\pm$ 0.03
BNST-AV	83	-69.5 $\pm$ 0.9	799 $\pm$ 34.1	36.7 $\pm$ 1.9	-39.3 $\pm$ 0.7	68.9 $\pm$ 1.4	1.06 $\pm$ 0.03

### 3.3.3. Rare cell types

Together, LTB and RS cells accounted for nearly 80% of BNST-A neurons. However, three other cell types were also encountered, albeit less frequently. We describe them in turn below. The first one corresponds to the *Type-III cells* of Rainnie and colleagues (Fig. 3.5A; Hammack et al. 2007). Like RS cells, these neurons exhibited spike frequency adaptation during prolonged depolarizations (Fig 3.5A, top). However, unlike RS cells, they displayed **fast inward rectification** in response to hyperpolarizing current pulses (Fig. 3.5A, inset), hence the

acronym fIR. The incidence of fIR neurons varied significantly depending on the BNST-A region (AL, 29%; AM, 8%; AV, 6%;  $\chi^2 = 17.1$ ,  $p < 0.0002$ ).

Another, even less frequent type of cells were *late-firing neurons* (LF; Fig. 3.5B), observed only in BNST-AL (4% of cells). In response to supra-threshold depolarizations, LF neurons displayed a conspicuous delay to firing that was especially pronounced when the current injection was performed from negative to -75 mV (compare Fig. 3.5B1 and B2 from -65 and -80 mV, respectively). Also characteristic of LF cells was a marked change in the rising phase of voltage responses to depolarizing current pulses as the stimulus intensity was increased (Fig. 3.5B2, inset). In light of prior findings, this behavior likely reflects the expression of a slowly inactivating potassium current ( $I_D$ ; Storm 1988). LF cells had the most negative resting potential and lowest  $R_{in}$  of all the cell types identified in this study (see Table 3.1).

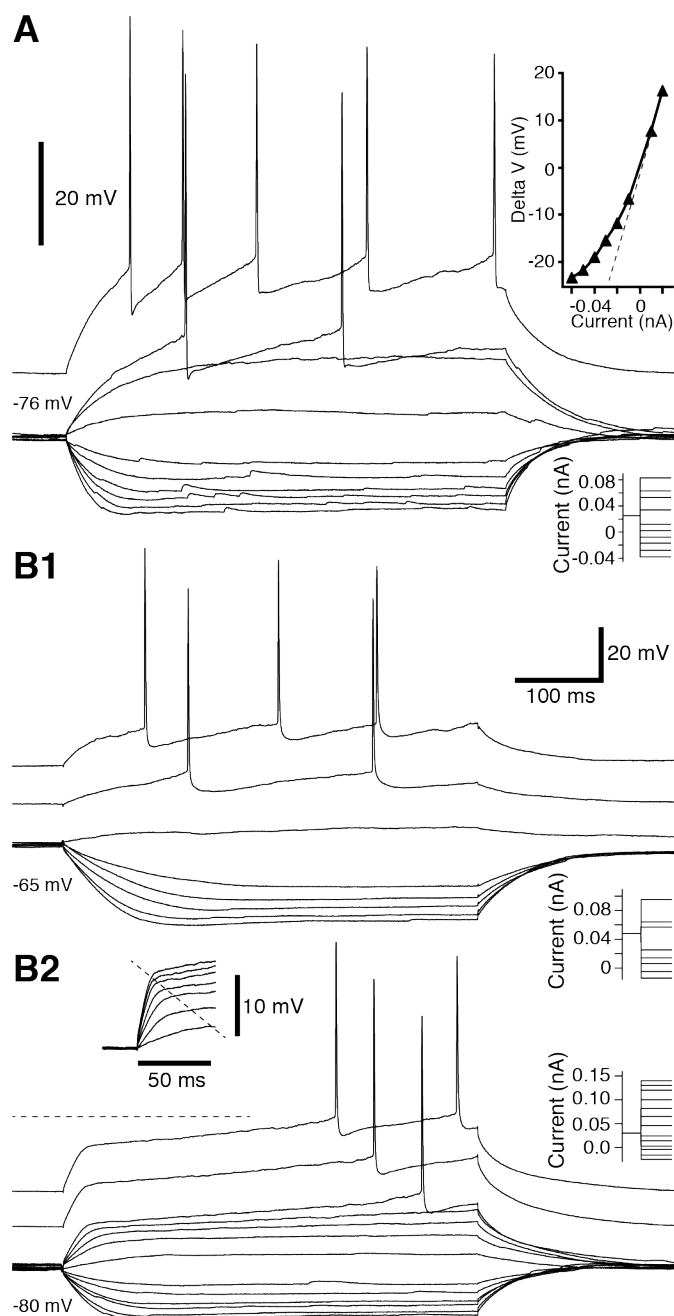


**Figure 3.5.** Type-III (flR; **A**) and late-firing (LF; **B**) neurons recorded in BNST-AM and AL, respectively. Voltage responses to gradually increasing pulses of positive or negative current applied from -76 mV (**A**), -65 mV (**B1**) or -80 mV (**B2**). Inset in **A** plots amplitude of voltage response to current pulses (y-axis) as a function of current (x-axis). Inset in **B2** shows expanded view of initial voltage response to current injection. Note that the top trace in panel A was offset graphically for clarity; the pre-pulse potential was -76 mV, as for the traces just below. In B1 and B2, the top two traces were also offset graphically for clarity; the pre-pulse potentials were -65 mV and -80 mV, respectively, as for the traces just below.

Finally, a small subset of cells stood out because of its highly regular spontaneous activity at rest (hence the designation *SA neurons*; Fig. 3.6A). Spontaneous firing rates averaged  $4.2 \pm 1.1$  Hz in whole cell mode at rest ( $n = 7$ ). It is unlikely that these spontaneous discharges were due to injury because they could be seen in cell-attached mode, albeit at a higher frequency ( $7.3 \pm 1.5$  Hz;  $n = 4$ ). Also inconsistent with the injury hypothesis, SA cells were only encountered in BNST-AV, where they accounted for 8% of the cells. Moreover, action potential duration was markedly lower in SA neurons ( $0.78 \pm 0.05$  ms) than in all other BNST-A cell types (Table 3.1). When depolarized, SA neurons displayed no evidence of spike frequency adaptation (as seen in RS, LTB, and fIR neurons) or acceleration (as seen in LF cells). Instead, they maintained a stable firing rate that increased with the amount of depolarization until challenged by strong currents, in which case spiking started to fail (Fig. 3.6B-C, top traces and arrows). SA cells did not display evidence of  $I_H$  or  $I_T$  (Fig. 3.6B-C).

To summarize the above (Fig. 3.7A), RS and LTB neurons were predominant in the three BNST-A regions, together accounting for 66.9-91.9% of the cells. In addition, 29% of BNST-AL cells were fIR neurons compared to  $\leq 8\%$  of the cells in BNST-AV and AM. Finally, the last two cell types (LF and SA neurons) were rare and only encountered in one of the three regions: SA neurons in BNST-AV and LF cells in BNST-AL. The distribution of these various cell types in the three regions is illustrated in Figure 3.7B. RS and LTB cells were homogeneously intermingled in BNST-AM and AL, including its oval nucleus.

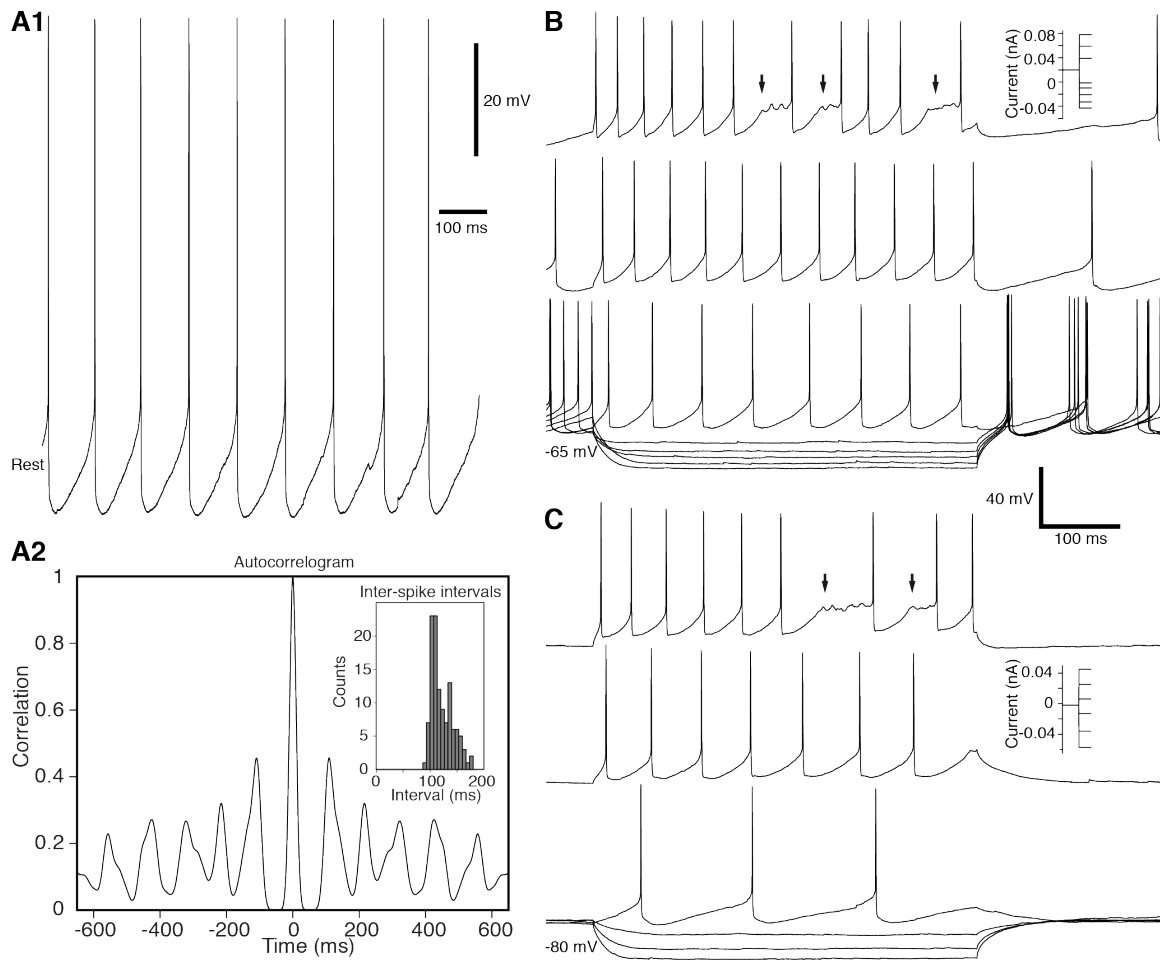


**Figure 3.6.** Spontaneously active (SA) neuron recorded in BNST-AV. **(A1)** Spontaneous firing at rest. **(A2)** Autocorrelogram of spontaneous activity (inset shows corresponding distribution of interspike intervals). **(B-C)** Voltage responses to gradually increasing pulses of positive or negative current applied from  $-65$  mV **(B)**, or  $-80$  mV **(C)**. In B and C, the top two traces were also offset graphically for clarity; the pre-pulse potentials were  $-65$  mV and  $-80$  mV, respectively, as for the traces just below. Arrows in **B** and **C** point to periods of depolarization when spiking started to fail.

In contrast, in BNST-AV, RS cells were more concentrated ventrally. Unexpectedly, fIR neurons were concentrated along the internal capsule, in a region corresponding to the juxtacapsular subregion of BNST-AL, although it cannot be ruled out that this concentration overlapped with the oval nucleus. In BNST-AL, outside the juxtacapsular/oval subregions, only one fIR cell was encountered. This is in contrast with BNST-AV and AM where a uniform, albeit

low concentration of fIR cells was encountered.

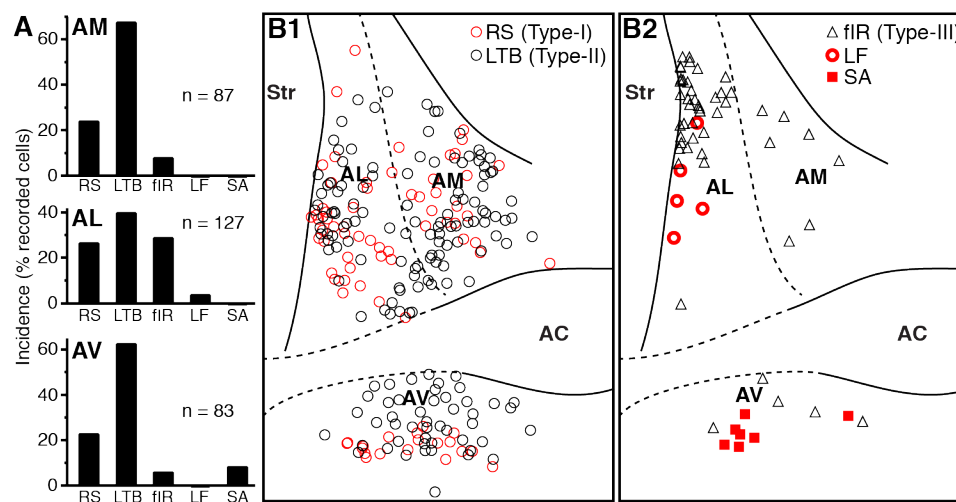


**Figure 3.7.** Incidence (**A**) and spatial distribution (**B**) of the various physiological cell types in different sectors of BNST-A. (**A**) Incidence: AM, top; AL, middle; AV, bottom. (**B1**) Distribution of RS (Type-I; red circles) and LTB (Type-II; black circles) neurons. (**B2**) Distribution of fIR (Type-III; black triangles), LF (thick red circles), and SA (red squares) neurons.

### 3.3.4. Passive properties and spike characteristics in different BNST-A regions

Although the above indicates that, for the most part, the three BNST-A regions are characterized by a similar complement of cell types, it remains possible that they differ in other ways such as passive properties or spike characteristics. Unfortunately, most of these variables did not meet the requirements of parametric ANOVAs (variance homogeneity and normality of distributions). Thus, to address this question, we computed Kruskal-Wallis one-way ANOVAs and corrected the significance level for the number of comparisons (Bonferroni). To minimize the number of comparisons and avoid stringent significance levels, when two variables were correlated (e.g.  $R_{in}$  and time constant or spike duration and amplitude), we considered only one of them.

We first compared resting potential ( $V_r$ ),  $R_{in}$ , and spike duration (at half amplitude) of neurons in the three regions (all classes combined; Table 3.4). A significant region effect was observed for  $R_{in}$  ( $H=48.8$ ,  $p<0.001$ ) and spike duration ( $H=37.2$ ,  $p<0.001$ ). Post-hoc Mann-Whitney tests corrected for multiple comparisons revealed that  $R_{in}$  was significantly lower in BNST-AL than AV and AM neurons ( $p$ 's  $<0.001$ ) with no difference between the latter two regions. Also, spike durations were significantly lower in BNST-AV compared to the other two regions ( $p<0.001$ ) with no difference between AM and AL.

Since these results could be due to the differing incidence of the various cell types in the three regions, we then repeated these analyses, but separately for the two most frequent cell types (RS, Table 3.2; LTB, Table 3.3). Again, we obtained a significant effect of region on  $R_{in}$  and spike duration for RS ( $R_{in}$ ,  $H=15.6$ ,  $p=0.0007$ ; spike duration,  $H=9.8$ ,  $p=0.007$ ) and LTB ( $R_{in}$ ,  $H=21.4$ ,  $p=0.00002$ ; spike duration,  $H=15.3$ ,  $p=0.0005$ ) cells. Post-hoc Mann-Whitney tests yielded nearly identical results in the two cell types. As we observed when comparing regions irrespective of cell types,  $R_{in}$  was significantly lower in BNST-AL's RS and LTB neurons than the corresponding cell classes in BNST-AV and AM ( $p$ 's  $<0.001$ ) with no difference between the latter two regions. Also, spike durations were significantly lower in BNST-AV's RS and LTB neurons compared to the corresponding cell classes in BNST-AL and AM ( $p$ 's  $<0.001$ ) with no difference between the latter two regions.

### 3.3.5. Morphological correlates of electroresponsive properties

A total of 60 biocytin-filled neurons were recovered (13 RS, 39 LTB, 6 fIR, and 2 SA) from BNST-AL (n=24), BNST-AM (n=22), and BNST-AV (n=14). Examples of these morphologically identified cells are provided in figures 3.8-3.9. In both figures, panel A shows the position and general morphology of the cells depicted in subsequent panels (red, presumed axons; black, soma and dendrites). We identified two main morphological cell types whose prevalence varied depending on the BNST-A region.

The first type of cells had long dendrites that ramified sparingly (Fig. 3.8A-E, Fig. 3.9F). They usually exhibited a low density of dendritic spines, typically of the stubby type. These spines were most common proximally (Fig. 3.8C2, E3, arrowheads); more distal dendrites typically lacked spines but usually displayed varicosities (Fig. 3.8B2, C3). These cells prevailed in BNST-AV (12 of 14), AM (17 of 22), and the ventral part of AL (9 of 11).

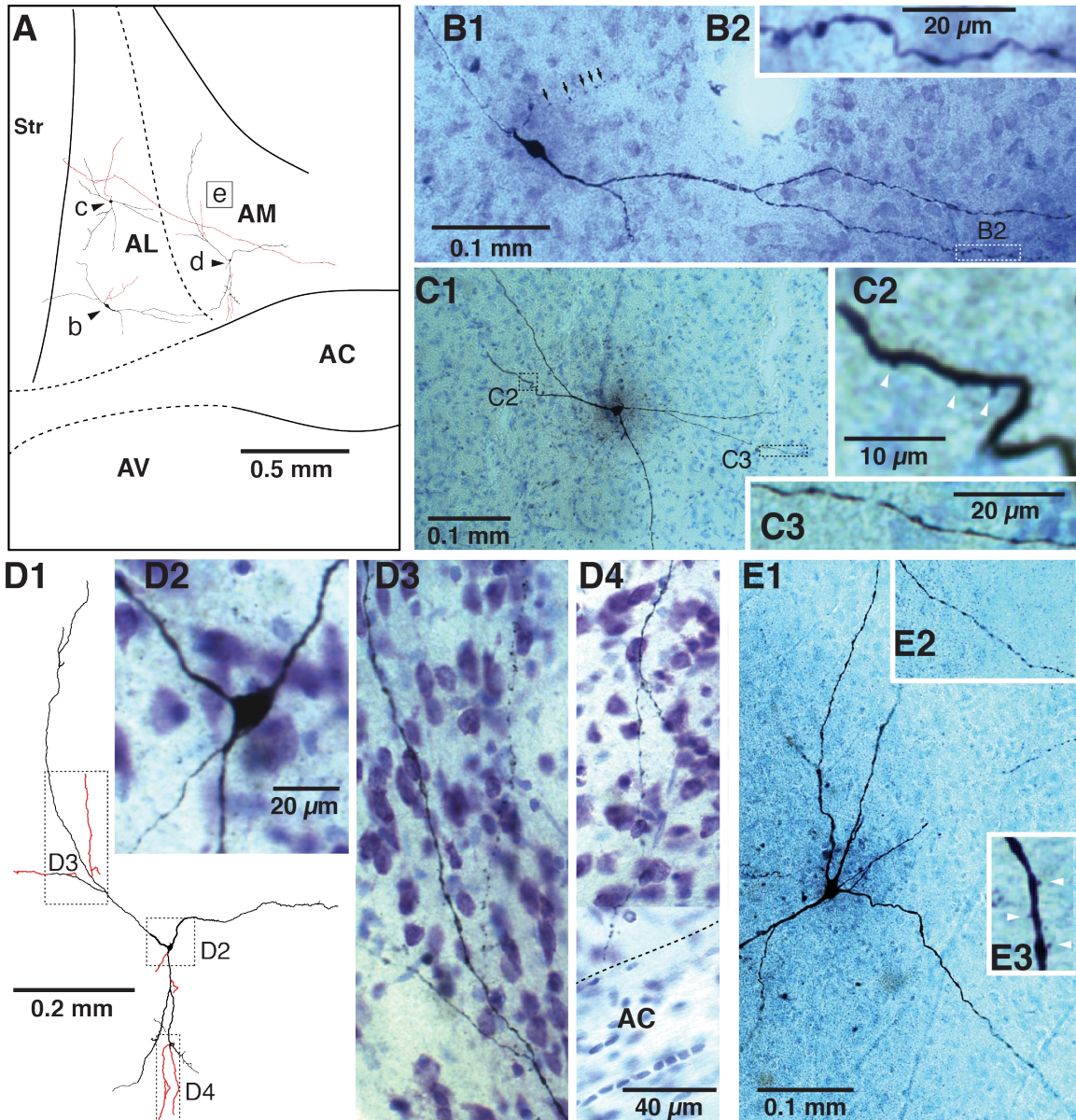


**Figure 3.8.** Morphological properties of BNST-A neurons. **(A)** Scheme showing position and overall morphology of cells depicted in panels B-E (red, axon-like processes, black dendrites and soma). For cell e, only its position is shown because its dendrites overlapped extensively with those of cell d. **(B)** AL cell (RS, Type-I). Dendritic region enclosed in white dashed rectangle of B1 (lower right) is shown at higher magnification in B2. Note dendritic varicosities in B2. **(C)** AL neuron (LTB, Type-II). Regions enclosed in dashed rectangles of C1 are shown at higher magnification in C2, and C3. Arrowheads point to stubby spines. **(D)** AM neuron (RS type). **(D1)** Drawing of the cell. Regions enclosed in dashed rectangle are shown at higher magnification in D2-4. Panels D3 and D4 show axon-like processes emerging from distal dendrites. **(E)** AM neuron (LTB type). **E2-3** show dendritic segments with varicosities (E2) or stubby spines (E3, arrowheads).

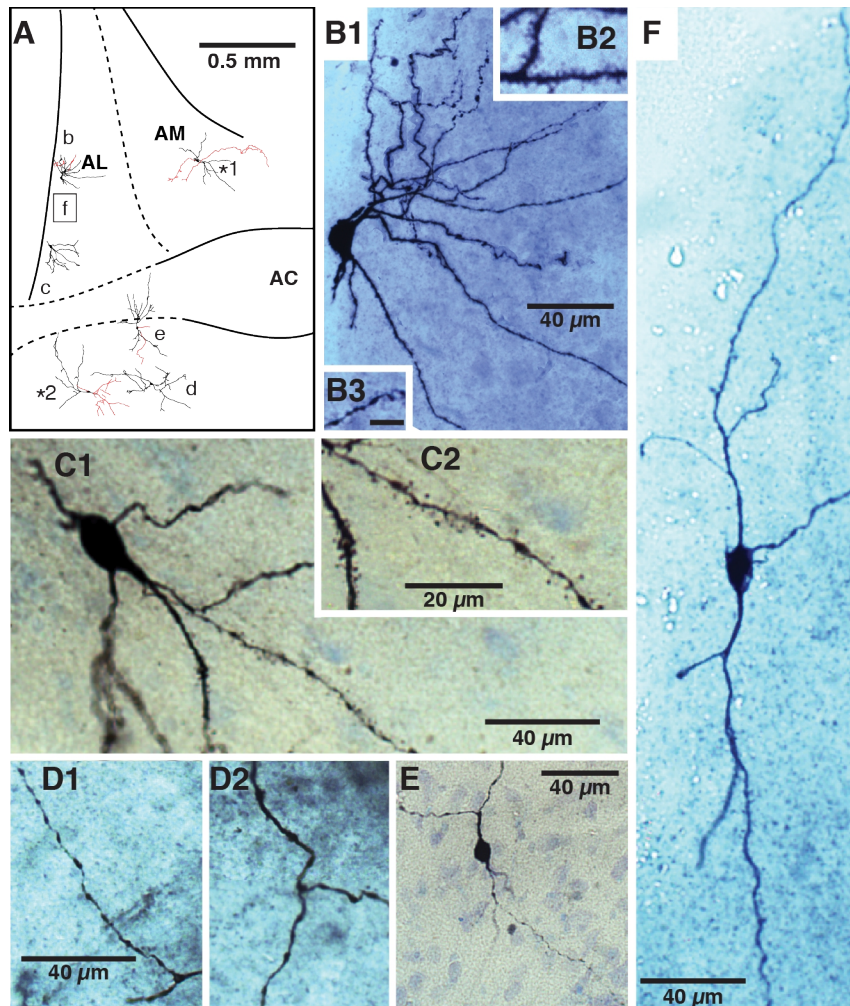


**Figure 3.9.** Morphological properties of BNST-A neurons. **(A)** Scheme showing position and overall morphology of cells depicted in panels B-F (red, axon-like processes, black dendrites and soma). For cell f, only its position is shown because its dendrites overlapped with those of cells b and c. Neurons labeled \*1 and \*2 are not depicted in subsequent panels. **(B)** AL neuron (LTB, Type-II). **(B2)** Dendritic segments with high density of spines. **(B3)** More distal dendritic segment with varicosities. **(C)** AL neuron (fIR, Type-III). **(D)** AV neuron (RS, Type-I) labeled “d” in panel A. Distal **(D1)** and proximal **(D2)** dendritic segments of cell. **(E)** AV neuron (LTB, Type-II). **(F)** AL neuron (fIR, Type-III). Scale bar in B3 is 15  $\mu\text{m}$  and valid for B2. Scale bar in D1 valid for D2.

The second type of neurons had smaller, but highly branched dendritic trees (Fig. 3.9B,C). Whereas their proximal dendrites lacked spines, more distal dendritic segments typically displayed a moderate to high density of thin dendritic spines (Fig. 3.9B2, C2). Most of these cells were recovered from the dorsal part of AL (4 of 6) and along the internal capsule (4 of 7), in regions that correspond to

the oval and juxtacapsular regions, respectively.

A previously unreported characteristic, exhibited by both cell types, was the variable emergence site of presumed axons. Axon-like processes could emerge from somata (Fig. 3.8A, cells c and d; Fig. 3.9A, cells b, \*1, and \*2), proximal dendrites (Fig. 3.8A, cell B; Fig. 3.9A, cells E and \*1) or distal dendrites (Fig. 3.8A, cells c and d), as far as 200  $\mu\text{m}$  from the soma. In 10% of cells (6 of 60), two or more distinct axon-like branches were seen to emerge from a combination of these sites. Note that in order for a cell to be considered as having more than one putative axon, each had to meet the following criteria. First, its emergence site had to be visible in the microscope by repeatedly changing the focal plane back and forth. Second, these axon-like processes had to emerge from two clearly different parts of the cells. Ambiguous cases were ignored.

Figure 3.8D illustrates a cell with multiple axon-like processes. This BNST-AM neuron had a putative axon emerging from its soma (Fig. 3.8D1), two more emerging from dorsally directed dendrites (one of which is visible in Fig. 3.8D3), and others from ventrally directed dendrites (Fig. 3.8D4). One of the latter appeared to merge into the anterior commissure. Overall, 28% of BNST-A cells had dendritically-emerging axon-like processes with no significant difference between regions (AL, 29%; AM, 27%; AV, 39%). On average, these axon-like processes emerged  $66.5 \pm 11.2 \mu\text{m}$  from the soma (AL,  $49.8 \pm 10.1 \mu\text{m}$ ; AM,  $89.6 \pm 28.1 \mu\text{m}$ ; AV,  $78.8 \pm 26.9 \mu\text{m}$ ).

Importantly, it should be noted that it is unclear whether these axon-like

processes truly are axons or extremely thin dendrites that bear varicosities. Unambiguous determination of their identity will require triple immunofluorescence for biocytin as well as dendritic and axonal markers such as MAP2 and synaptophysin.

The most frequently encountered property were dendritic varicosities, a feature exhibited by 75, 81, and 93% of BNST-AL, AV, and AM neurons, respectively. This property showed no consistent association with the presence or absence of dendritic spines or overall dendritic morphology. For instance, some cells had aspiny distal dendrites with varicosities (Fig. 3.9B3) and more proximal dendritic segments densely covered with spines, but lacking varicosities (Fig. 3.9B2). Other cells with dendritic varicosities had uniformly aspiny or sparsely spiny dendrites (Fig. 3.8B2, C3, E2; Fig. 3.9D1).

Surprisingly, we found no systematic relationship between the morphological and electroresponsive properties of RS and LTB cells. That is, there was as much morphological variability between RS and LTB of neurons as among both of these cell types considered independently. For instance, cells B-E in figure 3.8 had similar morphological properties including long, poorly ramified dendrites with a low density of dendritic spines, yet two of them were RS cells (Fig. 3.8B,D) and two were LTB neurons (Fig. 3.8C,E). Moreover, the RS and LTB phenotypes were also encountered among densely spiny neurons (Fig. 3.9B, LTB). In fact, the proportion of spiny cells corresponding to RS (30%) and LTB neurons (70%) was nearly identical to that seen among aspiny neurons (RS, 24%; LTB, 76%). Differences in other properties (Table 3.5) such as soma size,

number of primary dendrites, distance to first dendritic branching point, incidence of dendritic varicosities also failed to reach significance between these two prevalent cell types.

Due to their low incidence, our samples of fIR (n = 6) and SA (n =2) neurons are small. With one exception (Fig. 3.9F), all recovered fIR had densely spiny dendrites and moderately branching dendrites (Fig. 3.9C). In contrast, both SA cells had aspiny dendrites (Fig. 3.9, cell labeled \*2).

Table 3.5 *Morphological properties of BNST neurons* (values are means  $\pm$  SEM)

Cell Type	n	Soma diameter ( $\mu\text{m}$ )		Number of Primary Dendrites	Distance to first dendritic branch from soma ( $\mu\text{m}$ )	Length of the inter-varicose axonal segments ( $\mu\text{m}$ )*
		Maximum	Minimum			
RS (type-I)	13	19.2 $\pm$ 1.1	10.2 $\pm$ 0.6	2.8 $\pm$ 0.3	30.1 $\pm$ 5.6	4.4 $\pm$ 0.3
LTB (type-II)	39	19.7 $\pm$ 0.7	11.3 $\pm$ 0.4	3.2 $\pm$ 0.1	28.3 $\pm$ 2.2	5.1 $\pm$ 0.3
fIR (type-III)	6	19.4 $\pm$ 2.2	9.9 $\pm$ 0.7	2.8 $\pm$ 0.2	32.5 $\pm$ 6.5	4 $\pm$ 0.1
SA	2	19.5 $\pm$ 4.5	9 $\pm$ 1	2.5 $\pm$ 0.5	13.2 $\pm$ 1.7	5

\*For this analysis, we only considered primary dendrites that could be seen to branch at least once.

### 3.3.6. Other approaches to classification

The apparent lack of correlation between the physiological cell types described above and their morphological properties led us to consider other approaches to classification. In particular, for a large array of variables ( $V_r$ ,  $R_{in}$ , time constant, spike duration, amplitude and threshold, sag amplitude, amplitude and duration of spike after hyperpolarization), we computed frequency

distributions and scrutinized them for evidence of discrete clusters (multimodality) we might have missed by adopting the classification of Rainnie and colleagues. We also plotted different combinations of physiological and morphological variables against each other, two or three at a time and in principal component analysis space. However, these various approaches failed to reveal physiological variables that could support a different classification scheme consistent with morphology. Although multidimensional cluster analyses might have identified clusters, these approaches are counter-indicated in the absence of positive evidence that such groupings exist.

### **3.4. Summary of results**

We characterized the electroresponsive and morphological properties of neurons in BNST-A. Previously, Rainnie and colleagues distinguished three cell types in BNST-A: low-threshold bursting cells (LTB; Type-II) and regular spiking that display time-dependent (RS, Type-I) or fast (fIR; Type-III) inward rectification in the hyperpolarization direction. In this study, we found that the same neuronal types exist in BNST-AM and AV. In addition, we observed two hitherto unreported cell types: LF cells, only seen in BNST-AL, that display conspicuous delay to firing, and SA neurons, only present in BNST-AV, firing continuously at rest. However, the feature that most clearly distinguished the three BNST regions was the incidence of LTB cells (~40-70%) and the strength of their bursting behavior (both higher in BNST-AM and AV relative to AL). The incidence of RS cells was similar in the three regions (~25%), whereas that of fIR

cells was higher in BNST-AL (~25%) than AV or AM ( $\leq 8\%$ ). Using biocytin, two dominant morphological cell classes were identified but they were not consistently related to particular physiological phenotypes. One neuronal class had highly branched and spiny dendrites; the second had longer but poorly branched and sparsely spiny dendrites. Both often exhibited dendritic varicosities. Since LTB cells prevail in BNST, it will be important to determine what inputs set their firing mode (tonic vs. bursting) and in what behavioral states. See chapter VI for a complete discussion of the findings obtained in this chapter.

## **CHAPTER IV**

### **Intrinsic Connections in the Anterior Part of the Bed Nucleus of the Stria Terminalis**

#### **4.1. Rationale**

As I previously mentioned in the general introduction (chapter I), the different BNST regions form contrasting connections (Sofroniew et al., 1983; Holstege et al., 1985; Moga et al., 1989; Sun and Cassell 1993; McDonald et al., 1999b; Dong et al., 2001a; Ulrich-Lai and Herman 2009). While this heterogeneous connectivity suggests a degree of functional specialization within the BNST-A, a seminal series of tracing studies by Swanson and colleagues (Dong and Swanson 2003, 2004, 2006a, 2006b, 2006c) suggest that different BNST-A regions do not act as independent processing channels, but that they interact via inter-nuclear connections. For instance, they reported that components of BNST-AL, particularly, the oval nucleus, strongly projects to parts of BNST-AV, such as the fusiform nucleus (Dong and Swanson 2004). However, interpretation of these findings is complicated by the fact that the distance between different BNST regions is small relative to the considerable extent of dendritic trees in the BNST (McDonald 1983; Larriva-Sahd 2006). Moreover, this problem is compounded by tracer diffusion from the injection site in the small volume of BNST, particularly along the tract of the pipettes used to inject the tracers.

Another unresolved question relates to the transmitter(s) used by intrinsic BNST axons. Indeed, previous work has revealed that BNST-A contains GABAergic and glutamatergic neurons (Cullinan et al., 1993; Sun and Cassell 1993; Polston et al., 2004; Poulin et al., 2009) with GABAergic cells accounting for the majority of BNST-A cells, and glutamatergic neurons for a minority. Thus,

the experiments described in this chapter were undertaken to shed light on the organization of intrinsic BNST-A connections using a method that has higher spatial resolution than tract tracing and allows identification of the transmitters involved: glutamate uncaging coupled to patch recordings in vitro.

#### **4.2. Brief overview of methods**

Brain slices of BNST-A were prepared according to the procedures described in the chapter II. After incubation, slices were then transferred one at a time to the recording chamber perfused with aCSF (5 ml/min) plus caged glutamate (4-Methoxy-7-nitroindolinyI-caged-L-glutamate, 1.0 mM; Tocris Bioscience, Bristol, UK).

To study the intrinsic connectivity of the BNST-A, we used ultra-violet (UV) uncaging of glutamate (GU) at various sites with respect to the recorded cells. UV light pulses (50 ms) were delivered at 0.1 Hz by a LED source (365 nm, 60 mW; CoolLED, Andover, UK) via a 60X immersion objective, yielding UV light spots of  $\approx 150\mu\text{m}$  in diameter. The microscope rested on a computer-controlled motorized stage, allowing us to move the light spot in a grid-like pattern (50 or 110  $\mu\text{m}$  steps) with respect to the recorded cell (Fig. 4.1). At least three UV light pulses were applied at each site while keeping the cells at -90 mV with DC current injection. If a synaptic response was observed, the pre-stimulus membrane potential of recorded cells was sequentially set to two additional values (-80, and -65 mV), each for at least three light stimuli, and more when response latencies were variable. With this approach,  $\approx 60$  min was required to

scan the entire BNST-A region in search of sites where UV light application elicited responses in a given postsynaptic cell. PSPs  $\leq 0.2$  mV from a membrane potential of -90 mV were excluded.

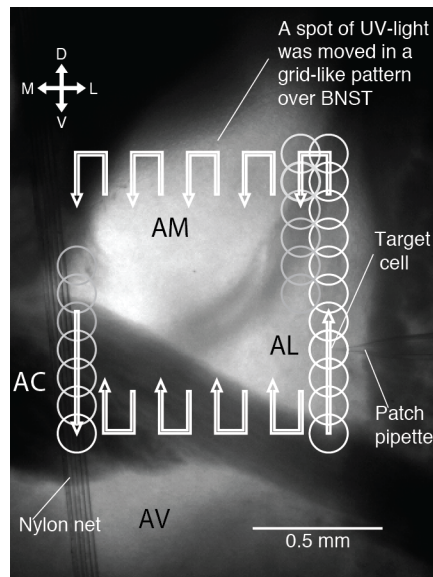


**Figure 4.1.** Approach used to study intrinsic BNST-A connections. Glutamate uncaging was used to study the intrinsic connectivity of BNST-A. Patch recordings of BNST-A cells were obtained under visual guidance. Pulses (50 ms) of UV light were delivered (0.1 Hz) at sites of 150  $\mu\text{m}$  in diameter (white circles), uncaging glutamate at the stimulation site. The site of UV light stimulation was systematically moved over the entire BNST-A in a grid-like pattern. Multiple light pulses were applied at each site and from different membrane potentials.

GU-evoked PSPs could easily be distinguished from spontaneous synaptic events because the latter occurred infrequently and showed no temporal relationship with respect to the light stimulus. Nevertheless, since anterior BNST neurons display spontaneous synaptic events (Dumont et al., 2005, 2008; Kash et al., 2008; Guo and Rainnie 2010; Gosnell et al., 2011) that could be erroneously interpreted as GU-elicited PSPs, the following approach was used to distinguish spontaneous vs. GU-evoked PSPs. For each cell, we estimated the average interval between spontaneous PSPs (inter spontaneous PSP interval,

IsPSPI) during the pre-stimulus period. Across all recorded cells, the average was  $331 \pm 30$  ms. We then used the IsPSPI of each cell to determine the duration of a temporal window within which we required PSPs in at least 8 of 9 trials in order to consider them considered as GU-elicited. This “detection window” was set to a quarter of the cell’s IsPSPI. Within this window, the probability of getting 8 or more spontaneous PSPs in 9 traces by chance (i.e. the false positive rate) is then  $p = 0.000107$  (Binomial test). We searched for GU-elicited PSPs in a 300 ms period after stimulus onset by moving our detection window in non-overlapping steps. The average number of non-overlapping detection windows was 4, resulting in a false positive probability of 0.000428 per stimulation site. The average number of stimulus sites per cell was 77, resulting in an average false positive probability of  $p = 0.0329$  per cell. Since we recorded a total of 75 cells, the number of stimulus positions with PSPs falsely labeled as GU-elicited is equal to  $(0.0329 * 75 = 2.467)$ . Given that we observed 277 connections, this represents less than 1% of false positives.

### **4.3. Results**

#### 4.3.1. Spatial specificity of glutamate uncaging to study intra-BNST connectivity

The usefulness of the GU method to study intrinsic BNST connections depends on whether it meets the following two criteria. First, that the rise in glutamate concentration produced by UV light be high and rapid enough to reliably fire neurons located where the light stimulus is applied. Second, that the decay of the glutamate concentration with distance from the UV light stimulus be

sufficiently steep such that nearby neurons, not directly exposed to UV light, are not depolarized enough to fire. We first aimed to test whether the GU method meets these criteria in the BNST.

To this end, the spot of UV light (150  $\mu\text{m}$  in diameter and 50 ms in duration) was centered over recorded cells ( $n = 10$ ) and then gradually displaced away from this site in various directions (steps of 50  $\mu\text{m}$ ). In these recordings, the pipette solution included biocytin to allow post-hoc correlation of morphology and responsiveness to uncaged glutamate. A representative example of such an experiment is shown in figure 4.2A. Red and white dots mark the sites of UV light application that elicited supra- or subthreshold responses, respectively. Application of UV light over the soma (Fig. 4.2A4) and its immediate vicinity always elicited robust spiking. This is a direct response to uncaged glutamate. However, when the center of the UV spot was moved away from the soma, these direct depolarizing responses eventually became sub-threshold or vanished. These variations (amplitude reduction vs. disappearance) depended on the exact position of the cells' dendrites with respect to the position of the light spot, with stimuli located  $\geq 150$   $\mu\text{m}$  from dendrites never eliciting spiking from rest. For instance, in the case depicted in figure 4.2A, GU elicited spiking when the UV light was applied over the soma and proximal dendrites (red dots and Fig. 4.2A2-4) but not when the stimulus was applied over more distal dendrites or at sites  $\geq 150$   $\mu\text{m}$  from the soma and dendrites. At some of these sites (Fig. 4.2A5,6), evidence of GABAergic synaptic connections was obtained. Across all the cells tested in this manner, we did not observe a single case where spiking could be

elicited from stimulation sites located  $>200\ \mu\text{m}$  from their somata. Typically, direct responses vanished within  $150\ \mu\text{m}$ . Thus, these results suggest that the GU method has sufficient spatial selectivity to study intrinsic BNST connections.

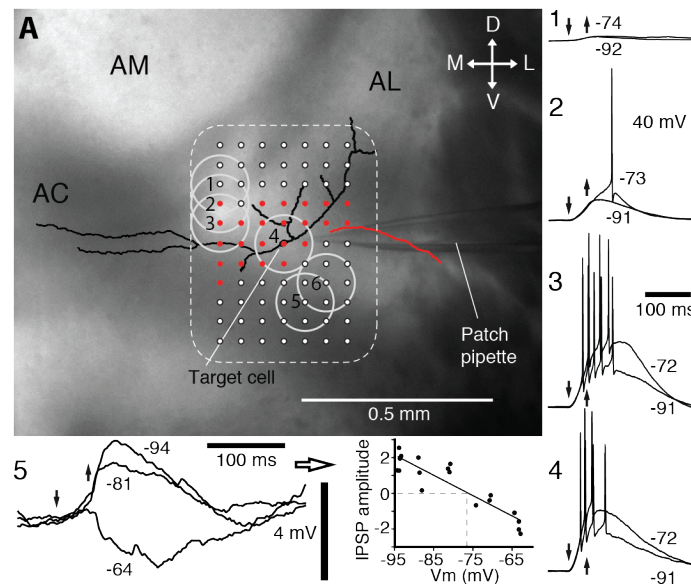


**Figure 4.2.** (A) Spatial selectivity of glutamate uncaging. A patch recording of a BNST-AL neuron was obtained and the morphology of the cell revealed with biocytin (black, soma and dendrites; red, axon). UV light was applied over, and in the vicinity of, the recorded cell. The center of the UV-light spot was moved in steps of  $50\ \mu\text{m}$ . Sites evoking direct supra-threshold responses are indicated by **red dots**; **white circles** indicate sub-threshold responses. No supra-threshold responses could be elicited when the center of the UV-light spot was  $>150\ \mu\text{m}$  from the cell. Examples of direct responses are provided in 1-4. GU at sites 5 and 6 elicited GABA-A IPSPs. Responses elicited from site 5 from different membrane potentials are shown on the bottom left.

Another important consideration when assessing the usefulness of GU to study intrinsic BNST connections is whether depolarizing PSPs can be distinguished from direct subthreshold responses to uncaged glutamate. Indeed, when UV stimuli are applied near recorded cells, it is possible that the evoked depolarizations are not due to synaptically released transmitter, but uncaged glutamate. Fortunately, these two types of responses could be readily distinguished. Figure 4.3A1 shows three superimposed direct sub-threshold responses to uncaged glutamate. As was typically observed when the light

stimulus was applied near the recorded cell, this direct response started shortly after the onset of the light pulse, rose gradually for its entire duration, and began decaying shortly after its offset (Fig. 4.3A1).

Compared to direct responses, synaptically evoked PSPs had a longer latency (PSPs,  $79.0 \pm 4.4$ ; direct,  $8.3 \pm 0.1$  ms), they peaked more rapidly (PSPs,  $27.8 \pm 1.5$  ms; direct,  $74.7 \pm 0.4$  ms), the onset of their decay phase was not time-locked to the offset of the light stimulus, and they sometimes showed conspicuous latency variations. The most direct illustration of the distinction between direct and synaptic responses are cases where both phenomena are elicited by UV light application at the same site. In the example shown in figure 4.3A2, the responses elicited by multiple consecutive light stimuli are superimposed. All trials started with a direct response to uncaged glutamate that showed no latency variations. Superimposed on the decaying phase of these direct responses were depolarizing PSPs whose exact latencies and number varied from trial to trial. These latency variations, coupled to the differing time course of the two types of responses leave no doubt as to their distinct origin. Of course, in the case of GABAergic PSPs, the distinction was further facilitated by the fact that IPSPs reversed in polarity when the cells were depolarized (see below and Fig. 4.2A5).

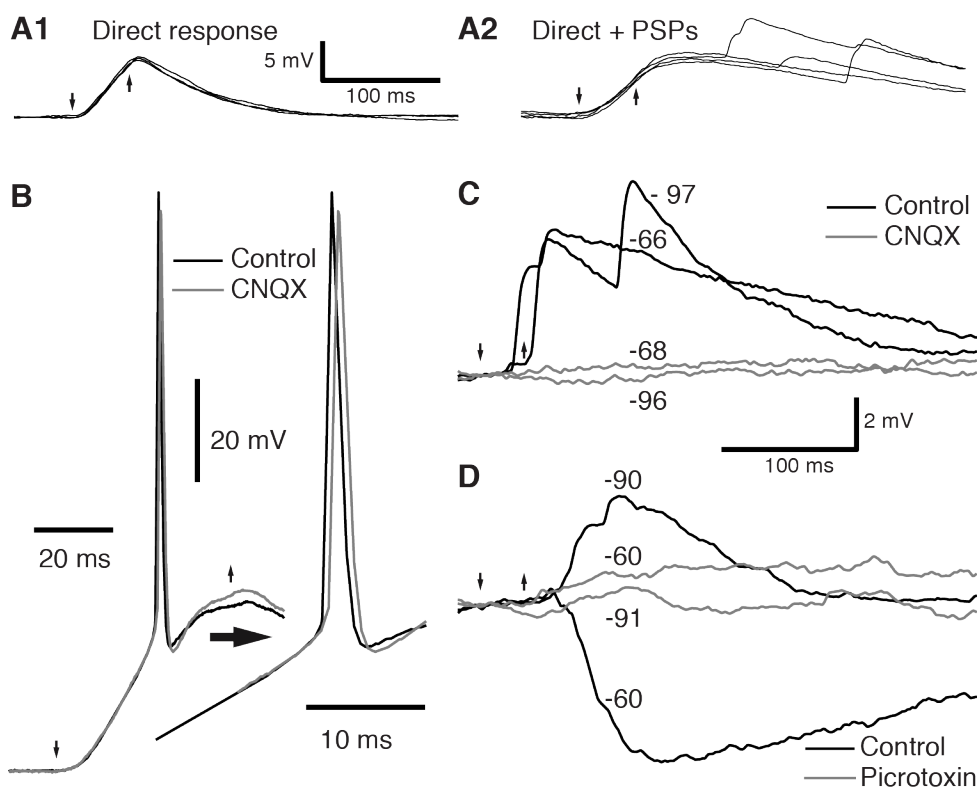


**Figure 4.3.** Distinguishing responses to uncaged glutamate vs. synaptically released transmitters. **(A1)** Direct sub-threshold response to uncaged glutamate (three superimposed sweeps) from  $-90$  mV. Note slow and invariant rising phase. Downward and upward arrows indicate onset and offset of UV light stimuli, respectively. **(A2)** Case where a direct response and PSPs are triggered from the same stimulation site. Again, note slow and invariant rising phase of the direct response that contrasts with the fast rising phase, variable latency and number of evoked PSPs (four superimposed sweeps). **(B)** Example of direct suprathreshold response to uncaged glutamate and **(C-D)** of PSPs in control aCSF (black), after addition of CNQX **(B-C)**, gray) or picrotoxin **(D)**, gray). Direct supra-threshold response to uncaged glutamate resists CNQX **(B)** whereas indirect glutamatergic responses are abolished **(C)**. As shown in **D**, picrotoxin blocked IPSPs elicited by GU.

It should be noted that latency variations were typically much smaller than in figure 4.3A2, as will become clear in subsequent figures. However, since anterior BNST neurons display spontaneous synaptic events (Dumont et al., 2005, 2008; Kash et al., 2008b; Guo and Rainnie 2010; Gosnell et al., 2011) that could be erroneously interpreted as GU-elicited PSPs, the following approach was used to distinguish spontaneous vs. GU-evoked PSPs. For each target cell independently, we computed the frequency of spontaneous PSPs and only

considered PSPs that largely exceeded the chance expected (see details in section 4.2). With the approach we used, the estimated false-positive rate was around 1%.

#### 4.3.2. Distinguishing GABAergic and glutamatergic PSPs elicited by glutamate uncaging

To identify the transmitters mediating GU-evoked PSPs, we primarily relied on their reversal potentials. That is, PSPs with extrapolated reversal potentials near 0 mV were assumed to be mediated by ionotropic glutamatergic receptors, whereas PSPs with reversal potentials negative to – 60 mV were classified as being mediated by GABA-A receptors (Fig. 4.2A5). In several cases, we verified these inferences by testing whether presumed glutamatergic or GABAergic PSPs were sensitive to drugs that block non-NMDA glutamate receptors (6-cyano-7-nitroquinoxaline-2,3-dione, CNQX, 10  $\mu$ M; Fig. 4.3B-C) or GABA-A (picrotoxin, 75  $\mu$ M; Fig. 4.3D) responses. In all tested cases (EPSP, n = 5; IPSP, n = 7), the pharmacological experiment confirmed our electrophysiological inference. Here, it should be noted that due to the large rise in glutamate concentration produced by GU, the competitive receptor antagonist CNQX application did not block (only delayed) direct supra-threshold responses to uncaged glutamate (Fig. 4.3B). In contrast, EPSPs elicited by synaptically released glutamate were completely abolished (Fig. 4.3C). The differential sensitivity of direct vs. synaptically mediated glutamatergic responses to CNQX was previously reported in a study relying on local pressure applications of glutamate (Apergis-Schoute et al.,

2007).

#### 4.3.3. Mapping of intrinsic BNST-A connections with glutamate uncaging

We studied GU-evoked responses in 75 cells where long-term recording stability ( $\leq 10\%$  variations in input resistance and  $\leq 5$  mV in resting potential) allowed extensive mapping of their intra-BNST connections with GU. These include 25 BNST-AL, 28 BNST-AM, and 22 BNST-AV neurons. Consistent with earlier reports on the electroresponsive properties of BNST-A neurons (Hammack et al., 2007; Guo et al., 2009; Hazra et al., 2011, 2012), regular spiking and low-threshold bursting neurons accounted for the vast majority of cells in the three regions examined. However, because no differences in the intrinsic connections were seen between physiological cell types ( $\chi^2(N = 75) = 7.64$ ,  $p = 0.27$ ), the results obtained in the various cell types are pooled below. In all cells combined, we tested the effects of UV light stimuli at 5739 sites, usually separated by 110  $\mu\text{m}$ . Overall, 5.1% of the stimulation sites elicited a synaptic response. Typical examples of intrinsic BNST-A connections evidenced with GU are shown for individual BNST-AM (Fig. 4.4A), AL (Fig. 4.4B), and AV (Fig. 4.4C) neurons. We first provide a qualitative description of these response patterns; quantitative population analyses will follow.

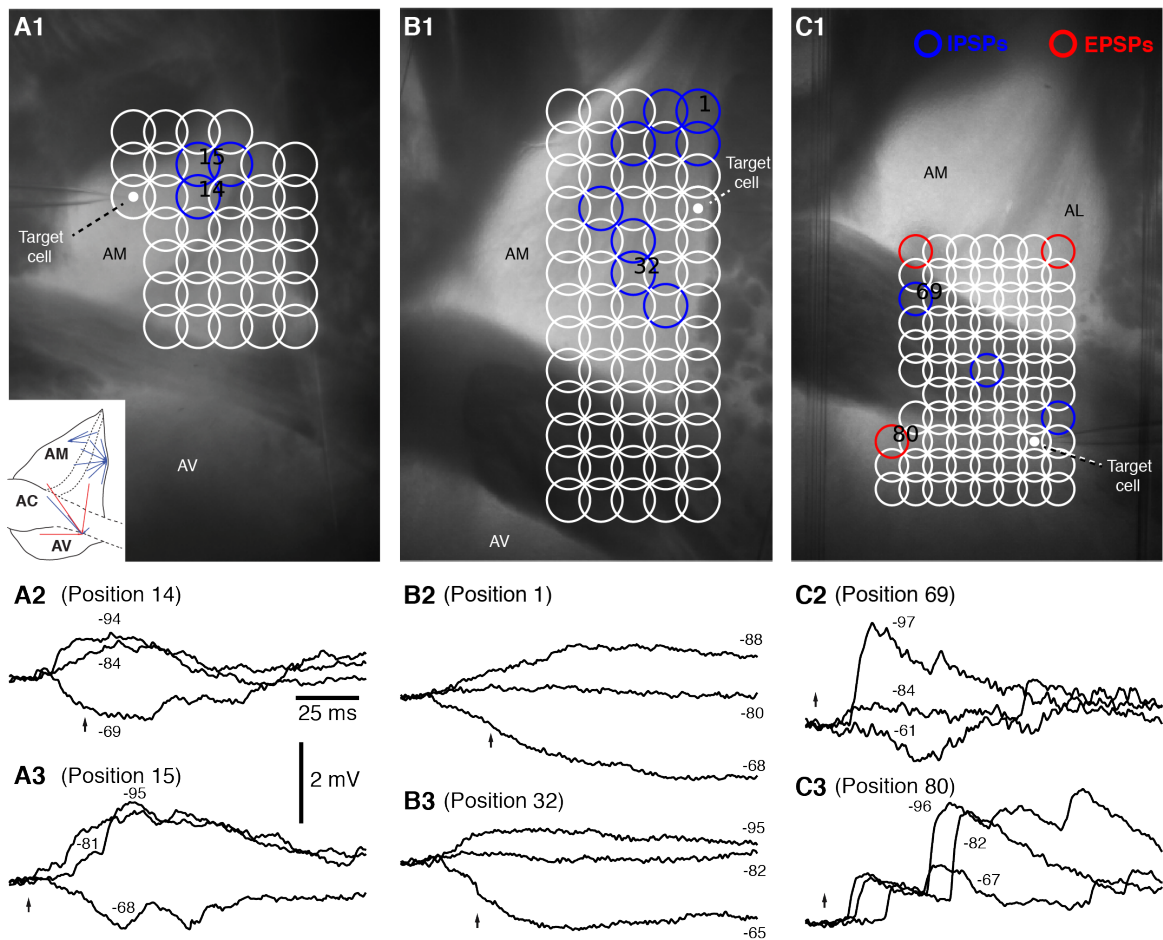


**Figure 4.4.** Examples of response patterns observed in BNST-AM (A), AL (B) and AV (C) neurons with glutamate uncaging. (1) Photomicrographs of the trans-illuminated slices with position of recorded cells (target cell, white dot) and UV stimulation sites (circles). **White circles** indicate sites of UV light application that elicited no response. At sites marked by **blue circles**, UV light elicited IPSPs. At sites marked by **red circles**, EPSPs were evoked. Examples of IPSPs (A2-3, B2-3, C2) and EPSPs (C3) are provided at the bottom. Numbers indicate the pre-stimulus membrane potentials (mV) at which the responses were observed. Upward arrows indicate offset of 50-ms UV light stimuli that elicited the responses. **Inset in A1** (lower left): graphical summary of connections found in the three cells depicted in panels A-C. **Blue:** inhibitory connections. **Red:** excitatory connections.

In figure 4.4A1-C1, colored circles are used to mark UV stimulation sites that elicited IPSPs (blue), EPSPs (red) or no responses (white). As was typically the case, these three cells responded to a minority of stimulation sites. Also representative of the overall response pattern, a majority of PSPs elicited with GU

were IPSPs. Examples evoked of IPSPs (Fig. 4.4A2-3, B2-3, C2) and EPSPs (Fig. 4.4C3) are provided. The rise time and duration of evoked PSPs varied within and between cells. This variability probably reflects a number of factors such as electrotonic distances between the activated synapse(s) and soma as well as differences in the number of spikes (and instantaneous firing frequency) of presynaptic neurons recruited by GU. Of course, it is also possible that the number of presynaptic neurons varies between stimulation sites.

The inset in figure 4.4A1 (lower left) provides a different representation of the results obtained in the same three neurons shown in figure 4.4. The same representation is used to illustrate the responsiveness of 20 additional neurons in figure 4.5. We will refer to the results obtained in these cells later on, when describing the general trends identified in this study.

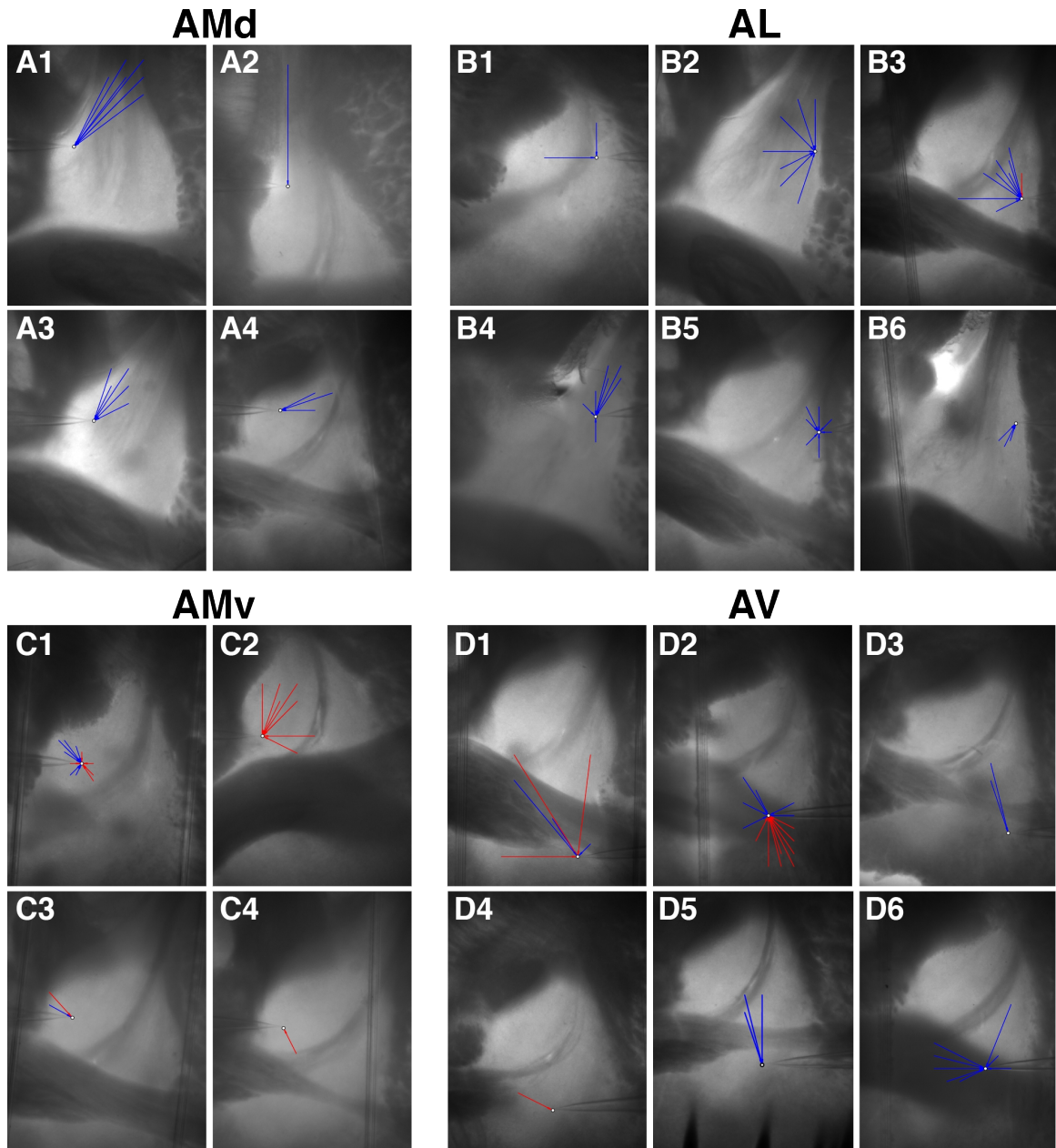


**Figure 4.5.** Plots of intra-BNST connections evidenced with glutamate uncaging in the dorsal (**A**) and ventral (**B**) parts of AM, AL (**C**), and AV (**D**). Each of the 20 panels illustrates a different cell. Note that in dorsally located AM cells, intrinsic inputs prevalently run dorsoventrally. This trend was generally not seen in cells recorded in BNST-AL (**B**), AV (**D**) or ventral part of AM (**C**). While excitatory connections to neurons in BNST-AL and the dorsal part of BNST-AM were rare, they were frequently encountered in AV and ventrally-located BNST-AM cells.

#### 4.3.4. Intrinsic BNST-A connections: population analyses

Consistent with the fact that GABAergic cells represent the main cell type in the BNST-A, most of the intrinsic connections disclosed with GU were inhibitory. Figure 4.6 shows this in two ways: first (Fig. 4.6A) by plotting the proportion of cells in which only IPSPs (blue circles), EPSPs (red circles) or both (intersection between the circles) were evoked by GU, and second (Fig. 4.6B-C) by depicting the proportion of stimulation sites that were effective in eliciting EPSPs or IPSPs across all cells. With the first approach, the prevalence of inhibitory connections was apparent when we considered all BNST-A cells together (Fig. 4.6A1;  $\chi^2(1, N = 75) = 7.18, p = 0.0074$ ) or neurons in different parts of the BNST-A separately (Fig. 4.6A2-4). However, the differing incidence of inhibitory and excitatory connections was especially marked in the BNST-AL (Fig. 4.6A2;  $\chi^2(1, N = 25) = 4.53, p = 0.033$ ), and progressively less so in the BNST-AM (Fig. 4.6A3,  $p = 0.12$ ) and the BNST-AV (Fig. 4.6A4,  $p = 0.6$ ). This result pattern was confirmed using a different statistical approach whereby the proportion of effective stimulation sites was first determined for each cell, averaged across cells separately for IPSPs and EPSPs and then compared with a paired t-test (Fig. 4.7A). This was used for all BNST-A cells combined ( $t(74) = 3.87, p = 0.0002$ ) as well as separately for AL ( $t(24) = 2.77, p = 0.011$ ), AM ( $t(27) = 2.65, p = 0.013$ ), and AV neurons ( $t(21) = 1.29, p = 0.212$ ).

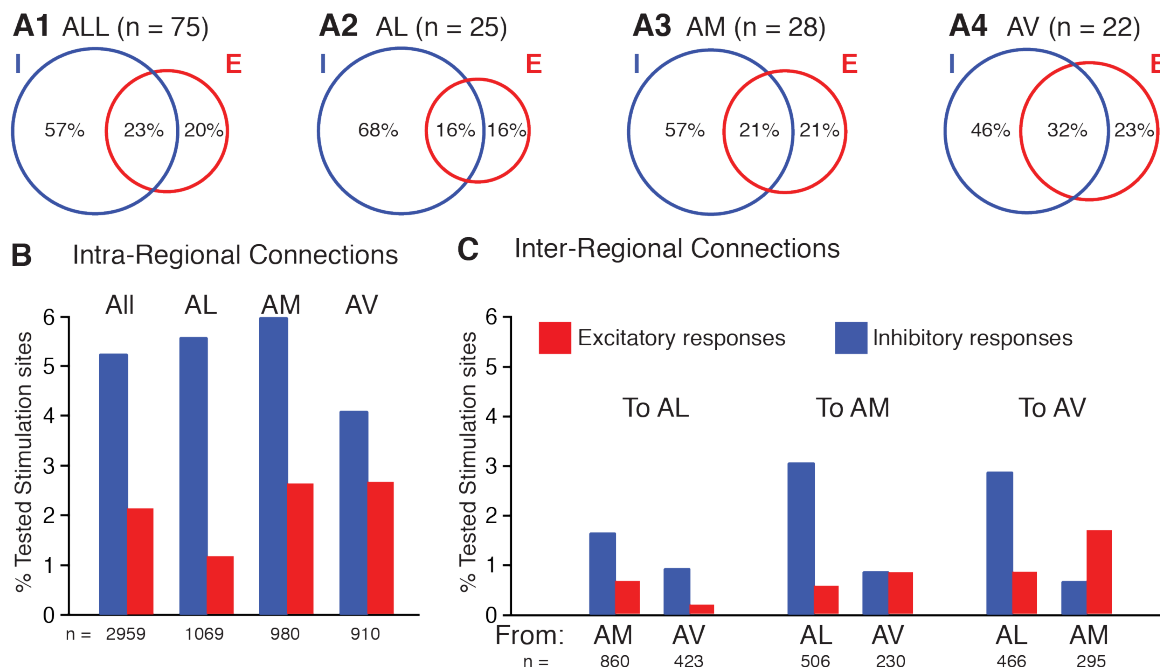


**Figure 4.6.** Relative incidence of inhibitory and excitatory connections within BNST-A. **(A)** Proportion of cells that responded with glutamatergic (red; E) and/or GABAergic (blue; I) PSPs to GU. From left to right: all recorded cells irrespective of location, AL, AM, and AV cells. **(B-C)** Proportion of tested stimulation sites eliciting GABAergic (blue) or glutamatergic (red) PSPs when the stimulation and recording sites were in the same **(B, intraregional)** or different **(C, interregional)** sectors of BNST-A.

The same conclusions emerged from the overall analysis of effective stimulation sites (Fig. 4.6B-C). For intra-regional connections (Fig. 4.6B), that is cases where the stimulation sites and recorded neurons were in the same BNST-A region, a chi-squared test revealed a significant dependence between response type (IPSP, EPSP, no response) and BNST region (BNST-AV, BNST-AM and BNST-AL) ( $\chi^2(4, N = 2959) = 9.62, p = 0.047$ ). Post-hoc tests showed that the proportion of stimulation sites eliciting IPSPs was higher in the BNST-AL than BNST-AV ( $\chi^2(2, N = 1979) = 7.56, p = 0.023$ ), and that the proportions in the BNST-AM are intermediate, and not significantly different from either the BNST-AL ( $p = 0.07$ ) or BNST-AV ( $p = 0.23$ ).

For inter-regional connections (Fig. 4.6C), namely instances where the recording and stimulation sites were located in different BNST-A regions, a more complex picture emerged. First, irrespective of the type of response observed (IPSPs or EPSPs), the incidence of effective stimulation sites was much lower than seen in intra-regional connections (intra-regional: 7.41%, inter-regional: 2.63%,  $\chi^2(1, N = 5775) = 84.34, p < 0.0001$ ). As shown in figure 4.7B, the same conclusion was reached using a different statistical approach, namely first determining the proportion of effective stimulation sites per cell for intra- vs. inter-regional connections, averaging these values, and then comparing them with a paired t-test ( $t(74) = 2.93; p = 0.004$ ).

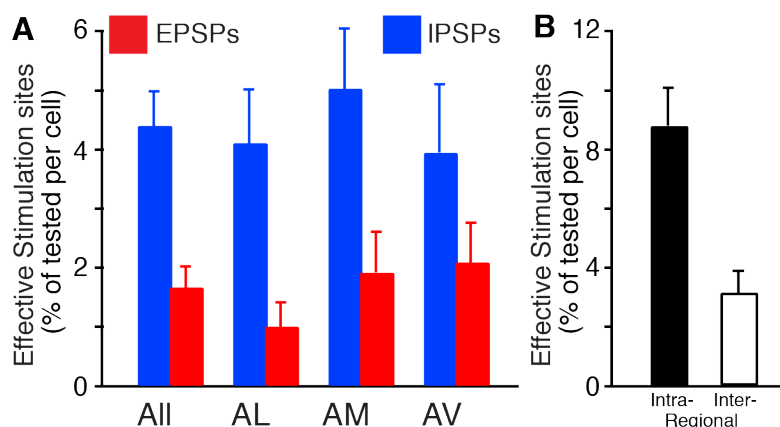


**Figure 4.7.** Properties of intrinsic BNST connections. **(A)** Proportion of stimulation sites that elicited EPSPs (red) or IPSPs (blue) in BNST neurons. In contrast to figure 5, the proportion of effective sites was computed for each cell separately and then averaged across cells (values are averages  $\pm$  SEMs). **(B)** Proportion of effective stimulation sites (EPSPs and IPSPs combined) in intranuclear (black) or internuclear connections (empty bar). As for panel A, the proportion of effective sites was computed for each cell separately and then averaged across cells.

Second, IPSPs did not prevail in all interregional connections. They did in connections from and to BNST-AL neurons ( $n_{\text{ipsp}} = 46$ ,  $n_{\text{epsp}} = 16$ ; binomial test,  $p < 0.0001$ ), whereas in connections from and to the BNST-AV, the incidence of inhibitory connections could be equal to (AV to AM) or even lower than (AM to AV) that of excitatory connections. However, because the proportion of effective stimulation sites was low in these inter-regional connections, the latter difference did not reach statistical significance (binomial test,  $p = 0.5$ ).

Properties of GU-evoked PSPs (rise-time, amplitude, duration) did not vary depending on the BNST-A region where the target cells were recorded or where the light stimuli were applied. This was true of EPSPs and IPSPs, even with significance levels uncorrected for multiple comparisons. Figure 4.8 therefore shows frequency distributions of IPSP and EPSP properties using results obtained in the three BNST-A regions combined. See figure legend for methodological details. It should be noted that for these analyses, compound PSPs were not included; only well isolated PSPs (presumed single-axon PSPs) that could be measured unambiguously. However, note that the rise time of compound events, particularly of IPSPs, were markedly slower than those of isolated PSPs.

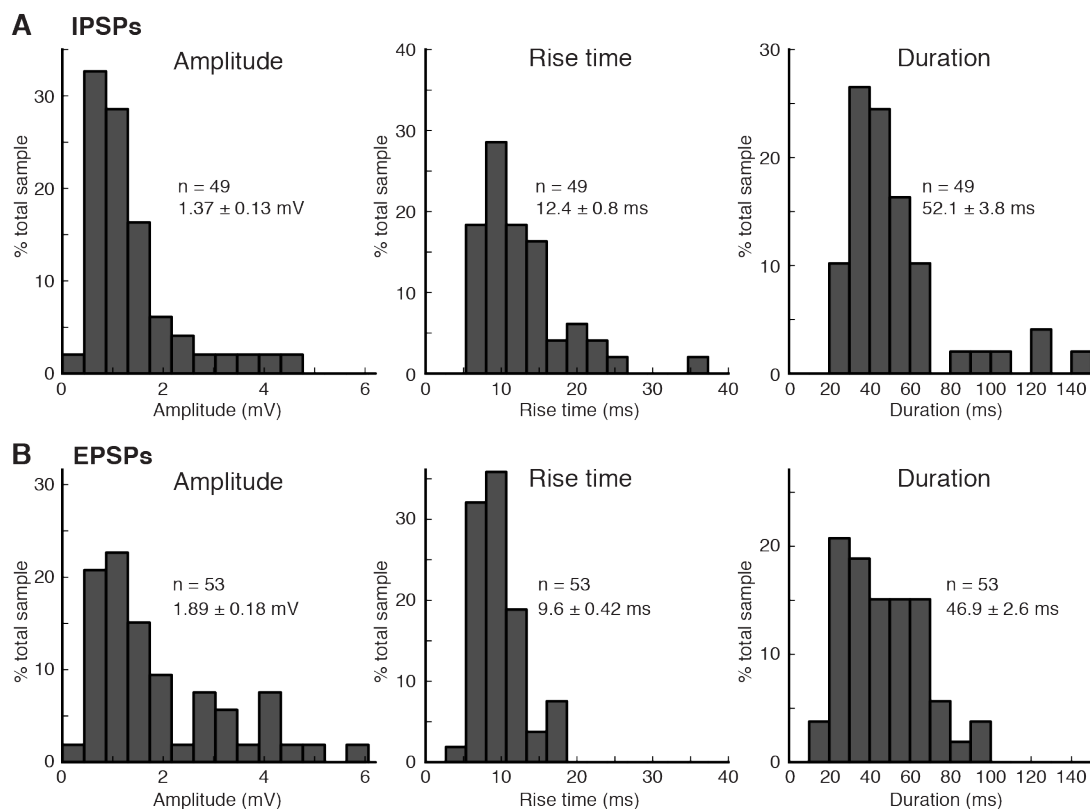


**Figure 4.8.** Properties of IPSPs and EPSPs elicited by GU in intra- and interregional connections in all recorded neurons combined. **(A)** Frequency distributions of IPSP amplitudes (left), rise times (middle) and durations (right). **(B)** Frequency distribution of EPSP amplitudes (left), rise times (middle) and durations (right). This analysis only includes connections where individual PSPs could be resolved; compound events were excluded. All measures were performed from a membrane potential of  $-90$  mV. PSP rise times correspond to time to half of peak amplitude.

#### 4.3.5. Heterogeneous directionality and polarity of intrinsic BNST connections

There were marked differences in the directionality of intra-regional connections in different sectors of the BNST-A. In the dorsal but not ventral portions of the BNST-AM, connections had a preferential directionality, with dorsal GU sites eliciting IPSPs in more ventrally located cells far more frequently than stimulation sites located ventrally to the recorded neurons (Fig. 4.5A). Although a few cells exhibited this phenomenon in other BNST regions (Fig. 4.5B4, C2, D3,5), no overall preferential directionality of connections emerged in the BNST-AL (Fig. 4.5B1-3,5-6), BNST-AV (Fig. 4.5D1,24,6) or the ventral part of BNST-AM

(Fig. 4.5C1,3,4).

Another obvious difference between the dorsal (Fig. 4.5A) and ventral parts (Fig. 4.5C) of the BNST-AM was the incidence of neurons receiving excitatory inputs. All but one of the BNST-AM neurons in which intrinsic glutamatergic connections were disclosed (12 of 28) were found in the ventral part of the BNST-AM. As in the ventral part of BNST-AM, a high incidence of neurons receiving intrinsic glutamatergic inputs was found in the BNST-AV (12 of 22 or 55%; Fig. 4.5D), significantly higher than in the BNST-AL where intrinsic glutamatergic inputs were infrequent (7 cells of 25 or 28%; Fisher Exact test,  $p = 0.045$ ).

Inter-regional connections were also asymmetric (Fig. 4.6C). Indeed, GU in BNST-AM or AL elicited PSPs in BNST-AV cells (3.66%) much more frequently than in the opposite direction (1.38%, Fisher exact test,  $p = 0.007$ ). In addition, while reciprocal connections were found between BNST-AL and AM, BNST-AL to AM connections were more frequent than in the opposite direction (% tested stimulated sites: AM to AL, 2.78%; AL to AM, 3.56%; Fisher exact test,  $p = 0.042$ ).

#### 4.3.6. Morphological correlates

To test whether the contrasting directionality of intrinsic connections observed in different BNST-A sectors was dependent on the morphology of BNST-A neurons, we filled 38 neurons with biocytin (AM,  $n = 12$ ; AL,  $n = 19$ ; AV,  $n = 7$ ). Representative examples of biocytin-filled neurons are provided in figure 4.9A. After filling, the slices were placed in fixative, re-sectioned at 100  $\mu\text{m}$  and

the biocytin revealed. The morphology of recorded cells was reconstructed by performing drawings of all labeled elements found in the different sections. Then, based on the matching position of blood vessels and of the cut ends of dendritic and/or axonal segments, the labeling found in the different sections was aligned. Figure 4.9B provides examples of such reconstructions.

Consistent with the prevalent dorsoventral connectivity seen in the dorsal portion of the BNST-AM, 11 of 12 cells recovered from BNST-AM ( $n = 12$ ) had dendrites that extended more in the dorsal ( $370 \pm 157 \mu\text{m}$ ) than the ventral ( $205 \pm 69 \mu\text{m}$ ) direction (t-test,  $p = 0.047$ ). Moreover, all cells located in the dorsal portion of the BNST-AM ( $n = 4$ ) contributed ventrally directed axons (Fig. 4.9B1-2, AM). In contrast, cells in other parts of BNST-A displayed no consistent morphological polarization (Fig. 4.9B1-2, AL, AV). Of note, whereas the dendritic arbors of BNST-AL ( $n = 19$ ) and AM ( $n = 12$ ) neurons were typically confined to the BNST region where their soma was located, BNST-AV neurons often (4 of 7) had dendrites that extended dorsally beyond the anterior commissure and into BNST-AM or AL. This suggests that interregional connections targeting BNST-AL or AM neurons typically depended on axons that extended beyond the BNST sector where the parent soma was located. In contrast, for BNST-AV neurons, this was not necessarily the case.

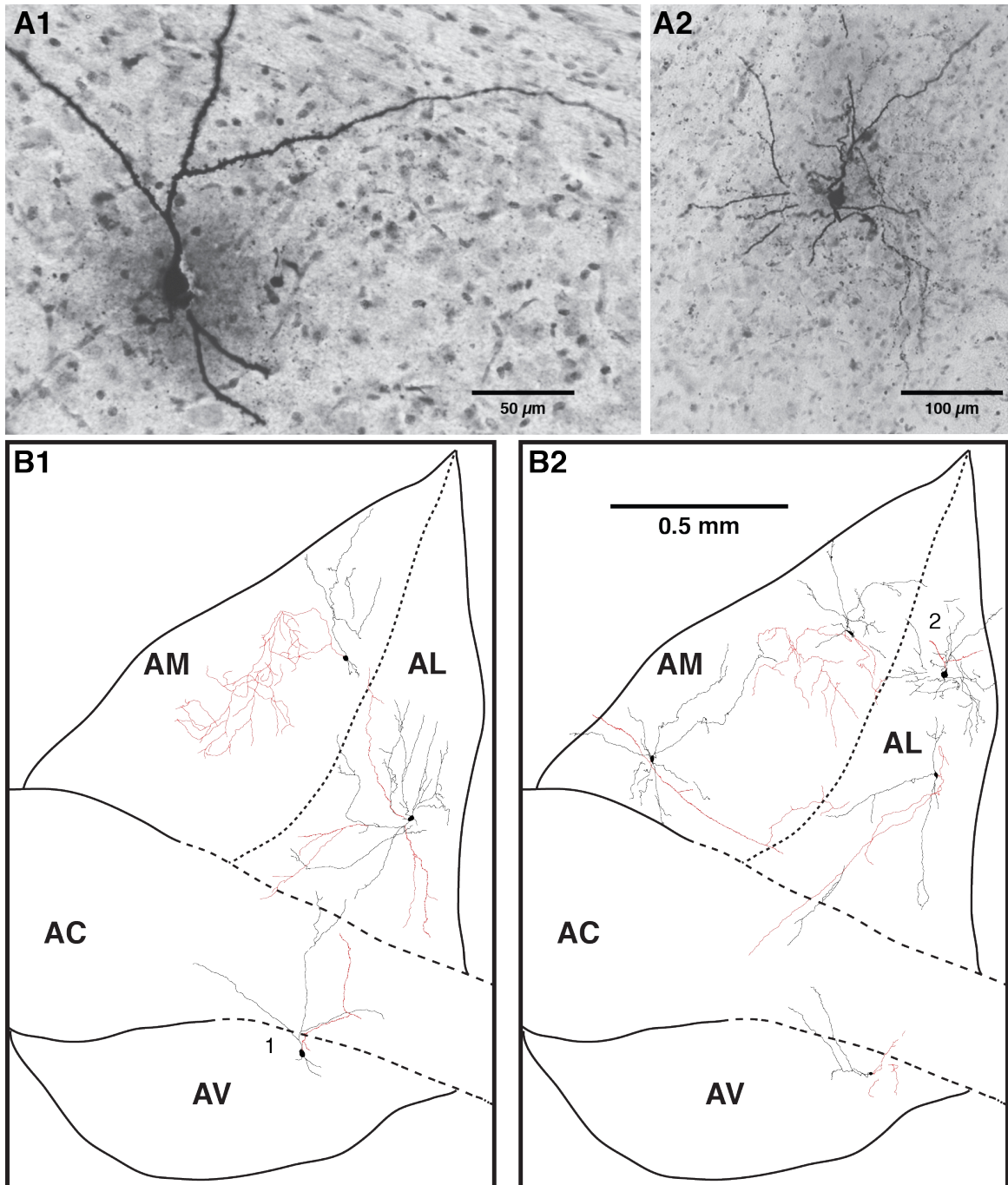


**Figure 4.9.** Morphological correlates of intrinsic connectivity. **(A)** Photomicrographs showing examples of BNST neurons labeled with biocytin (**A1**, BNST-AV; **A2**, BNST-AL). **(B)** Drawings of eight BNST-A neurons (red, axons; black, somata and dendrites). The neurons labeled 1 in B1 and 2 in B2 are the same cells as shown in A1 and A2, respectively. Note that because all our recordings were performed in the anterior portion of BNST, the rostrocaudal position of recorded cells did not vary much in our experiments ( $\pm 250 \mu\text{m}$ ).

#### 4.4. Summary of results

The intrinsic connections of BNST-A were studied using patch recordings and GU *in vitro*. UV light was delivered at small BNST-A sites in a grid-like pattern while monitoring evoked responses in different BNST-A regions. Overall, GU elicited GABAergic IPSPs more frequently than EPSPs. The incidence of intra-regional connections was higher than inter-regional links. With respect to the latter, asymmetric connections were seen between different parts of BNST-A. Indeed, while reciprocal connections were found between BNST-AL and AM, BNST-AL to AM connections were more frequent than in the opposite direction. Similarly, while GU in BNST-AM or AL often elicited IPSPs in BNST-AV cells, the opposite was rarely seen. Within BNST-AM, connections were polarized with dorsal GU sites eliciting IPSPs in more ventrally located cells more frequently than the opposite. This trend was not seen in other regions of BNST. Consistent with this, most BNST-AM cells had dorsally directed dendrites and ventrally ramified axons whereas this morphological polarization was not seen in other parts of BNST-A. Overall, our results reveal a hitherto unsuspected level of asymmetry in the connections within and between different BNST-A regions, implying a degree of inter-dependence in their activity. See chapter VI for a complete discussion of the findings obtained in this chapter.

## **CHAPTER V**

**Altered synaptic responsiveness of BNST-A neurons in resilient  
and PTSD-like rats**

## 5.1. Rationale

A highly conserved network of brain structures regulates fear/anxiety in mammals. Many of these structures display abnormal activity levels in PTSD. However, some of them, like the BNST, lie beneath the spatial resolution of human neuroimaging techniques. As a result, there is no human data about potential BNST contributions to PTSD.

To shed light on this question, in this chapter I used a well-characterized rat model of PTSD. In this model, Lewis rats are subjected to a species-relevant threatening experience, predatory threat, involving exposure to cat smell (Cohen et al., 2006a, b). Following predatory threat, a subset of rats (termed “PTSD-like” rats) develops severe and persistent (>2 weeks) behavioral manifestations of anxiety that includes extremely compromised exploratory behavior and increased startle (Cohen et al., 2006a, 2006b). Importantly, this model reproduces salient features of the human syndrome. For instance, human twin studies have shown that PTSD is characterized by (1) a fear extinction deficit that develops *after* trauma (Milad et al., 2008) and (2) a hippocampal-dependent allocentric spatial processing deficit that *predates* trauma (Gilbertson et al., 2002, 2007). The Lewis rat model of PTSD reproduces these two deficits, including their different temporal relationship to trauma (Goswami et al., 2010, 2012).

In the following experiments, I examined the physiological alterations of BNST-A neurons after Lewis rats underwent predatory threat using patch recordings *in vitro*. We compared the intrinsic and synaptic responsiveness of BNST-A neurons in the different regions in resilient versus PTSD-like rats.

## 5.2. Brief overview of methods

Upon delivery, adult male Lewis rats (200-225 g upon delivery) were group-housed for three days. They were then housed individually and habituated to handling for four days prior to the experiments. Figure 5.1A describes the overall timeline of the experiments. Rats were first subjected to predator threat and, seven days later, tested on the EPM, a well-accepted behavioral test of anxiety. Depending on their behavior in the EPM, rats were then classified as “PTSD-like” or “Resilient”, according to the criteria described below. One to three days later, the rats were anesthetized, their brains extracted, and coronal slices of the BNST prepared. Visually guided patch-clamp recordings of BNST neurons were then obtained by an investigator that was blind to the rats’ phenotype.

Chapter II, section 2.4, described the behavioral procedures for these experiments. Briefly, Lewis rats were exposed for 10 minutes to soiled cat litter. Predator odors are extremely potent stimuli: they can be used as unconditioned stimuli to support cued or contextual fear conditioning (Blanchard et al., 2001; McGregor et al., 2002). One week after, anxiety levels were assessed in the EPM. Their behavior was recorded by video camera and scored offline. The criterion to count an arm entry required the rat to have all four paws into the arm. We used exploratory behavior in the EPM to distinguish Resilient from PTSD-like rats. Rats with extremely compromised exploratory behavior, that is spending *none* of the available time in the EPM’s open arms, were classified as PTSD-like. Rats exploring the open and closed arms were classified as Resilient. Previously (Cohen et al., 2006b; Goswami et al., 2010), it was reported that predatory threat

exposure greatly increased the incidence of the PTSD-like phenotype in the EPM: from around 10% in rats exposed to clean litter to nearly 50% after predatory threat. Reproducing these earlier observations, 45% of our rats were classified as PTSD-like in the present study. Three days after the EPM test, brain slices from BNST-A were prepared following the procedure described in section 2.1 in the methods chapter.

To activate synaptic inputs to the recorded cells, stimulating electrodes were positioned in the stria terminalis (ST). To minimize variability, we always selected the same coronal level of BNST, at the level of the crossing of the anterior commissure, and positioned the stimulating electrodes at the same distance from the ventricle. Unless otherwise noted, electrical stimuli (100  $\mu$ s) were delivered at a low frequency (0.1 Hz), in a range of intensities (100-600  $\mu$ A), and from a membrane potential of -65 mV. At least three stimuli were delivered at each intensity and responses averaged. The data was analyzed off-line with the software IGOR (Wavemetrics, Oregon), clampfit (Axon instruments, Foster City, CA), and custom software written using Numpy and Scipy (<http://www.scipy.org>). Values are expressed as means  $\pm$  SEM.

### **5.3. Results**

Lewis rats ( $n = 83$ ) were subjected to predatory threat and tested on the EPM one week later (Fig. 5.1A). Rats with extremely compromised exploratory behavior (zero time in the open arms of the EPM) were categorized as PTSD-like (45% or 37 of 83) and the others as resilient (55% or 46 of 83). One to three days

later, the rats were anesthetized, their brains extracted, and coronal BNST slices prepared for visually guided patch clamp recordings (Fig. 5.1B). We focused on the anterior BNST region (BNST-A) because it has been most frequently implicated in fear and anxiety (reviewed in Walker et al., 2009a).

Our experiments aimed to determine whether the intrinsic or synaptic responsiveness of BNST-A cells differs depending on the rats' phenotype. We recorded 163 neurons in three different BNST-A regions (Fig. 5.1B and Table 5.1). Indeed, the BNST is in fact a collection of nuclei (as many as 18 according to Ju and Swanson, 1989) that form contrasting connections with fear effector neurons (Bota et al., 2012). However, there is much disagreement regarding the exact number and location of these nuclei (see Ju and Swanson, 1989; Moga et al., 1989). Compounding this problem, individual BNST nuclei cannot be identified with precision in living slices. Therefore, we used a simpler parcellation BNST-A in three regions, based on the position of major fiber bundles that can be easily identified in trans-illuminated slices (Fig. 5.1B): the AC, dividing the BNST-A in dorsal and ventral (BNST-AV) sectors, and the intra-BNST component of the stria terminalis, subdividing the dorsal portion in medial (BNST-AM) and lateral (BNST-AL) regions.

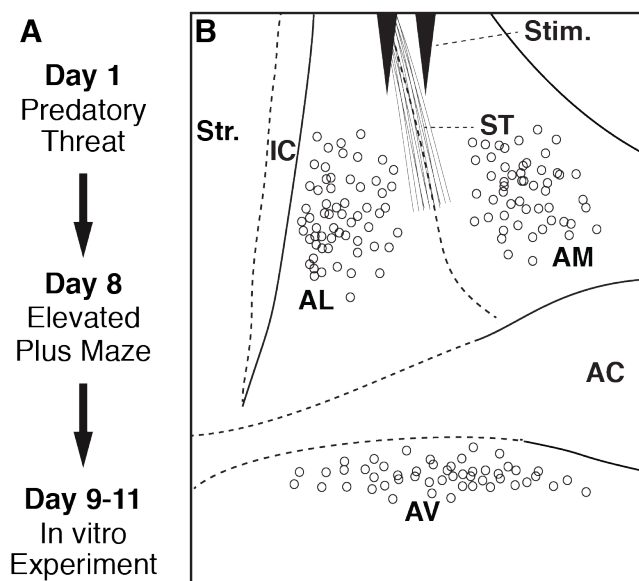


**Figure 5.1.** Experimental paradigm and recording sites. **(A)** Timeline of the experiments. **(B)** Scheme showing stimulation (stim.) and recording (circles) sites. To activate inputs to BNST-A neurons, a pair of tungsten electrodes was positioned in the stria terminalis (ST). Visually-guided patch clamp recordings were performed in three different BNST-A regions: anterolateral (AL), anteromedial (AM), and anteroventral (AV). Other abbreviations: AC, anterior commissure; IC, internal capsule; Str., Striatum.

The following is based on samples of 61 BNST-AL (Resilient,  $n = 33$ ; PTSD-like,  $n = 28$ ), 52 BNST-AM (Resilient,  $n = 27$ ; PTSD-like,  $n = 25$ ), and 50 BNST-AV neurons (Resilient,  $n = 24$ ; PTSD-like,  $n = 26$ ). These cells had stable resting potentials negative to  $-60$  mV and generated overshooting action potentials. For each BNST region, at least 12 rats of each phenotype were used. We first compare the passive properties and incidence of physiological cell types between resilient and PTSD-like rats and then consider their synaptic responsiveness.

### 5.3.1. Incidence, passive properties, and spike characteristics of BNST-A neurons in resilient vs. PTSD-like rats

In chapter III, I described that the BNST-A contains as many as five different physiological cell types (Hammack et al., 2007; Francesconi et al., 2009; Szucs et al., 2010; Rodriguez-Sierra et al., 2013). In decreasing order of incidence (Table 5.1), these cell types are LTB cells, RS cells, fIR cell, SA cells, and LF neurons (see section 3.3). Unfortunately, whether there is a relationship between the physiological properties of BNST-A neurons and their transmitter content is currently unclear. Indeed, most BNST-A neurons, including output cells, are GABAergic neurons (Cullinan et al., 1993; Sun and Cassell, 1993; Polston et al., 2004; Poulin et al., 2009) that express a number of peptides in various combinations (Woodhams et al., 1983). A few glutamatergic cells have also been identified in BNST-AM and AV (Poulin et al., 2009; Kudo et al., 2012), but most are intermingled with the prevalent GABAergic neurons. Thus, it is likely that the vast majority of the cells we recorded belong to the prevalent class of GABAergic neurons, a conclusion supported by a recent study that correlated physiological properties and GAD67 mRNA expression in single BNST-A cells (Hazra et al., 2011).

As detailed in Table 5.1, we found no phenotype-related variations in the incidence of the physiological cell types (Chi-square tests,  $p \geq 0.51$ ). Because three of the five cell types are rare, we focused our comparisons of passive properties and spike characteristics on the two prevalent classes of BNST-A neurons: regular spiking and low-threshold bursting cells. As detailed in Tables

5.2-5.7, we found no significant differences between the two rat phenotypes (Kruskal-Wallis one-way ANOVAs).

Table 5.1 *Incidence of BNST-A cell types in resilient and PTSD-like rats*

Cell Type	BNST-AL		BNST-AM		BNST-AV	
	Resilient %	PTSD-like %	Resilient %	PTSD-like %	Resilient %	PTSD-like %
LTB	42.4	35.7	81.5	68	50	65.4
RS	42.4	46.4	14.8	20	29.2	23
fIR	12.1	10.7	3.7	12	0	3.8
LF	3	7.1	0	0	0	0
SA	0	0	0	0	20.8	7.7

### 5.3.2. Synaptic responsiveness of BNST-A neurons in resilient vs. PTSD-like rats

To study the synaptic responsiveness of BNST-A neurons, we positioned a pair of stimulating electrodes in the stria terminalis (ST; Fig. 5.1B). This fiber bundle carries inputs from the main afferent of BNST, the amygdala. Indeed, the BNST-A receives very strong glutamatergic and GABAergic inputs from the basal and central nuclei of the amygdala, respectively (Krettek and Price, 1978a; Sun and Cassell, 1993; Dong et al., 2001a). Therefore, we activated these axons at a low frequency (0.1 Hz) by delivering brief (100  $\mu$ s) electrical stimuli in a range of intensities (0.1-0.6 mA) through the ST electrodes. At least 3 stimuli were delivered at each intensity and averaged independently. These tests were carried out at a membrane potential of -65 mV, as determined by intracellular current injection. When the ST stimuli elicited a mixture of sub- and supra-threshold responses, more stimuli were applied and the two types of responses were considered separately.

As described below, we found marked differences in synaptic responsiveness of BNST-A neurons between the two rat phenotypes. However, the polarity of these differences was expressed in a region-specific fashion. Moreover, these differences were expressed similarly in the various physiological cell types. Thus, for simplicity, the results obtained in all neurons are pooled below.

### 5.3.3. BNST-AL neurons

The synaptic responsiveness of BNST-AL neurons was *lower* in PTSD-like than resilient rats (Fig. 5.2). Indeed, the amplitude of ST-evoked IPSPs was significantly higher in BNST-AL cells from PTSD-like than resilient rats (Fig. 5.2A; repeated measure ANOVA,  $F = 8.821$ ,  $P = 0.006$ ; post-hoc t-test,  $p = 0.012$ ). Although there was a trend for ST-evoked EPSPs to have lower amplitudes in BNST-AL neurons from PTSD-like than resilient rats (Fig. 5.2A), the difference did not reach significance ( $F = 2.4$ ,  $P = 0.07$ ). Consistent with this, the slope of ST-evoked EPSPs did not differ significantly between the two rat phenotypes (Fig. 5.2B). Despite the similar properties of ST-evoked EPSPs in the two rat phenotypes, the likelihood that ST stimuli would elicit spiking was significantly higher in neurons from resilient than PTSD-like rats (Fig. 5.2C). Overall, these results suggest that differences in the potency of ST-evoked inhibition contribute to reduce the orthodromic responsiveness of BNST-AL neurons in PTSD-like relative to resilient rats.

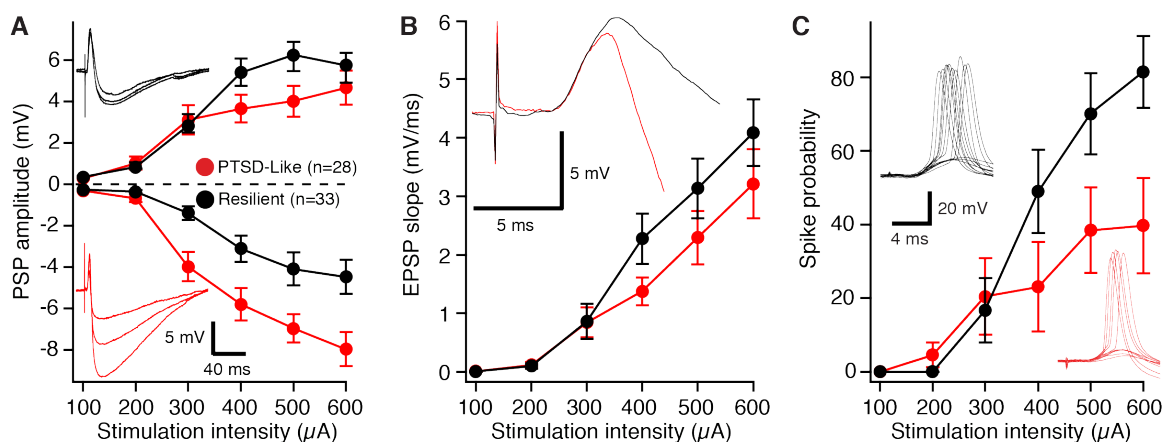


**Figure 5.2.** Synaptic responsiveness of BNST-AL neurons to ST stimuli in resilient (black) and PTSD-like (red) rats. In panels **A-C**, the x-axis represents stimulation intensity whereas the y-axis shows **(A)** the amplitude of evoked EPSPs and IPSPs (positive and negative values, respectively), **(B)** EPSP slopes (measured in the first 2 ms), and **(C)** the proportion of trials eliciting orthodromic spikes. Insets show representative examples of evoked responses for neurons recorded in resilient (black) and PTSD-like rats (red).

Table 5.2 *Physiological Properties of RS cells in BNST-AL* (values are means  $\pm$  SEM)

	n	Rest (mV)	R <sub>in</sub> (M $\Omega$ )	Time Constant (ms)	Action Potential		
					Threshold (mV)	Amplitude (mV)	Duration (ms)
Resilient	13	-64 $\pm$ 1.2	563.9 $\pm$ 39.4	23.2 $\pm$ 2.4	-41.4 $\pm$ 1.7	84.5 $\pm$ 2	1.05 $\pm$ 0.05
PTSD-like	14	-64.7 $\pm$ 1.1	562.7 $\pm$ 30	22.3 $\pm$ 3.1	-42.5 $\pm$ 0.9	79.7 $\pm$ 1.2	1.17 $\pm$ 0.03

#### 5.3.4. BNST-AM neurons

Opposite to BNST-AL neurons, the responsiveness of BNST-AM cells was *higher* in PTSD-like than resilient rats. Indeed, the amplitude (Fig. 5.3A) and slope (Fig. 5.3B) of ST-evoked EPSPs were significantly higher in neurons recorded from PTSD-like than resilient rats (EPSPs,  $F = 5.762$ ,  $P = 0.02$ ; Slope,  $F = 4.95$ ,  $P = 0.03$ ; post-hoc t-test,  $p = 0.021$ ), with no difference in IPSP amplitudes (Fig. 5.3A;  $F = 0.179$ ,  $P = 0.67$ ). Accordingly, the probability that ST

stimuli would elicit supra-threshold responses was significantly higher in PTSD-like than resilient rats (Fig. 5.3C;  $F = 5.09$ ,  $P = 0.028$ ; post-hoc t-test,  $p = 0.029$ ).

Table 5.3 *Physiological Properties of LTB cells in BNST-AL* (values are means  $\pm$  SEM)

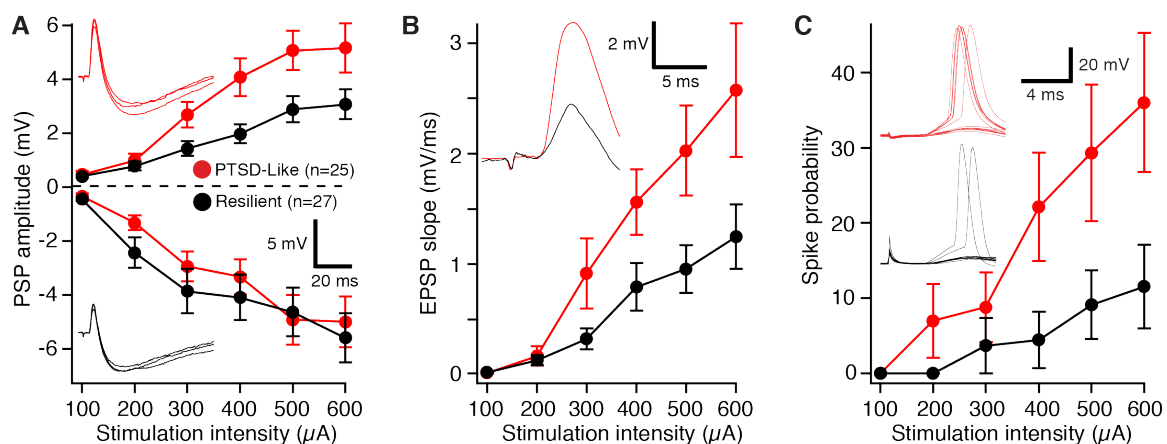
	n	Rest (mV)	Rin (M $\Omega$ )	Time Constant (ms)	Action Potential		
					Threshold (mV)	Amplitude (mV)	Duration (ms)
Resilient	10	-63.67 $\pm$ 1.2	577.6 $\pm$ 55.9	22.7 $\pm$ 2.9	-42 $\pm$ 1.4	79.7 $\pm$ 1.5	1.29 $\pm$ 0.1
PTSD-like	14	-62.17 $\pm$ 1.5	613.4 $\pm$ 50.8	20.6 $\pm$ 1.8	-41.4 $\pm$ 1.2	78.2 $\pm$ 1.3	1.09 $\pm$ 0.06

Table 5.4 *Physiological Properties of RS cells in BNST-AM* (values are means  $\pm$  SEM)

	n	Rest (mV)	Rin (M $\Omega$ )	Time Constant (ms)	Action Potential		
					Threshold (mV)	Amplitude (mV)	Duration (ms)
Resilient	4	-59 $\pm$ 4	855 $\pm$ 144.6	33.9 $\pm$ 4.8	-38.5 $\pm$ 3.6	69.9 $\pm$ 1.1	1.07 $\pm$ 0.31
PTSD-like	5	-53.1 $\pm$ 4.5	725.2 $\pm$ 229	40.9 $\pm$ 8.4	-42.4 $\pm$ 2	73.7 $\pm$ 2.3	1.38 $\pm$ 0.17

Table 5.5 *Physiological Properties of LTB cells in BNST-AM* (values are means  $\pm$  SEM)

	n	Rest (mV)	Rin (M $\Omega$ )	Time Constant (ms)	Action Potential		
					Threshold (mV)	Amplitude (mV)	Duration (ms)
Resilient	22	-55 $\pm$ 1.3	674.1 $\pm$ 54.4	34.5 $\pm$ 3.6	-39.5 $\pm$ 0.8	76.2 $\pm$ 0.8	1.45 $\pm$ 0.12
PTSD-like	17	-58.9 $\pm$ 1.5	692.8 $\pm$ 79.2	36.4 $\pm$ 3.5	-39.2 $\pm$ 1.1	75.8 $\pm$ 1	1.39 $\pm$ 0.08



**Figure 5.3.** Synaptic responsiveness of BNST-AM neurons to ST stimuli in resilient (black) and PTSD-like (red) rats. In panels **A-C**, the x-axis represents stimulation intensity whereas the y-axis shows (**A**) the amplitude of evoked EPSPs and IPSPs (positive and negative values, respectively), (**B**) EPSP slopes (measured in the first 2 ms), and (**C**) the proportion of trials eliciting orthodromic spikes. Insets show representative examples of evoked responses for neurons recorded in resilient (black) and PTSD-like rats (red).

### 5.3.5. BNST-AV neurons

Similar to BNST-AM cells, but opposite to BNST-AL neurons, the responsiveness of BNST-AV cells was *higher* in PTSD-like than in resilient rats. This was evidenced in the significantly higher amplitude (Fig. 5.4A) and slope (Fig. 5.4B) of ST-evoked EPSPs in PTSD-like rats (EPSPs,  $F = 9.65$ ,  $P = 0.003$ ; Slope,  $F = 9.309$ ,  $P = 0.004$ ; post-hoc t-test,  $p = 0.006$ ), with again no difference in IPSP amplitudes between the two rat phenotypes (Fig. 5.4B;  $F = 0.425$ ,  $p = 0.51$ ). Paralleling these results, spiking probability in response to ST stimuli was significantly higher in PTSD-like than resilient rats (Fig. 5.4C;  $F = 11.51$ ,  $p = 0.001$ ; post-hoc t-test,  $p = 0.006$ ).

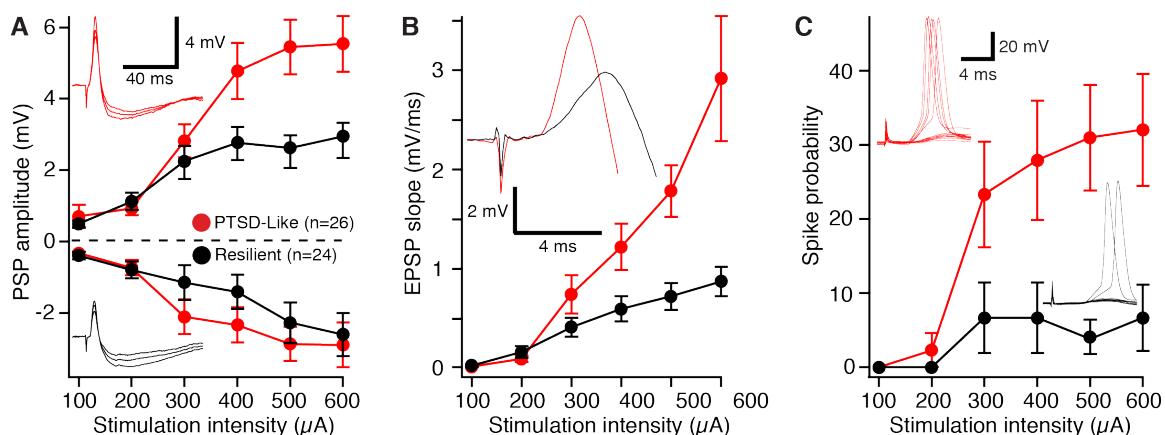


**Figure 5.4.** Synaptic responsiveness of BNST-AV neurons to ST stimuli in resilient (black) and PTSD-like (red) rats. In panels **A-C**, the x-axis represents stimulation intensity whereas the y-axis shows (A) the amplitude of evoked EPSPs and IPSPs (positive and negative values, respectively), (B) EPSP slopes (measured in the first 2 ms), and (C) the proportion of trials eliciting orthodromic spikes. Insets show representative examples of evoked responses for neurons recorded in resilient (black) and PTSD-like rats (red).

Table 5.6 *Physiological Properties of RS cells in BNST-AV* (values are means  $\pm$  SEM)

	n	Rest (mV)	R <sub>in</sub> (M $\Omega$ )	Time Constant (ms)	Action Potential		
					Threshold (mV)	Amplitude (mV)	Duration (ms)
Resilient	7	-56.2 $\pm$ 5.4	780.6 $\pm$ 114.6	42.8 $\pm$ 5.5	-39 $\pm$ 2.8	73.4 $\pm$ 1.8	1.22 $\pm$ 0.16
PTSD-like	6	-51.5 $\pm$ 1.1	887.8 $\pm$ 128.2	31.6 $\pm$ 3.2	-36 $\pm$ 1.9	75.1 $\pm$ 2.2	1.11 $\pm$ 0.16

Table 5.7 *Physiological Properties of LTB cells in BNST-AV* (values are means  $\pm$  SEM)

	n	Rest (mV)	R <sub>in</sub> (M $\Omega$ )	Time Constant (ms)	Action Potential		
					Threshold (mV)	Amplitude (mV)	Duration (ms)
Resilient	12	-57.8 $\pm$ 1.67	621.8 $\pm$ 69.3	31.2 $\pm$ 1.8	-37.9 $\pm$ 1.8	74.0 $\pm$ 1	1.1 $\pm$ 0.07
PTSD	17	-56.3 $\pm$ 1.81	807.5 $\pm$ 59	35.2 $\pm$ 4.2	-39 $\pm$ 1	74.8 $\pm$ 1	1.29 $\pm$ 0.09

### 5.3.6. Mechanisms underlying phenotype-related differences in synaptic responsiveness

To determine whether the phenotypic differences in EPSP properties described above are dependent on a presynaptic mechanism, we compared the amount of paired-pulse facilitation (PPF) in the two groups (Fig. 5.5). In this analysis (Katz and Miledi, 1968), two identical stimuli are applied in rapid succession. PPF magnitude was repeatedly shown to be inversely proportional to transmitter release probability: manipulations that increase release probability decrease PPF and conversely (Creager et al., 1980; Manabe et al., 1993; reviewed in Zucker and Regehr, 2002).

Therefore, in the presence of picrotoxin (100  $\mu$ M) and in voltage-clamp mode, we applied two ST stimuli separated by 50 ms and computed the ratio of the EPSC amplitude elicited by the two stimuli (EPSC2/EPSC1) in BNST- AM (Fig. 5.5A), and AV (Fig. 5.5B) neurons from PTSD-like and resilient rats. In both types, the paired pulse ratio did not differ significantly between the two groups (Fig. 5.5A; t-tests, AM,  $p = 0.8$ ; AV,  $p = 0.1$ ).

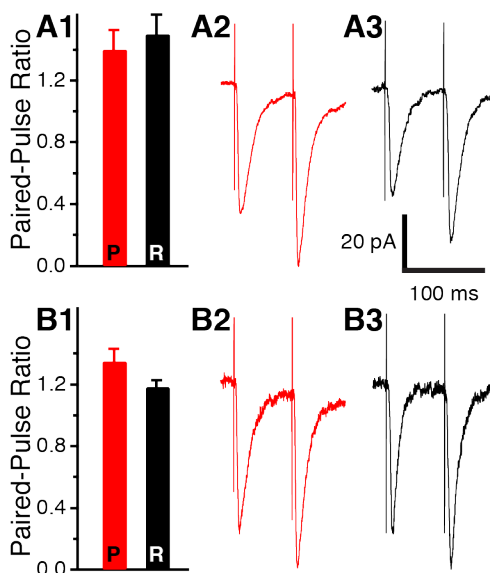


**Figure 5.5.** Properties of paired-pulse facilitation at glutamatergic inputs to BNST-AM (**A**,  $n = 8$ ) and AV (**B**,  $n = 8$ ) neurons does not vary as a function of the rats' phenotype. (**1**) Ratio of second to first EPSC amplitudes. Representative examples of responses evoked by two ST stimuli separated by 70 ms in neurons from PTSD-like (**2**) and resilient (**3**) rats.

#### 5.4. Summary of results

A highly conserved network of brain structures regulates fear/anxiety in mammals. Many of these structures display abnormal activity levels in PTSD. However, some of them, like the BNST, lie beneath the spatial resolution of human neuroimaging techniques. Therefore, we used a well-characterized rat model of PTSD to compare the properties of BNST neurons in resilient vs. PTSD-like rats using patch recordings *in vitro*. In this model, a persistent state of extreme anxiety is induced in a subset of susceptible rats following predator threat. Previously, it was found that the AL and AM portions of BNST-A exert anxiolytic and anxiogenic influences, respectively (Haufler et al., 2013). Consistent with this, the excitability of AL neurons was lower in PTSD-like than resilient rats whereas AM cells showed the opposite. Overall, these findings

suggest that BNST contributions to fear/anxiety are increased in PTSD-like rats. See chapter VI for a complete discussion of the findings obtained in this chapter.

## **CHAPTER VI**

### **General Discussion**

The work presented in this thesis was undertaken to investigate the functional organization of BNST-A. Previous studies have examined the electroresponsive properties of BNST-AL but not other regions. This thesis broadens our understanding of BNST-A by systematically studying the electroresponsive properties of neurons throughout BNST-A. Further, I investigated the intrinsic connections in BNST-A, opening future research avenues aiming at understanding the neural computations performed in intrinsic BNST-A circuits. Finally, by comparing the excitability of BNST-A neurons in resilient vs. PTSD-like rats, this thesis contributed towards our understanding of the role of BNST-A in fear and anxiety.

In the following sections, I will discuss the significance of my findings for our understanding of BNST-A and its role in fear, anxiety, and stress.

### **6.1. Physiological properties of BNST-A neurons**

In many brain regions, a systematic relationship was found between the physiological properties, firing pattern, morphology, connections, and transmitter content of different neuronal types (e.g. thalamus, Steriade and Llinas 1998; striatum, Tepper and Bolam 2004). This knowledge has proven invaluable in interpreting extracellularly recorded unit activity. In contrast, our understanding of BNST is far less advanced. Thus, the present study was undertaken to characterize the electroresponsive and morphological properties of BNST-A neurons. Our experiments revealed that two cell types (RS, LTB) account for the majority of neurons in different BNST-A regions. Three additional physiological

cell types were also identified but their incidence was lower and varied markedly depending on the BNST-A region. Surprisingly, the physiological properties of BNST-A cells showed little correlation with their morphology.

#### 6.1.1. Prior studies on the cellular physiology of BNST-A neurons

The electroresponsive properties of BNST neurons have received little attention so far. Indeed, most electrophysiological studies have focused on other aspects of BNST physiology such as the influence of various peptides/transmitters (Grueter and Winder, 2005; McElligott and Winder, 2008; Shields et al., 2009; Puente et al., 2010; Krawczyk et al., 2011a; Nobis et al., 2011; Li et al., 2012; Lungwitz et al., 2012), particularly CRF (Kash and Winder 2006; Gafford et al., 2012; Oberlander and Henderson 2012; Ide et al., 2013; Silberman et al., 2013), mechanisms of addiction and relapse to drug seeking (Dumont and Williams 2004; Dumont et al., 2005, 2008; Davis et al., 2008; Kash et al., 2008a, 2008b, 2009; Grueter et al., 2008; Krawczyk et al., 2011b; Conrad et al., 2012), synaptic plasticity (Weitlauf et al., 2005), and the impact of stress (Conrad et al., 2011).

Although a few studies compared the passive properties of neurons in different BNST-A sectors (e.g. Egli and Winder 2003), most did not examine the temporal dynamics of current-evoked spiking. To our knowledge, a systematic physiological characterization of BNST-A neurons has only been performed in the AL region in general (Rainnie 1999; Hammack et al., 2007; Guo et al., 2009, 2012; Hazra et al., 2011, 2012) and its juxtacapsular sector in particular

(Francesconi et al., 2009; Szucs et al., 2010). Three BNST-AL cell types were distinguished, with marked differences in their incidence: LTB cells (Type-II, 55%) and regular spiking neurons that display time-dependent (Type-I, 29%) or near instantaneous (fIR, 16%) inward rectification in the hyperpolarizing direction (Hammack et al., 2007).

This classification of BNST-AL neurons found support in a single-cell RT-PCR study where the alpha sub-unit expression profile of key ionic channels correlated with the electrophysiological classification (Hazra et al., 2011). Moreover, another study revealed that serotonergic receptor subtypes were differentially expressed in the three cell types. For instance, 5HT-2C receptors were almost exclusively expressed by Type-III neurons whereas 5HT-7 receptors were commonly expressed by Type-I and II neurons but not Type-III cells (Guo et al., 2009; Hazra et al., 2012).

#### 6.1.2. Similarities and differences in the physiological properties of neurons in different parts of BNST-A

The present study corroborates the findings of Rainnie and colleagues regarding the dominant cell types found in BNST-AL and extends them by showing that the same classes of neurons prevail in other BNST-A regions. Within BNST-AL, our results closely match what Rainnie and colleagues reported except for resting potential and  $R_{in}$ . However, differences in methodology (correction or not for junction potential; how the slices were prepared) or age/strain of the rats are probably responsible. Within BNST-AM and AV, more

than 80% of neurons were RS or LTB cells. However, there were significant inter-regional variations in some of their properties. For LTB cells, the number of spikes per rebound burst and the peak instantaneous firing rate reached during these bursts were higher in BNST-AV and AM cells than in BNST-AL neurons. Moreover, LTB cells accounted for a higher proportion of neurons in BNST-AV and AM than in BNST-AL. Also, for RS and LTB cells, the magnitude of the depolarizing sag, presumably due to  $I_H$ , was on average lower in BNST-AV and AM than in BNST-AL. Also noteworthy, the  $R_{in}$  of RS and LTB cells was significantly lower in BNST-AL than in the other two regions. Finally, the incidence of fIR neurons was much lower in BNST-AV and AM than in BNST-AL. In the latter region, fIR neurons were concentrated along the internal capsule, in a region that appears to overlap with the juxtacapsular nucleus. However, outside this region, the incidence of fIR neurons was homogeneously low in all three BNST-A sectors, again consistent with the findings of Rainnie and colleagues.

In addition to the cell classes identified previously, we encountered two hitherto unreported types of neurons, both of which showed little or no evidence of  $I_H$  or  $I_T$ : LF neurons found only in BNST-AL (4% of the cells) and SA neurons only seen in BNST-AM (8% of the cells). In response to supra-threshold depolarizations, LF neurons displayed a delay to firing that was especially pronounced when the current injection was performed from negative to -75 mV. During this delay, the membrane potential depolarized gradually, a behavior that likely reflects the time-dependent inactivation of a slow, A-like potassium current ( $I_D$ ; Storm 1988). Finally, SA neurons spontaneously generated thin (<0.8 ms)

spikes at a rate of around 4 Hz from rest. When depolarized, SA neurons displayed no evidence of spike frequency accommodation (as seen in RS, LTB, and fIR neurons) or acceleration (as seen in LF cells). Instead, they maintained a stable firing rate that augmented with depolarization.

### 6.1.3. Morphological correlates of electroresponsive properties

Three prior Golgi studies described the morphological properties of BNST-A neurons (McDonald 1983; Larriva-Sahd 2004, 2006). For the juxtacapsular nucleus, there is consensus that the majority of neurons are small cells with spiny and often bipolar dendritic trees (McDonald 1983; Larriva-Sahd 2004), consistent with our results. For BNST-AL, there is also agreement that the dominant cell type cell is characterized by an ovoid soma from which emerge 4-5 dendrites that branch several times, are aspiny proximally, moderately to densely spiny more distally, and often exhibit dendritic varicosities (McDonald 1983; Larriva-Sahd 2006). McDonald (1983) likened these cells to the medium spiny neurons found in the central lateral amygdala. However, Larriva-Sahd (2006), focusing on the oval sub-region of BNST-AL, identified 10 additional types of neurons. Although the text of his paper does not comment on more ventrally located-BNST-AL neurons, his figures 3-5 indicate that the proportion of densely spiny neurons is substantially lower in this sub-region. Instead, similar to what McDonald (1983) reported for BNST-AM neurons, a majority of these cells contribute few dendritic branches that ramify sparingly and exhibit a low spine density.

Overall, these results closely match the properties and distribution of the two classes of biocytin-filled neurons we recovered. However, one feature, not reported previously, was that a proportion of cells appeared to contribute multiple axon-like processes that could emerge from multiple sites. These axon-like processes could emerge from somata or dendrites, in one case 200  $\mu\text{m}$  from the soma. Moreover, several cells contributed two or more axon-like processes emerging from different cellular compartments (soma and dendrite or different dendritic branches). Although novel for BNST, there are many precedents in the literature for dendritically-emerging axons. This was observed in many types of cerebellar, cortical, and hippocampal GABAergic neurons (Palay and Chan-Palay 1974; Amaral 1978; Feldman and Peters 1978; Gulyas et al., 1992) and in dopaminergic cells of the substantia nigra (Juraska et al., 1977; Preston et al., 1981; Tepper et al., 1987). In the latter cell type, action potentials are initiated in dendritically-emerging axons (Hausser et al., 1995), suggesting that in such cells, the main site of synaptic integration is not the soma but the dendritic segment near the point of axonal emergence. However, it is unclear whether the axon-like processes we saw in a proportion of BNST neurons truly are axons or extremely thin dendrites that bear varicosities. Unambiguous determination of their identity will require triple immunofluorescence for biocytin as well as dendritic and axonal markers such as MAP2 and synaptophysin.

Unfortunately, we found little correlation between the morphological and electroresponsive properties of BNST-A neurons. In Type I (RS) and II (LTB) neurons, the only morpho-physiological correlations we found were trivial ones

such as an inverse correlation between  $R_{in}$  and soma size. Both physiological cell types could display the morphology of the medium spiny class or the ones with long poorly branched aspiny dendrites.

While these negative results are disappointing, they are consistent with the marked phenotypic heterogeneity among BNST-A neurons. Indeed, BNST-A contains a small group of glutamatergic cells interspersed among a dominant population of GABAergic neurons (Esclapez et al., 1993; Sun and Cassell 1993; Day et al., 1999; Hur and Zaborszky 2005; Poulin et al., 2009; Kudo et al., 2012). Moreover, BNST-A neurons express numerous peptides than can coexist in various combinations (Woodhams et al., 1983). In light of these variations, and given that only two main morphological cell types prevail in BNST-A, one would expect that each morphological cell class includes multiple subsets of neurons with marked phenotypic variations between them.

Thus it appears that in contrast to the thalamus or striatum where physiological properties, firing patterns, and cellular identity are closely related, it will be more challenging to understand BNST-A. A promising approach would be to correlate projection site(s) with physiological and neurochemical properties. Also, given the prevalence of LTB cells in the three regions, it will be important to determine in what behavioral states these neurons fire tonically vs. in bursts. Given that BNST-AL sends strong GABAergic projections to BNST-AM and AV (chapter IV; Turesson et al., 2013), it is likely that these inhibitory inputs play a critical role in setting the firing mode of LTB cells in the other two regions.

## 6.2. Intrinsic BNST-A connections

It has been proposed that the BNST and the central amygdala are part of an anatomical entity termed the extended amygdala (Alheid and Heimer 1988; de Olmos and Heimer 1999). This concept is based on similarities in neuronal morphology and transmitter content (for a review, see McDonald 2003), common inputs from the basolateral amygdala (Krettek and Prince 1978a, 1978b; Paré et al., 1995; Savander et al., 1995; Dong et al., 2001a) as well as overlapping projections to a network of motor and autonomic brainstem nuclei thought to generate various aspects of fear/anxiety responses (Hopkins and Holstege 1978; Veening et al., 1984; Holstege et al., 1985; Dong et al., 2000; Dong and Swanson 2003, 2004, 2006a, 2006b, 2006c).

In contrast to the amygdala however, the physiological organization of the BNST is poorly understood. The BNST is comprised of several subnuclei with much disagreement regarding their exact number and location (Andy and Stephan 1964; De Olmos et al., 1985; Ju and Swanson 1989; Ju et al., 1989; Moga et al., 1989). However, it is commonly accepted that different BNST regions form contrasting connections with the rest of the brain. This suggests a degree of functional specialization within the BNST, raising the question of whether different BNST regions interact with each other or whether they constitute independent processing modules.

Experiments in chapter IV were undertaken to address this question, focusing on the intrinsic connections that exist in the anterior part of the BNST. Below, we summarize the pattern of intrinsic connections evidenced in the

present study and discuss these results in light of earlier findings regarding the anatomy and physiology of BNST-A. Because the incidence of inhibitory and excitatory connections varied as a function of the region contributing or receiving these intrinsic connections, our findings raise the possibility that both cooperative and competitive interactions take place within the BNST.

### 6.2.1. Nature of the synaptic connections

Several factors suggest that the vast majority of the synaptic connections evidenced in the present study are monosynaptic and had an intrinsic origin (the pre- and postsynaptic neurons were located within the BNST). All the glutamatergic EPSPs we elicited with the GU method were  $\leq 6$  mV in amplitude (mode of 1 mV). Since all the BNST neurons we recorded had a resting potential negative to -65 mV, it seems extremely unlikely that such low amplitude EPSPs could cause enough depolarization to reach spiking threshold ( $-49.8 \pm 0.3$  mV) in a neuron not directly exposed to uncaged glutamate. Indeed, our control experiments (Fig. 4.2) revealed that unless the UV light stimulus was applied directly over the recorded soma or the proximal portion of the dendritic tree, it never elicited spiking. As a result, it seems extremely unlikely that the responses we observed were polysynaptic. Regarding the intrinsic vs. extrinsic origin of the connections, the vast majority of the UV light stimuli used to uncage glutamate were applied entirely within the BNST. While some of the effective stimulation sites straddled BNST boundaries, they accounted for a minority of the connections we observed. Furthermore, many of these peripheral stimulation

sites were located in the internal capsule, which is largely devoid of neurons, and the lateral ventricle.

One confound we cannot completely exclude however, is the possibility that uncaged glutamate affected axon terminals contributed by neurons located in the BNST or elsewhere. Indeed, prior studies have revealed that the BNST contains a sub-population of GABAergic axon terminals expressing NMDA receptors (Gracy and Pickel 1995; Paquet and Smith 2000). Under this scenario, uncaged glutamate would bind to presynaptic NMDA receptors and cause sufficient depolarization to trigger GABA release. While this phenomenon cannot be responsible for the glutamatergic EPSPs we observed, it could account for some of the GABAergic IPSPs. However, for this effect to occur, the axon terminal expressing NMDA receptors and its postsynaptic target would have to be located where the light stimulus is applied. Thus, unless such receptors are expressed in the axons themselves (not only in terminals), this effect could only be involved in cases where both a direct response to uncaged glutamate and an IPSP were observed. However, such instances were rare in our database (<7.3% of the connections) and therefore cannot account for the pattern of results we obtained. Finally, while there is clear evidence that axon terminals in the BNST express metabotropic glutamate receptors (Grueter and Winder 2005; Grueter et al., 2006; Muly et al., 2007; Gosnell et al., 2011), it is unlikely that activation of these receptors by uncaged glutamate generated the fast synaptic events we examined because mGluRs are G-protein coupled receptors that exert slow modulatory effects, but do not mediate fast PSPs. Since BNST neurons express

a wide variety of peptides, it is conceivable that GU led to some peptide release. However, this possibility remains unclear at this time because we could see no electrophysiological manifestations of such release.

### 6.2.2. Overall pattern of intrinsic BNST-A connections

*Intraregional connections.* With respect to intraregional connections, a marked difference was found between the dorsal part of BNST-AM and the rest of BNST-A. In most of the BNST-A, intra-regional connections displayed no preferential directionality. However, in the dorsal part of BNST-AM, intrinsic connections had a predominant dorsoventral orientation (Fig. 6.1). Importantly, we found a parallel for this in the morphology of individual BNST-A neurons. Indeed, our reconstructions of biocytin-filled cells revealed that most BNST-AM neurons were morphologically polarized in a way consistent with the directionality of intrinsic connections. That is, their dendrites extended more in the dorsal than in the ventral direction and contributed axons that coursed ventrally. In contrast, neurons recovered from other sectors of the BNST-A showed no consistent orientation of their axons and dendrites.

Although a prior study examined the connectivity of the BNST-AM with *Phaseolus vulgaris*- leucoagglutinin (PHAL) (Dong and Swanson 2006a), it did not comment on the peculiar organization we observed in the dorsal part of the BNST-AM. However, this is likely due to technical limitations inherent to tracing techniques. In order to disclose the type of organization we observed with GU, one would need to perform extremely small tracer injections, which is nearly

impossible.

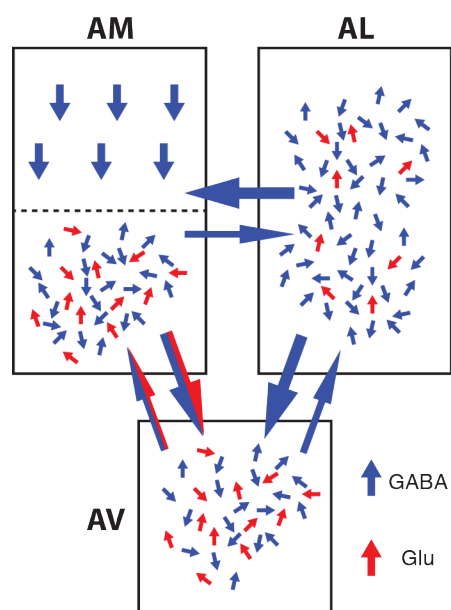


**Figure 6.1.** Overall pattern of intrinsic BNST-A connections revealed with GU. Red and blue arrows correspond to glutamatergic and GABAergic connections respectively. For intra-regional connections, the number of blue and red arrows approximates the relative frequency of inhibitory and excitatory connections, respectively. For inter-regional connections, the thickness of the arrows was adjusted to represent the relative incidence of connections.

Another finding that emerged from our study is that the relative incidence of GABAergic and glutamatergic connections varied markedly in the different regions examined. Although GABAergic connections were prevalent overall, in some BNST-A regions glutamatergic connections were nearly as frequent. The incidence of glutamatergic connections was lowest in the BNST-AL and dorsal part of BNST-AM. By contrast, in the BNST-AV and the ventral region of BNST-AM, they accounted for about half the connections (Fig. 4.9).

The varying incidence of GABAergic and glutamatergic connections in different BNST-A regions is consistent with the results of previous reports that used immunohistochemistry (Esclapez et al., 1993; Sun and Cassell 1993; Hur

and Zaborszky 2005) or in situ hybridization (Day et al., 1999; Poulin et al., 2009; Kudo et al., 2012) to study the distribution of neurons that are GABAergic (expressing mRNA for glutamic acid decarboxylase [GAD] 65 and/or 67) and/or glutamatergic (expressing mRNA for the vesicular glutamate transporter 2 – VGLUT2) in the BNST. Considered together, these studies indicate that GABAergic neurons are abundant in all divisions of the BNST-A whereas the incidence of glutamatergic neurons shows marked inter-regional variations. In particular, consistent with our observations, no (or very few) VGLUT2 positive cells were seen in the BNST-AL whereas a significant number was seen in the BNST-AV and AM.

*Interregional connections.* The connections between different BNST-A regions were asymmetric. That is, for all pairs of regions examined, connections were significantly more frequent in one direction than the other (Fig. 4.10). This was the case of all inter-regional projections involving the BNST-AL: higher incidence from BNST-AL to BNST-AM and AV than from the latter two to BNST-AL. Conversely, all inter-regional connections ending in the BNST-AV were stronger than the reciprocal connections: lower incidence from BNST-AV to BNST-AM and AL than from the latter two to BNST-AV.

This pattern of connections is consistent with the findings of earlier anterograde (Dong and Swanson 2004, 2006a) and retrograde (Shin et al., 2008) tracing studies. Indeed, these studies revealed that components of the BNST-AV receive convergent inputs from the BNST-AL and AM and that subregions of the BNST-AL and AM are reciprocally connected. However, it is difficult to compare

the relative strength of the connections evidenced here with that seen in tracing studies because the size of the various PHAL injection sites was not constant. Nevertheless, the results of Swanson and colleagues appear generally consistent with the notion that BNST-AL to AM connections (Dong and Swanson 2004) are stronger than in the opposite direction (Dong and Swanson 2006a). Also consistent with our findings, BNST-AL projections to BNST-AV (Dong and Swanson 2004) appear denser than in the opposite direction (Dong et al., 2001b).

Inter-regional connections also differed in the relative incidence of GABAergic and glutamatergic inputs (Fig. 4.10). Paralleling the intra-regional connections, the projections of BNST-AL to BNST-AM or AV were almost exclusively GABAergic. Similarly, return projections from BNST-AM and AV to BNST-AL were also characterized by a scarcity of glutamatergic connections. In contrast, the connections between BNST-AM and AV included both glutamatergic and GABAergic projections.

### 6.2.3 Functional implications of the intrinsic pattern of connectivity in BNST-A

The pattern intrinsic connectivity disclosed in the chapter IV implies that different BNST-A sectors do not act independently. In particular, because the projections of the BNST-AL to BNST-AM and AV are purely inhibitory and stronger than the reciprocating pathways, the BNST-AL is strategically positioned to determine, or at least modulate, activity levels in the rest of the BNST-A. This suggests an arrangement where the BNST-AL, via its inhibitory projections to

BNST-AM and AV, acts as a gating mechanism for many BNST-A outputs. When BNST-AL activity is high, this would tend to reduce firing rates in BNST-AM and AV neurons. Conversely, a reduction in BNST-AL activity could cause a positive (or self-reinforcing) feedback effect where disinhibition of BNST-AM from BNST-AL inputs would increase return inhibitory projections from BNST-AM to BNST-AL, resulting in a further disinhibition of the BNST-AM, and so on. In addition to these competitive interactions, our findings raise the possibility that other sectors of BNST-A entertain cooperative relations. Indeed, the high incidence of glutamatergic connections between the BNST-AV and ventral part of BNST-AM suggest that neurons in these two regions may mutually enhance their excitability.

At present, it is difficult to assess how significant the impact of intrinsic BNST-A connections might be. While the incidence of interregional connections was relatively low, it was likely underestimated because many connections, particularly the longer ones, are lost when slices are prepared. In addition, it is likely that intrinsic inputs ending in the distal dendrites of BNST neurons could not be detected due to electrotonic attenuation. Besides, the influence of intrinsic BNST connections will depend on a variety of factors including moment-to-moment variations in the activity of extrinsic afferents as well as modulatory inputs. In any event, the above considerations highlight the difficulty of interpreting lesion and pharmacobehavioral studies. Depending what exact BNST-A sector is lesioned or inactivated, opposite behavioral consequences can emerge.

### **6.3. Altered synaptic responsiveness of BNST-A neurons in a rat model of PTSD**

In chapter V, we studied the intrinsic and synaptic responsiveness of BNST-A neurons in a rat model of PTSD. In this model, a persistent state of extreme anxiety is induced in a subset of susceptible rats after exposure to an ethologically relevant stressor that mimics the type of life-and-death situation known to precipitate PTSD in humans. Thus, we compared the properties of BNST-A neurons in resilient vs. PTSD-like rats and observed region-specific differences in synaptic excitability. Overall, the excitability of BNST-AL neurons was lower in PTSD-like relative to resilient rats, whereas the opposite was seen in BNST-AM and AV neurons.

#### 6.3.1. Limitations of the *ex vivo* approach

Although investigating the synaptic responsiveness of BNST-A neurons in brain slices *in vitro* has substantial analytical power, this approach also has significant limitations. On the positive side, the *ex vivo* paradigm allows identification of phenotypic differences in neuronal excitability, independently of emotion and cognition. This is contrast with human functional imaging studies where differences in activity cannot be dissociated from ongoing emotional processes. In other words, the altered activity seen in human symptom provocation studies could be a consequence, not an antecedent condition.

On the negative side, many connections, particularly those involving

distant structures, are lost in brain slices. This results in abnormally hyperpolarized membrane potentials and reduced spontaneous activity (Paré et al., 1998). Consequently, network phenomena that might play an important role in PTSD cannot be studied with this approach. Thus, it is unclear whether the phenotypic differences in synaptic responsiveness evidenced in the present study are expressed *in vivo*. In particular, it is conceivable that some of the differences we observed are overwhelmed by increased or decreased activity in afferents to different BNST-A regions. *In vivo* extracellular recordings comparing BNST-A neurons in resilient and PTSD-like rats will be required to address this question.

#### 6.3.2. Functional organization of BNST-A

Early lesion and inactivation studies that lacked the spatial resolution to selectively affect different BNST sub-regions led to the view that BNST activity promotes the development of long-lasting anxiety states (LeDoux et al., 1988; Gewirtz et al., 1998; Hammack et al., 2004; Sullivan et al., 2004; Duvarci et al., 2009; Walker et al., 2009b). However, more recent studies, using approaches that permit selective manipulations of different BNST regions (Kim et al., 2013) or cell types within these regions (Jennings et al., 2013), indicate that BNST is functionally heterogeneous.

Consistent with this, mounting evidence suggests that different BNST-A regions exert opposing influences over fear and anxiety. For instance, a recent unit recording study revealed that many BNST-AL neurons acquire inhibitory

responses to conditioned stimuli predicting adverse outcomes, whereas most BNST-AM cells exhibit the opposite behavior (Hauffler et al., 2013). Importantly, BNST-AL and AM neurons displayed the same inverse behavior in relation to the expression of contextual fear (Hauffler et al., 2013). Moreover, intra-BNST infusions of calcitonin gene-related peptide, a peptide that inhibits BNST-AL neurons (Gungor and Paré, 2013), increase fear-potentiated startle and Fos expression targets of BNST-AL (Sink et al., 2011). Last, the results in chapter IV revealed that BNST-AL sends purely GABAergic projections to BNST-AM and AV, raising the possibility of reciprocal activity fluctuations between these two BNST-A regions. Interestingly, in contrast with BNST-AL, BNST-AM and AV send glutamatergic projections to each other. Overall, these findings support the view that BNST-AM and AL exert opposite influences over the expression of fear/anxiety, with the former exerting anxiogenic and the latter anxiolytic influences. The presence of glutamatergic connections between BNST-AM and AV further suggests that these two regions might exert synergistic influences over fear and anxiety.

The region-specific regulation of neuronal excitability observed here is consistent with this model. BNST-AL neurons showed a reduced level of synaptic excitability in PTSD-like rats, in keeping with evidence that BNST-AL exerts anxiolytic influences. Opposite to BNST-AL, BNST-AM and AV neurons had a higher synaptic excitability in PTSD-like relative to resilient rats, consistent with the notion that these regions exert an anxiogenic influence.

### 6.3.3. Nature and origin of the altered neuronal responsiveness

Although we observed phenotypic differences in the efficacy of glutamatergic synapses onto BNST-AM and AV neurons, PPF properties did not differ as a function of the rats' phenotype. It is thus possible that postsynaptic factors, such as a change in the number and/or biophysical properties of AMPA receptors are involved. Interestingly, a recent study on central lateral amygdala (CeL) neurons also reached this conclusion (Goswami et al., 2012). In this case, the efficacy of BL inputs to CeL neurons was higher in PTSD-like than resilient rats. As seen in BNST-AM and AV neurons, this difference was not associated with altered properties of PPF, but with an increased sensitivity to uncaged glutamate in PTSD-like rats. In contrast, the responsiveness of CeM neurons to BL inputs was lower in PTSD-like rats. This is surprising given that CeM constitutes the main source of amygdala projections to brainstem fear effector neurons (Hopkins and Holstege, 1978; Veening et al., 1984).

Overall, the above suggests that between PTSD-like and resilient rats, are distributed changes in neuronal excitability within fear/anxiety networks. BNST-AL and CeM neurons have a lower responsiveness in PTSD-like relative to resilient rats, whereas BNST-AM, AV, and CeL neurons show the opposite. Interestingly, CeL emerges as a key regulator in this context because it contributes with GABAergic projections to CeM (Petrovich and Swanson, 1997) and BNST-AL (Dong et al., 2001a).

The phenotypic differences in neuronal excitability described above lead to

a startling prediction. In PTSD-like rats, control of fear expression is altered such that the influence of CeM is minimized whereas that of BNST-AM and AV is enhanced. This prediction could be tested experimentally by comparing the effects of BNST lesions on the expression of conditioned fear responses to cues in the two rat phenotypes. Indeed, prior studies have found that cued fear is unaffected by BNST lesions or inactivations (Walker and Davis 1997; Gewirtz et al., 1998; Sullivan et al., 2004; Duvarci et al., 2009). However, our *in vitro* results predict that, after predatory threat, such interventions will reduce cued fear in PTSD-like but not resilient rats. If supported, this prediction might explain the greater resistance of conditioned fear to extinction training in PTSD-like rats (Goswami et al., 2010). Because mechanisms of fear expression would differ between the two rat phenotypes, so would mechanisms of extinction.

Another important challenge for future investigations will be to determine whether the phenotypic differences in neuronal excitability we disclosed develop after predatory threat or whether they predate it. The latter might contribute to individual differences in trauma susceptibility; the former might contribute to maintenance of the PTSD-like state. Thus, many exciting lines of investigations lie ahead.

## References

Adamec R (1997) Transmitter systems involved in neural plasticity underlying increased anxiety and defense--implications for understanding anxiety following traumatic stress. *Neurosci Biobehav Rev* 21:755–765.

Adamec R, Head D, Blundell J, Burton P, Berton O (2006) Lasting anxiogenic effects of feline predator stress in mice: sex differences in vulnerability to stress and predicting severity of anxiogenic response from the stress experience. *Physiol Behav* 88:12–29.

Adamec R, Kent P, Anisman H, Shallow T, Merali Z (1998) Neural plasticity, neuropeptides and anxiety in animals--implications for understanding and treating affective disorder following traumatic stress in humans. *Neurosci Biobehav Rev* 23:301–318.

Adamec RE, Blundell J, Burton P (2003) Phosphorylated cyclic AMP response element binding protein expression induced in the periaqueductal gray by predator stress: its relationship to the stress experience, behavior and limbic neural plasticity. *Prog Neuropsychopharmacol Biol Psychiatry* 27:1243–1267.

Adamec RE, Blundell J, Burton P (2005) Neural circuit changes mediating lasting brain and behavioral response to predator stress. *Neurosci Biobehav Rev* 29:1225–1241.

Adamec RE, Blundell J, Collins A (2001) Neural plasticity and stress induced changes in defense in the rat. *Neurosci Biobehav Rev* 25:721–744.

Adamec RE, Shallow T (1993) Lasting effects on rodent anxiety of a single exposure to a cat. *Physiol Behav* 54:101–109.

Afifi TO, Asmundson GJG, Taylor S, Jang KL (2010) The role of genes and environment on trauma exposure and posttraumatic stress disorder symptoms: a review of twin studies. *Clin Psychol Rev* 30:101–112

Alheid GF, Heimer L (1988) New perspectives in basal forebrain organization of special relevance for neuropsychiatric disorders: the striatopallidal, amygdaloid, and corticopetal components of substantia innominata. *Neuroscience* 27:1–39.

Amano T, Duvarci S, Popa D, Paré D (2011) The fear circuit revisited: contributions of the basal amygdala nuclei to conditioned fear. *J Neurosci* 31:15481–15489.

Amaral DG (1978) A Golgi study of cell types in the hilar region of the hippocampus in the rat. *J Comp Neurol* 182:851–914.

American Psychiatric Association (2013) Diagnostic and statistical manual of mental disorders (5th ed.) Arlington, VA: American Psychiatric Publishing.

Amir A, Amano T, Paré D (2011) Physiological identification and infralimbic responsiveness of rat intercalated amygdala neurons. *J Neurophysiol* 105:3054–3066.

Andy OJ, Stephan H (1964) The septum of the cat. Springfield: Charles C Thomas.

Apergis-Schoute J, Pinto A, Paré D (2007) Muscarinic control of long-range GABAergic inhibition within the rhinal cortices. *J Neurosci* 27:4061–4071.

Association AP (1994) Diagnostic and Statistical Manual of Mental Disorders, 4th ed. Washington, D.C.: American Psychiatric Publishing, Inc.

Aston-Jones G, Delfs JM, Druhan J, Zhu Y (1999) The bed nucleus of the stria terminalis. A target site for noradrenergic actions in opiate withdrawal. *Ann N Y Acad Sci* 877:486–498.

Baker DG, West SA, Nicholson WE, Ekhtor NN, Kasckow JW, Hill KK, Bruce AB, Orth DN, Geraciotti TD (1999) Serial CSF corticotropin-releasing hormone levels and adrenocortical activity in combat veterans with posttraumatic stress disorder. *Am J Psychiatry* 156:585–588.

Bernard-Bonnin A-C, Hébert M, Daignault I V, Allard-Dansereau C (2008) Disclosure of sexual abuse, and personal and familial factors as predictors of post-traumatic stress disorder symptoms in school-aged girls. *Paediatr Child Health* 13:479–486.

Bienkowski MS, Rinaman L (2013) Common and distinct neural inputs to the medial central nucleus of the amygdala and anterior ventrolateral bed nucleus of stria terminalis in rats. *Brain Struct Funct* 218:187–208.

Binder EB, Bradley RG, Liu W, Epstein MP, Deveau TC, Mercer KB, Tang Y, Gillespie CF, Heim CM, Nemeroff CB, Schwartz AC, Cubells JF, Ressler KJ (2008) Association of FKBP5 polymorphisms and childhood abuse with risk of posttraumatic stress disorder symptoms in adults. *JAMA* 299:1291–1305.

Blair HT, Schafe GE, Bauer EP, Rodrigues SM, LeDoux JE (2001) Synaptic plasticity in the lateral amygdala: a cellular hypothesis of fear conditioning. *Learn Mem* 8:229–242.

Blanchard DC, Griebel G, Blanchard RJ (2001) Mouse defensive behaviors: pharmacological and behavioral assays for anxiety and panic. *Neurosci Biobehav Rev* 25:205–218.

Blechert J, Michael T, Vriends N, Margraf J, Wilhelm FH (2007) Fear conditioning in posttraumatic stress disorder: evidence for delayed extinction of autonomic, experiential, and behavioural responses. *Behav Res Ther* 45:2019–2033.

Blundell J, Adamec R, Burton P (2005) Role of NMDA receptors in the syndrome of behavioral changes produced by predator stress. *Physiol Behav* 86:233–243.

Bota M, Sporns O, Swanson LW (2012) Neuroinformatics analysis of molecular expression patterns and neuron populations in gray matter regions: the rat BST as a rich exemplar. *Brain Res* 1450:174–193.

Bremner JD, Licinio J, Darnell A, Krystal JH, Owens MJ, Southwick SM, Nemeroff CB, Charney DS (1997a) Elevated CSF corticotropin-releasing factor concentrations in posttraumatic stress disorder. *Am J Psychiatry* 154:624–629.

Bremner JD, Randall P, Scott TM, Capelli S, Delaney R, McCarthy G, Charney DS (1995) Deficits in short-term memory in adult survivors of childhood abuse. *Psychiatry Res* 59:97–107.

Bremner JD, Randall P, Vermetten E, Staib L, Bronen RA, Mazure C, Capelli S, McCarthy G, Innis RB, Charney DS (1997b) Magnetic resonance imaging-based measurement of hippocampal volume in posttraumatic stress disorder related to

childhood physical and sexual abuse--a preliminary report. *Biol Psychiatry* 41:23–32.

Bremner JD, Scott TM, Delaney RC, Southwick SM, Mason JW, Johnson DR, Innis RB, McCarthy G, Charney DS (1993) Deficits in short-term memory in posttraumatic stress disorder. *Am J Psychiatry* 150:1015–1019.

Bremner JD, Vermetten E, Schmahl C, Vaccarino V, Vythilingam M, Afzal N, Grillon C, Charney DS (2005) Positron emission tomographic imaging of neural correlates of a fear acquisition and extinction paradigm in women with childhood sexual-abuse-related post-traumatic stress disorder. *Psychol Med* 35:791–806.

Bremner JD, Vythilingam M, Vermetten E, Adil J, Khan S, Nazeer A, Afzal N, McGlashan T, Elzinga B, Anderson GM, Heninger G, Southwick SM, Charney DS (2003) Cortisol response to a cognitive stress challenge in posttraumatic stress disorder (PTSD) related to childhood abuse. *Psychoneuroendocrinology* 28:733–750.

Britton JC, Phan KL, Taylor SF, Fig LM, Liberzon I (2005) Corticolimbic blood flow in posttraumatic stress disorder during script-driven imagery. *Biol Psychiatry* 57:832–840.

Ciocchi S, Herry C, Grenier F, Wolff SBE, Letzkus JJ, Vlachos I, Ehrlich I, Sprengel R, Deisseroth K, Stadler MB, Müller C, Lüthi A (2010) Encoding of conditioned fear in central amygdala inhibitory circuits. *Nature* 468:277–282.

Cohen H, Matar MA, Richter-Levin G, Zohar J (2006a) The contribution of an animal model toward uncovering biological risk factors for PTSD. *Ann N Y Acad Sci* 1071:335–350.

Cohen H, Zohar J (2004) An animal model of posttraumatic stress disorder: the use of cut-off behavioral criteria. *Ann N Y Acad Sci* 1032:167–178.

Cohen H, Zohar J, Gidron Y, Matar M a, Belkind D, Loewenthal U, Kozlovsky N, Kaplan Z (2006b) Blunted HPA axis response to stress influences susceptibility to posttraumatic stress response in rats. *Biol Psychiatry* 59:1208–1218.

Cohen H, Zohar J, Matar M (2003) The Relevance of Differential Response to Trauma in an Animal Model of Posttraumatic Stress Disorder. *Biol Psychiatry*

3223:463–473.

Collins DR, Paré D (2000) Differential fear conditioning induces reciprocal changes in the sensory responses of lateral amygdala neurons to the CS(+) and CS(-). *Learn Mem* 7:97–103.

Conrad KL, Davis AR, Silberman Y, Sheffler DJ, Shields AD, Saleh SA, Sen N, Matthies HJG, Javitch JA, Lindsley CW, Winder DG (2012) Yohimbine depresses excitatory transmission in BNST and impairs extinction of cocaine place preference through orexin-dependent, norepinephrine-independent processes. *Neuropsychopharmacology* 37:2253–2266.

Conrad KL, Louderback KM, Gessner CP, Winder DG (2011) Stress-induced alterations in anxiety-like behavior and adaptations in plasticity in the bed nucleus of the stria terminalis. *Physiol Behav* 104:248–256.

Creager R, Dunwiddie T, Lynch G (1980) Paired-pulse and frequency facilitation in the CA1 region of the in vitro rat hippocampus. *J Physiol* 299:409–424.

Cullinan WE, Herman JP, Watson SJ (1993) Ventral subicular interaction with the hypothalamic paraventricular nucleus: evidence for a relay in the bed nucleus of the stria terminalis. *J Comp Neurol* 332:1–20.

Cullinan WE, Ziegler DR, Herman JP (2008) Functional role of local GABAergic influences on the HPA axis. *Brain Struct Funct* 213:63–72.

Davidson JRT, Tharwani HM, Connor KM (2002) Davidson Trauma Scale (DTS): normative scores in the general population and effect sizes in placebo-controlled SSRI trials. *Depress Anxiety* 15:75–78.

Davis AR, Shields AD, Brigman JL, Norcross M, McElligott ZA, Holmes A, Winder DG (2008) Yohimbine impairs extinction of cocaine-conditioned place preference in an alpha2-adrenergic receptor independent process. *Learn Mem* 15:667–676.

Davis M (2000) The role of the amygdala in conditioned and unconditioned fear and anxiety. In: *The Amygdala*, edited by Aggleton AP (Oxford, Oxford Univ. Press).

Davis M, Walker DL, Miles L, Grillon C (2010) Phasic vs sustained fear in rats and humans: role of the extended amygdala in fear vs anxiety. *Neuropsychopharmacology* 35:105–135.

Day HE, Curran EJ, Watson SJ, Akil H (1999) Distinct neurochemical populations in the rat central nucleus of the amygdala and bed nucleus of the stria terminalis: evidence for their selective activation by interleukin-1beta. *J Comp Neurol* 413:113–128.

Dayas C V, Buller KM, Crane JW, Xu Y, Day TA (2001) Stressor categorization: acute physical and psychological stressors elicit distinctive recruitment patterns in the amygdala and in medullary noradrenergic cell groups. *Eur J Neurosci* 14:1143–1152.

De Kloet CS, Vermetten E, Geuze E, Kavelaars a, Heijnen CJ, Westenberg HGM (2006) Assessment of HPA-axis function in posttraumatic stress disorder: pharmacological and non-pharmacological challenge tests, a review. *J Psychiatr Res* 40:550–567.

De Olmos JS, Heimer L (1999) The concepts of the ventral striatopallidal system and extended amygdala. *Ann N Y Acad Sci* 877:1–32.

De Olmos JS, Alheid GF, Beltramino CA (1985) Amygdala. In: *The Rat Nervous System. Forebrain and Midbrain*, edited by Paxinos G. Orlando, FL: Academic, vol. 1, p. 509-603.

Dielenberg R a, Hunt GE, McGregor IS (2001) “When a rat smells a cat”: the distribution of Fos immunoreactivity in rat brain following exposure to a predatory odor. *Neuroscience* 104:1085–1097.

Dielenberg RA, McGregor IS (2001) Defensive behavior in rats towards predatory odors: a review. *Neurosci Biobehav Rev* 25:597–609.

Diorio D, Viau V, Meaney MJ (1993) The role of the medial prefrontal cortex (cingulate gyrus) in the regulation of hypothalamic-pituitary-adrenal responses to stress. *J Neurosci* 13:3839–3847.

Dong H, Petrovich GD, Swanson LW (2000) Organization of projections from the juxtacapsular nucleus of the BST: a PHAL study in the rat. *Brain Res* 859:1–14.

Dong H-W, Swanson LW (2003) Projections from the rhomboid nucleus of the bed nuclei of the stria terminalis: implications for cerebral hemisphere regulation of ingestive behaviors. *J Comp Neurol* 463:434–472.

Dong H-W, Swanson LW (2004) Organization of axonal projections from the anterolateral area of the bed nuclei of the stria terminalis. *J Comp Neurol* 468:277–298.

Dong H-W, Swanson LW (2006a) Projections from bed nuclei of the stria terminalis, anteromedial area: cerebral hemisphere integration of neuroendocrine, autonomic, and behavioral aspects of energy balance. *J Comp Neurol* 494:142–178.

Dong H-W, Swanson LW (2006b) Projections from bed nuclei of the stria terminalis, dorsomedial nucleus: implications for cerebral hemisphere integration of neuroendocrine, autonomic, and drinking responses. *J Comp Neurol* 494:75–107.

Dong H-W, Swanson LW (2006c) Projections from bed nuclei of the stria terminalis, magnocellular nucleus: implications for cerebral hemisphere regulation of micturition, defecation, and penile erection. *J Comp Neurol* 494:108–141.

Dong HW, Petrovich GD, Swanson LW (2001a) Topography of projections from amygdala to bed nuclei of the stria terminalis. *Brain Res Brain Res Rev* 38:192–246.

Dong HW, Petrovich GD, Watts AG, Swanson LW (2001b) Basic organization of projections from the oval and fusiform nuclei of the bed nuclei of the stria terminalis in adult rat brain. *J Comp Neurol* 436:430–455.

Dumont EC, Mark GP, Mader S, Williams JT (2005) Self-administration enhances excitatory synaptic transmission in the bed nucleus of the stria terminalis. *Nat Neurosci* 8:413–414.

Dumont EC, Rycroft BK, Maiz J, Williams JT (2008) Morphine produces circuit-specific neuroplasticity in the bed nucleus of the stria terminalis. *Neuroscience* 153:232–239.

Dumont EC, Williams JT (2004) Noradrenaline triggers GABAA inhibition of bed nucleus of the stria terminalis neurons projecting to the ventral tegmental area. *J Neurosci* 24:8198–8204.

Duvarci S, Bauer EP, Paré D (2009) The bed nucleus of the stria terminalis mediates inter-individual variations in anxiety and fear. *J Neurosci* 29:10357–10361.

Duvarci S, Popa D, Paré D (2011) Central amygdala activity during fear conditioning. *J Neurosci* 31:289–294.

Egli RE, Winder DG (2003) Dorsal and ventral distribution of excitable and synaptic properties of neurons of the bed nucleus of the stria terminalis. *J Neurophysiol* 90:405–414.

Elzinga BM, Schmahl CG, Vermetten E, van Dyck R, Bremner JD (2003) Higher cortisol levels following exposure to traumatic reminders in abuse-related PTSD. *Neuropsychopharmacology* 28:1656–1665.

Esclapez M, Tillakaratne NJ, Tobin AJ, Houser CR (1993) Comparative localization of mRNAs encoding two forms of glutamic acid decarboxylase with nonradioactive in situ hybridization methods. *J Comp Neurol* 331:339–362.

Feldman ML, Peters A (1978) The forms of non-pyramidal neurons in the visual cortex of the rat. *J Comp Neurol* 179:761–793.

Fendt M, Endres T, Apfelbach R (2003) Temporary inactivation of the bed nucleus of the stria terminalis but not of the amygdala blocks freezing induced by trimethylthiazoline, a component of fox feces. *J Neurosci* 23:23–28.

Figueiredo HF, Bruestle A, Bodie B, Dolgas CM, Herman JP (2003) The medial prefrontal cortex differentially regulates stress-induced c-fos expression in the forebrain depending on type of stressor. *Eur J Neurosci* 18:2357–2364.

Forray MI, Gysling K (2004) Role of noradrenergic projections to the bed nucleus of the stria terminalis in the regulation of the hypothalamic-pituitary-adrenal axis. *Brain Res Brain Res Rev* 47:145–160.

Francesconi W, Berton F, Koob GF, Sanna PP (2009) Intrinsic neuronal plasticity in the juxtacapsular nucleus of the bed nuclei of the stria terminalis (jcBNST). *Prog Neuropsychopharmacol Biol Psychiatry* 33:1347–1355.

Gafford GM, Guo J, Flandreau EI, Hazra R, Rainnie DG, Ressler KJ (2012) Cell-type specific deletion of GABA(A) $\alpha$ 1 in corticotropin-releasing factor-containing neurons enhances anxiety and disrupts fear extinction. *Proc Natl Acad Sci U S A* 109:16330–16335.

Georges F, Aston-Jones G (2001) Potent regulation of midbrain dopamine neurons by the bed nucleus of the stria terminalis. *J Neurosci* 21:RC160

Georges F, Aston-Jones G (2002) Activation of ventral tegmental area cells by the bed nucleus of the stria terminalis: a novel excitatory amino acid input to midbrain dopamine neurons. *J Neurosci* 22:5173–5187.

Geraciotti TD, Baker DG, Ekhtor NN, West SA, Hill KK, Bruce AB, Schmidt D, Rounds-Kugler B, Yehuda R, Keck PE, Kasckow JW (2001) CSF norepinephrine concentrations in posttraumatic stress disorder. *Am J Psychiatry* 158:1227–1230.

Gewirtz JC, McNish KA, Davis M (1998) Lesions of the bed nucleus of the stria terminalis block sensitization of the acoustic startle reflex produced by repeated stress, but not fear-potentiated startle. *Prog Neuropsychopharmacol Biol Psychiatry* 22:625–648.

Gilbertson MW, Shenton ME, Ciszewski A, Kasai K, Lasko NB, Orr SP, Pitman RK (2002) Smaller hippocampal volume predicts pathologic vulnerability to psychological trauma. *Nat Neurosci* 5:1242–1247.

Gilbertson MW, Williston SK, Paulus LA, Lasko NB, Gurvits T V, Shenton ME, Pitman RK, Orr SP (2007) Configural cue performance in identical twins discordant for posttraumatic stress disorder: theoretical implications for the role of hippocampal function. *Biol Psychiatry* 62:513–520.

Gillespie CF, Phifer J, Bradley B, Ressler KJ (2009) Risk and resilience: genetic and environmental influences on development of the stress response. *Depress Anxiety* 26:984–992.

Gosnell HB, Silberman Y, Grueter BA, Duvoisin RM, Raber J, Winder DG (2011)

mGluR8 modulates excitatory transmission in the bed nucleus of the stria terminalis in a stress-dependent manner. *Neuropsychopharmacology* 36:1599–1607.

Goswami S, Cascardi M, Rodríguez-Sierra OE, Duvarci S, Paré D (2010) Impact of predatory threat on fear extinction in Lewis rats. *Learn Mem* 17:494–501.

Goswami S, Paré D (2012) Ex vivo analysis of alterations in the physiology of amygdala neurons in a rat model of PTSD. *Soc for Neurosci abstract*, 603.12.

Goswami S, Rodríguez-Sierra O, Cascardi M, Paré D (2013) Animal models of post-traumatic stress disorder: face validity. *Front Neurosci* 7:89.

Goswami S, Samuel S, Sierra OR, Cascardi M, Paré D (2012) A rat model of post-traumatic stress disorder reproduces the hippocampal deficits seen in the human syndrome. *Front Behav Neurosci* 6:26.

Gracy KN, Pickel VM (1995) Comparative ultrastructural localization of the NMDAR1 glutamate receptor in the rat basolateral amygdala and bed nucleus of the stria terminalis. *J Comp Neurol* 362:71–85.

Gray TS, Magnuson DJ (1987) Neuropeptide neuronal efferents from the bed nucleus of the stria terminalis and central amygdaloid nucleus to the dorsal vagal complex in the rat. *J Comp Neurol* 262:365–374.

Gray TS, Magnuson DJ (1992) Peptide immunoreactive neurons in the amygdala and the bed nucleus of the stria terminalis project to the midbrain central gray in the rat. *Peptides* 13:451–460.

Gray TS, Piechowski RA, Yracheta JM, Rittenhouse PA, Bethea CL, Van de Kar LD (1993) Ibotenic acid lesions in the bed nucleus of the stria terminalis attenuate conditioned stress-induced increases in prolactin, ACTH and corticosterone. *Neuroendocrinology* 57:517–524.

Grueter BA, Gosnell HB, Olsen CM, Schramm-Sapyta NL, Nekrasova T, Landreth GE, Winder DG (2006) Extracellular-signal regulated kinase 1-dependent metabotropic glutamate receptor 5-induced long-term depression in the bed nucleus of the stria terminalis is disrupted by cocaine administration. *J Neurosci* 26:3210–3219.

Grueter BA, McElligott ZA, Robison AJ, Mathews GC, Winder DG (2008) In vivo metabotropic glutamate receptor 5 (mGluR5) antagonism prevents cocaine-induced disruption of postsynaptically maintained mGluR5-dependent long-term depression. *J Neurosci* 28:9261–9270.

Grueter BA, Winder DG (2005) Group II and III metabotropic glutamate receptors suppress excitatory synaptic transmission in the dorsolateral bed nucleus of the stria terminalis. *Neuropsychopharmacology* 30:1302–1311.

Grupe DW, Nitschke JB (2013) Uncertainty and anticipation in anxiety: an integrated neurobiological and psychological perspective. *Nat Rev Neurosci* 14:488–501.

Gulyás AI, Miettinen R, Jacobowitz DM, Freund TF (1992) Calretinin is present in non-pyramidal cells of the rat hippocampus--I. A new type of neuron specifically associated with the mossy fibre system. *Neuroscience* 48:1–27.

Gungor NZ, Paré D (2013) CGRP inhibits neurons of the bed nucleus of the stria terminalis: implications for the regulation of fear and anxiety. *J Neurosci*, in press.

Guo J-D, Hammack SE, Hazra R, Levita L, Rainnie DG (2009) Bi-directional modulation of bed nucleus of stria terminalis neurons by 5-HT: molecular expression and functional properties of excitatory 5-HT receptor subtypes. *Neuroscience* 164:1776–1793.

Guo J-D, Hazra R, Dabrowska J, Muly EC, Wess J, Rainnie DG (2012) Presynaptic muscarinic M(2) receptors modulate glutamatergic transmission in the bed nucleus of the stria terminalis. *Neuropharmacology* 62:1671–1683.

Guo J-D, Rainnie DG (2010) Presynaptic 5-HT(1B) receptor-mediated serotonergic inhibition of glutamate transmission in the bed nucleus of the stria terminalis. *Neuroscience* 165:1390–1401.

Hammack SE, Mania I, Rainnie DG (2007) Differential expression of intrinsic membrane currents in defined cell types of the anterolateral bed nucleus of the stria terminalis. *J Neurophysiol* 98:638–656.

Hammack SE, Richey KJ, Watkins LR, Maier SF (2004) Chemical lesion of the bed nucleus of the stria terminalis blocks the behavioral consequences of uncontrollable stress. *Behav Neurosci* 118:443–448.

Hammack SE, Roman CW, Lezak KR, Kocho-Shellenberg M, Grimmig B, Falls WA, Braas K, May V (2010) Roles for pituitary adenylate cyclase-activating peptide (PACAP) expression and signaling in the bed nucleus of the stria terminalis (BNST) in mediating the behavioral consequences of chronic stress. *J Mol Neurosci* 42:327–340.

Hamner MB, Diamond BI (1993) Elevated plasma dopamine in posttraumatic stress disorder: a preliminary report. *Biol Psychiatry* 33:304–306.

Hannibal J (2002) Pituitary adenylate cyclase-activating peptide in the rat central nervous system: an immunohistochemical and in situ hybridization study. *J Comp Neurol* 453:389–417.

Hasue RH, Shammah-Lagnado SJ (2002) Origin of the dopaminergic innervation of the central extended amygdala and accumbens shell: a combined retrograde tracing and immunohistochemical study in the rat. *J Comp Neurol* 454:15–33.

Haubensak W, Kunwar PS, Cai H, Ciochi S, Wall NR, Ponnusamy R, Biag J, Dong H-W, Deisseroth K, Callaway EM, Fanselow MS, Lüthi A, Anderson DJ (2010) Genetic dissection of an amygdala microcircuit that gates conditioned fear. *Nature* 468:270–276.

Haufler D, Nagy FZ, Paré D (2013) Neuronal correlates of fear conditioning in the bed nucleus of the stria terminalis. *Learn Mem* 20:633–641.

Häusser M, Stuart G, Racca C, Sakmann B (1995) Axonal initiation and active dendritic propagation of action potentials in substantia nigra neurons. *Neuron* 15:637–647.

Hazra R, Guo J-D, Ryan SJ, Jasnow AM, Dabrowska J, Rainnie DG (2011) A transcriptomic analysis of type I-III neurons in the bed nucleus of the stria terminalis. *Mol Cell Neurosci* 46:699–709.

Hazra R, Guo JD, Dabrowska J, Rainnie DG (2012) Differential distribution of serotonin receptor subtypes in BNST(ALG) neurons: modulation by unpredictable shock stress. *Neuroscience* 225:9–21.

Heim C, Nemeroff CB (2009) Neurobiology of posttraumatic stress disorder. *CNS Spectr* 14:13–24.

Herman JP, Figueiredo H, Mueller NK, Ulrich-Lai Y, Ostrander MM, Choi DC, Cullinan WE (2003) Central mechanisms of stress integration: hierarchical circuitry controlling hypothalamo-pituitary-adrenocortical responsiveness. *Front Neuroendocrinol* 24:151–180.

Herman JP, Mueller NK (2006) Role of the ventral subiculum in stress integration. *Behav Brain Res* 174:215–224.

Hitchcock JM, Davis M (1991) Efferent pathway of the amygdala involved in conditioned fear as measured with the fear-potentiated startle paradigm. *Behav Neurosci* 105:826–842.

Holstege G, Meiners L, Tan K (1985) Projections of the bed nucleus of the stria terminalis to the mesencephalon, pons, and medulla oblongata in the cat. *Exp Brain Res* 58:379–391.

Hopkins DA, Holstege G (1978) Amygdaloid projections to the mesencephalon, pons and medulla oblongata in the cat. *Exp Brain Res* 32:529–547.

Huguenard JR (1996) Low-threshold calcium currents in central nervous system neurons. *Annu Rev Physiol* 58:329–348.

Hur EE, Zaborszky L (2005) Vglut2 afferents to the medial prefrontal and primary somatosensory cortices: a combined retrograde tracing in situ hybridization study [corrected]. *J Comp Neurol* 483:351–373.

Ide S, Hara T, Ohno A, Tamano R, Koseki K, Naka T, Maruyama C, Kaneda K, Yoshioka M, Minami M (2013) Opposing roles of corticotropin-releasing factor and neuropeptide Y within the dorsolateral bed nucleus of the stria terminalis in the negative affective component of pain in rats. *J Neurosci* 33:5881–5894.

Jalabert M, Aston-Jones G, Herzog E, Manzoni O, Georges F (2009) Role of the bed nucleus of the stria terminalis in the control of ventral tegmental area dopamine neurons. *Prog Neuropsychopharmacol Biol Psychiatry* 33:1336–1346.

Jatzko A, Rothenhöfer S, Schmitt A, Gaser C, Demiralpca T, Weber-Fahr W, Wessa M, Magnotta V, Braus DF (2006) Hippocampal volume in chronic posttraumatic stress disorder (PTSD): MRI study using two different evaluation methods. *J Affect Disord* 94:121–126.

Jennings JH, Sparta DR, Stamatakis AM, Ung RL, Pleil KE, Kash TL, Stuber GD (2013) Distinct extended amygdala circuits for divergent motivational states. *Nature* 496:224–228.

Joëls M, Baram TZ (2009) The neuro-symphony of stress. *Nat Rev Neurosci* 10:459–466.

Ju G, Swanson LW (1989) Studies on the cellular architecture of the bed nuclei of the stria terminalis in the rat: I. Cytoarchitecture. *J Comp Neurol* 280:587–602.

Ju G, Swanson LW, Simerly RB (1989) Studies on the cellular architecture of the bed nuclei of the stria terminalis in the rat: II. Chemoarchitecture. *J Comp Neurol* 280:603–621.

Juraska JM, Wilson CJ, Groves PM (1977) The substantia nigra of the rat: a Golgi study. *J Comp Neurol* 172:585–600.

Kash TL, Baucum AJ, Conrad KL, Colbran RJ, Winder DG (2009) Alcohol exposure alters NMDAR function in the bed nucleus of the stria terminalis. *Neuropsychopharmacology* 34:2420–2429.

Kash TL, Matthews RT, Winder DG (2008a) Alcohol inhibits NR2B-containing NMDA receptors in the ventral bed nucleus of the stria terminalis. *Neuropsychopharmacology* 33:1379–1390.

Kash TL, Nobis WP, Matthews RT, Winder DG (2008b) Dopamine enhances fast excitatory synaptic transmission in the extended amygdala by a CRF-R1-dependent process. *J Neurosci* 28:13856–13865.

Kash TL, Winder DG (2006) Neuropeptide Y and corticotropin-releasing factor bi-directionally modulate inhibitory synaptic transmission in the bed nucleus of the stria terminalis. *Neuropharmacology* 51:1013–1022.

Katz B, Miledi R (1968) The role of calcium in neuromuscular facilitation. *J Physiol* 195:481–492.

Kessler RC, Chiu WT, Demler O, Merikangas KR, Walters EE (2005) Prevalence, severity, and comorbidity of 12-month DSM-IV disorders in the National Comorbidity Survey Replication. *Arch Gen Psychiatry* 62:617–627.

Kessler RC, Sonnega A, Bromet E, Hughes M, Nelson CB (1995) Posttraumatic Stress Disorder in the National Comorbidity Survey. *Arch Gen Psychiatry* 52:1048–1060.

Kim S-Y, Adhikari A, Lee SY, Marshel JH, Kim CK, Mallory CS, Lo M, Pak S, Mattis J, Lim BK, Malenka RC, Warden MR, Neve R, Tye KM, Deisseroth K (2013) Diverging neural pathways assemble a behavioural state from separable features in anxiety. *Nature* 496:219–223.

Kingston S, Raghavan C (2009) The relationship of sexual abuse, early initiation of substance use, and adolescent trauma to PTSD. *J Trauma Stress* 22:65–68.

Kitayama N, Vaccarino V, Kutner M, Weiss P, Bremner JD (2005) Magnetic resonance imaging (MRI) measurement of hippocampal volume in posttraumatic stress disorder: a meta-analysis. *J Affect Disord* 88:79–86.

Krawczyk M, Georges F, Sharma R, Mason X, Berthet A, Bézard E, Dumont EC (2011a) Double-dissociation of the catecholaminergic modulation of synaptic transmission in the oval bed nucleus of the stria terminalis. *J Neurophysiol* 105:145–153.

Krawczyk M, Sharma R, Mason X, Debacker J, Jones AA, Dumont EC (2011b) A switch in the neuromodulatory effects of dopamine in the oval bed nucleus of the stria terminalis associated with cocaine self-administration in rats. *J Neurosci* 31:8928–8935.

Krettek JE, Price JL (1978a) Amygdaloid projections to subcortical structures within the basal forebrain and brainstem in the rat and cat. *J Comp Neurol* 178:225–254.

Krettek JE, Price JL (1978b) A description of the amygdaloid complex in the rat and cat with observations on intra-amygdaloid axonal connections. *J Comp Neurol* 178:255–280.

Kudo T, Uchigashima M, Miyazaki T, Konno K, Yamasaki M, Yanagawa Y, Minami M, Watanabe M (2012) Three types of neurochemical projection from the bed nucleus of the stria terminalis to the ventral tegmental area in adult mice. *J Neurosci* 32:18035–18046.

Lanius RA, Williamson PC, Hopper J, Densmore M, Boksman K, Gupta MA, Neufeld RWJ, Gati JS, Menon RS (2003) Recall of emotional states in posttraumatic stress disorder: an fMRI investigation. *Biol Psychiatry* 53:204–210.

Larriva-Sahd J (2004) Juxtacapsular nucleus of the stria terminalis of the adult rat: extrinsic inputs, cell types, and neuronal modules: a combined Golgi and electron microscopic study. *J Comp Neurol* 475:220–237.

Larriva-Sahd J (2006) Histological and cytological study of the bed nuclei of the stria terminalis in adult rat II. Oval Nucleus: extrinsic inputs, cell types, neuropil, and neuronal modules. *J Comp Neurol* 807:772–807.

LeDoux JE (2000) Emotion circuits in the brain. *Annu Rev Neurosci* 23:155–184.

LeDoux JE, Iwata J, Cicchetti P, Reis DJ (1988) Different projections of the central amygdaloid nucleus mediate autonomic and behavioral correlates of conditioned fear. *J Neurosci* 8:2517–2529.

Lemieux AM, Coe CL (1995) Abuse-related posttraumatic stress disorder: evidence for chronic neuroendocrine activation in women. *Psychosom Med* 57:105–115.

Li C, Pleil KE, Stamatakis AM, Busan S, Vong L, Lowell BB, Stuber GD, Kash TL (2012) Presynaptic inhibition of gamma-aminobutyric acid release in the bed

nucleus of the stria terminalis by kappa opioid receptor signaling. *Biol Psychiatry* 71:725–732.

Liberzon I, Abelson JL, Flagel SB, Raz J, Young EA (1999) Neuroendocrine and psychophysiologic responses in PTSD: a symptom provocation study. *Neuropsychopharmacology* 21:40–50.

Lindauer RJL, Vlieger E-J, Jalink M, Olf M, Carlier IVE, Majoie CBLM, den Heeten GJ, Gersons BPR (2004) Smaller hippocampal volume in Dutch police officers with posttraumatic stress disorder. *Biol Psychiatry* 56:356–363.

Llinás RR (1988) The intrinsic electrophysiological properties of mammalian neurons: insights into central nervous system function. *Science* 242:1654–1664.

Lowry CA (2002) Functional subsets of serotonergic neurones: implications for control of the hypothalamic-pituitary-adrenal axis. *J Neuroendocrinol* 14:911–923.

Lungwitz EA, Molosh A, Johnson PL, Harvey BP, Dirks RC, Dietrich A, Minick P, Shekhar A, Truitt WA (2012) Orexin-A induces anxiety-like behavior through interactions with glutamatergic receptors in the bed nucleus of the stria terminalis of rats. *Physiol Behav* 107:726–732.

Manabe T, Wyllie DJ, Perkel DJ, Nicoll RA (1993) Modulation of synaptic transmission and long-term potentiation: effects on paired pulse facilitation and EPSC variance in the CA1 region of the hippocampus. *J Neurophysiol* 70:1451–1459.

Maren S (2001) Neurobiology of Pavlovian fear conditioning. *Annu Rev Neurosci* 24:897–931.

Maren S, Phan KL, Liberzon I (2013) The contextual brain: implications for fear conditioning, extinction and psychopathology. *Nat Rev Neurosci* 14:417–428.

McDonald a J (1983) Neurons of the bed nucleus of the stria terminalis: a golgi study in the rat. *Brain Res Bull* 10:111–120.

McDonald a J, Shammah-Lagnado SJ, Shi C, Davis M (1999a) Cortical afferents

to the extended amygdala. *Ann N Y Acad Sci* 877:309–338.

McDonald AJ (2003) Is there an amygdala and how far does it extend? An anatomical perspective. *Ann N Y Acad Sci* 985:1–21.

McDonald AJ, Shammah-Lagnado SJ, Shi C, Davis M (1999b) Cortical afferents to the extended amygdala. *Ann N Y Acad Sci* 877:309–338.

McElligott ZA, Winder DG (2008) Alpha1-adrenergic receptor-induced heterosynaptic long-term depression in the bed nucleus of the stria terminalis is disrupted in mouse models of affective disorders. *Neuropsychopharmacology* 33:2313–2323.

McGregor IS, Schrama L, Ambermoon P, Dielenberg RA (2002) Not all “predator odours” are equal: cat odour but not 2,4,5 trimethylthiazoline (TMT; fox odour) elicits specific defensive behaviours in rats. *Behav Brain Res* 129:1–16.

Meewisse M-L, Reitsma JB, de Vries G-J, Gersons BPR, Olf M (2007) Cortisol and post-traumatic stress disorder in adults: systematic review and meta-analysis. *Br J Psychiatry* 191:387–392.

Meloni EG, Gerety LP, Knoll AT, Cohen BM, Carlezon WA (2006) Behavioral and anatomical interactions between dopamine and corticotropin-releasing factor in the rat. *J Neurosci* 26:3855–3863.

Milad MR, Orr SP, Lasko NB, Chang Y, Rauch SL, Pitman RK (2008) Presence and acquired origin of reduced recall for fear extinction in PTSD: results of a twin study. *J Psychiatr Res* 42:515–520.

Moga MM, Saper CB, Gray TS (1989) Bed nucleus of the stria terminalis: cytoarchitecture, immunohistochemistry, and projection to the parabrachial nucleus in the rat. *J Comp Neurol* 283:315–332.

Molineux ML, Fernandez FR, Mehaffey WH, Turner RW (2005) A-type and T-type currents interact to produce a novel spike latency-voltage relationship in cerebellar stellate cells. *J Neurosci* 25:10863–10873.

Moore SA (2009) Cognitive abnormalities in posttraumatic stress disorder. *Curr*

Opin Psychiatry 22:19–24.

Muly EC, Mania I, Guo J-D, Rainnie DG (2007) Group II metabotropic glutamate receptors in anxiety circuitry: correspondence of physiological response and subcellular distribution. *J Comp Neurol* 505:682–700.

Myers EA, Banihashemi L, Rinaman L (2005) The anxiogenic drug yohimbine activates central viscerosensory circuits in rats. *J Comp Neurol* 492:426–441.

Nobis WP, Kash TL, Silberman Y, Winder DG (2011)  $\beta$ -Adrenergic receptors enhance excitatory transmission in the bed nucleus of the stria terminalis through a corticotropin-releasing factor receptor-dependent and cocaine-regulated mechanism. *Biol Psychiatry* 69:1083–1090.

Oberlander JG, Henderson LP (2012) Corticotropin-releasing factor modulation of forebrain GABAergic transmission has a pivotal role in the expression of anabolic steroid-induced anxiety in the female mouse. *Neuro-psychopharmacology* 37:1483–1499.

Orr SP, Metzger LJ, Lasko NB, Macklin ML, Peri T, Pitman RK (2000) De novo conditioning in trauma-exposed individuals with and without posttraumatic stress disorder. *J Abnorm Psychol* 109:290–298.

Palay S, Chan-Palay V (1974) *Cerebellar Cortex*. (Berlin: Springer-Verlag).

Pape HC (1996) Queer current and pacemaker: the hyperpolarization-activated cation current in neurons. *Annu Rev Physiol* 58:299–327.

Paquet M, Smith Y (2000) Presynaptic NMDA receptor subunit immunoreactivity in GABAergic terminals in rat brain. *J Comp Neurol* 423:330–347.

Paré D, Quirk GJ, Ledoux JE (2004) New vistas on amygdala networks in conditioned fear. *J Neurophysiol* 92:1–9.

Paré D, Shink E, Gaudreau H, Destexhe A, Lang EJ (1998) Impact of spontaneous synaptic activity on the resting properties of cat neocortical pyramidal neurons *In vivo*. *J Neurophysiol* 79:1450–1460.

Paré D, Smith Y, Paré JF (1995) Intra-amygdaloid projections of the basolateral and basomedial nuclei in the cat: Phaseolus vulgaris-leucoagglutinin anterograde tracing at the light and electron microscopic level. *Neuroscience* 69:567–583.

Park J, Kile BM, Wightman RM (2009) In vivo voltammetric monitoring of norepinephrine release in the rat ventral bed nucleus of the stria terminalis and anteroventral thalamic nucleus. *Eur J Neurosci* 30:2121–2133.

Paxinos G, Watson C (2007) *The rat brain in stereotaxic coordinates*, 6th ed. New York: Academic Press.

Pellow S, Chopin P, File SE, Briley M (1985) Validation of open:closed arm entries in an elevated plus-maze as a measure of anxiety in the rat. *J Neurosci Methods* 14:149–167.

Pellow S, File SE (1986) Anxiolytic and anxiogenic drug effects on exploratory activity in an elevated plus-maze: a novel test of anxiety in the rat. *Pharmacol Biochem Behav* 24:525–529.

Petrovich GD, Swanson LW (1997) Projections from the lateral part of the central amygdalar nucleus to the postulated fear conditioning circuit. *Brain Res* 763:247–254.

Phelix CF, Liposits Z, Paull WK (1992) Monoamine innervation of bed nucleus of stria terminalis: an electron microscopic investigation. *Brain Res Bull* 28:949–965.

Phelps EA, LeDoux JE (2005) Contributions of the amygdala to emotion processing: from animal models to human behavior. *Neuron* 48:175–187.

Pitkänen A, Savander V, LeDoux JE (1997) Organization of intra-amygdaloid circuitries in the rat: an emerging framework for understanding functions of the amygdala. *Trends Neurosci* 20:517–523.

Pleil KE, Lopez A, McCall N, Jijon AM, Bravo JP, Kash TL (2012) Chronic stress alters neuropeptide Y signaling in the bed nucleus of the stria terminalis in DBA/2J but not C57BL/6J mice. *Neuropharmacology* 62:1777–1786.

Plotsky PM, Cunningham ET, Widmaier EP (1989) Catecholaminergic modulation of corticotropin-releasing factor and adrenocorticotropin secretion. *Endocr Rev* 10:437–458.

Polston EK, Gu G, Simerly RB (2004) Neurons in the principal nucleus of the bed nuclei of the stria terminalis provide a sexually dimorphic GABAergic input to the anteroventral periventricular nucleus of the hypothalamus. *Neuroscience* 123:793–803.

Poulin J-F, Arbour D, Laforest S, Drolet G (2009) Neuroanatomical characterization of endogenous opioids in the bed nucleus of the stria terminalis. *Prog Neuropsychopharmacol Biol Psychiatry* 33:1356–1365.

Preston RJ, McCrea RA, Chang HT, Kitai ST (1981) Anatomy and physiology of substantia nigra and retrorubral neurons studied by extra- and intracellular recording and by horseradish peroxidase labeling. *Neuroscience* 6:331–344.

Prewitt CM, Herman JP (1998) Anatomical interactions between the central amygdaloid nucleus and the hypothalamic paraventricular nucleus of the rat: a dual tract-tracing analysis. *J Chem Neuroanat* 15:173–185.

Puente N, Elezgarai I, Lafourcade M, Reguero L, Marsicano G, Georges F, Manzoni OJ, Grandes P (2010a) Localization and function of the cannabinoid CB1 receptor in the anterolateral bed nucleus of the stria terminalis. *PLoS One* 5:e8869.

Puente N, Elezgarai I, Lafourcade M, Reguero L, Marsicano G, Georges F, Manzoni OJ, Grandes P (2010b) Localization and function of the cannabinoid CB1 receptor in the anterolateral bed nucleus of the stria terminalis. *PLoS One* 5:e8869.

Quirk GJ, Mueller D (2008) Neural mechanisms of extinction learning and retrieval. *Neuropsychopharmacology* 33:56–72.

Quirk GJ, Reppas CB, LeDoux JE (1995) Fear conditioning enhances short-latency auditory responses of lateral amygdala neurons: parallel recordings in the freely behaving rat. *Neuron* 15:1029–1039.

Radley JJ, Arias CM, Sawchenko PE (2006) Regional differentiation of the medial prefrontal cortex in regulating adaptive responses to acute emotional stress. *J Neurosci* 26:12967–12976.

Radley JJ, Sawchenko PE (2011) A common substrate for prefrontal and hippocampal inhibition of the neuroendocrine stress response. *J Neurosci* 31:9683–9695.

Rainnie DG (1999) Neurons of the bed nucleus of the stria terminalis (BNST). Electrophysiological properties and their response to serotonin. *Ann N Y Acad Sci* 877:695–699.

Repa JC, Muller J, Apergis J, Desrochers TM, Zhou Y, LeDoux JE (2001) Two different lateral amygdala cell populations contribute to the initiation and storage of memory. *Nat Neurosci* 4:724–731.

Resnick HS, Yehuda R, Pitman RK, Foy DW (1995) Effect of previous trauma on acute plasma cortisol level following rape. *Am J Psychiatry* 152:1675–1677.

Rodriguez-Sierra OE, Turesson HK, Paré D (2013) Contrasting distribution of physiological cell types in different regions of the bed nucleus of the stria terminalis. *J Neurophysiol.* 110: 2017-2049.

Savander V, Go CG, LeDoux JE, Pitkänen A (1995) Intrinsic connections of the rat amygdaloid complex: projections originating in the basal nucleus. *J Comp Neurol* 361:345–368.

Schuff N, Neylan TC, Lenoci MA, Du AT, Weiss DS, Marmar CR, Weiner MW (2001) Decreased hippocampal N-acetylaspartate in the absence of atrophy in posttraumatic stress disorder. *Biol Psychiatry* 50:952–959.

Selye H (1978) *The Stress of Life*. McGraw-Hill.

Shields AD, Wang Q, Winder DG (2009)  $\alpha_2A$ -adrenergic receptors heterosynaptically regulate glutamatergic transmission in the bed nucleus of the stria terminalis. *Neuroscience* 163:339–351.

Shin J-W, Geerling JC, Loewy AD (2008) Inputs to the ventrolateral bed nucleus of the stria terminalis. *J Comp Neurol* 511:628–657.

Shin LM, Liberzon I (2010) The neurocircuitry of fear, stress, and anxiety disorders. *Neuropsychopharmacology* 35:169–191.

Shin LM, Orr SP, Carson MA, Rauch SL, Macklin ML, Lasko NB, Peters PM, Metzger LJ, Dougherty DD, Cannistraro PA, Alpert NM, Fischman AJ, Pitman RK (2004) Regional cerebral blood flow in the amygdala and medial prefrontal cortex during traumatic imagery in male and female Vietnam veterans with PTSD. *Arch Gen Psychiatry* 61:168–176.

Shin LM, Whalen PJ, Pitman RK, Bush G, Macklin ML, Lasko NB, Orr SP, McInerney SC, Rauch SL (2001) An fMRI study of anterior cingulate function in posttraumatic stress disorder. *Biol Psychiatry* 50:932–942.

Shin LM, Wright CI, Cannistraro PA, Wedig MM, McMullin K, Martis B, Macklin ML, Lasko NB, Cavanagh SR, Krangel TS, Orr SP, Pitman RK, Whalen PJ, Rauch SL (2005) A functional magnetic resonance imaging study of amygdala and medial prefrontal cortex responses to overtly presented fearful faces in posttraumatic stress disorder. *Arch Gen Psychiatry* 62:273–281.

Shurin MR, Kusnecov AW, Riechman SE, Rabin BS (1995) Effect of a conditioned aversive stimulus on the immune response in three strains of rats. *Psychoneuroendocrinology* 20:837–849.

Siegmund A, Wotjak CT (2006) Toward an animal model of posttraumatic stress disorder. *Ann N Y Acad Sci* 1071:324–334.

Silberman Y, Matthews RT, Winder DG (2013) A corticotropin releasing factor pathway for ethanol regulation of the ventral tegmental area in the bed nucleus of the stria terminalis. *J Neurosci* 33:950–960.

Simerly RB (2002) Wired for reproduction: organization and development of sexually dimorphic circuits in the mammalian forebrain. *Annu Rev Neurosci* 25:507–536.

Sink KS, Walker DL, Yang Y, Davis M (2011) Calcitonin gene-related peptide in the bed nucleus of the stria terminalis produces an anxiety-like pattern of behavior and increases neural activation in anxiety-related structures. *J Neurosci* 31:1802–1810.

Smith Y, Paré D (1994) Intra-amygdaloid projections of the lateral nucleus in the cat: PHA-L anterograde labeling combined with postembedding GABA and glutamate immunocytochemistry. *J Comp Neurol* 342:232–248.

Sofroniew M V (1983) Direct reciprocal connections between the bed nucleus of the stria terminalis and dorsomedial medulla oblongata: evidence from immunohistochemical detection of tracer proteins. *J Comp Neurol* 213:399–405.

Steriade M, Llinás RR (1988) The functional states of the thalamus and the associated neuronal interplay. *Physiol Rev* 68:649–742.

Stöhr T, Szuran T, Pliska V, Feldon J (1999) Behavioural and hormonal differences between two Lewis rat lines. *Behav Brain Res* 101:163–172.

Storm JF (1988) Temporal integration by a slowly inactivating K<sup>+</sup> current in hippocampal neurons. *Nature* 336:379–381.

Ströhle A, Scheel M, Modell S, Holsboer F (2008) Blunted ACTH response to dexamethasone suppression-CRH stimulation in posttraumatic stress disorder. *J Psychiatr Res* 42:1185–1188.

Sullivan GM, Apergis J, Bush DEA, Johnson LR, Hou M, Ledoux JE (2004) Lesions in the bed nucleus of the stria terminalis disrupt corticosterone and freezing responses elicited by a contextual but not by a specific cue-conditioned fear stimulus. *Neuroscience* 128:7–14.

Sun N, Cassell MD (1993) Intrinsic GABAergic neurons in the rat central extended amygdala. *J Comp Neurol* 330:381–404.

Szücs A, Berton F, Nowotny T, Sanna P, Francesconi W (2010) Consistency and diversity of spike dynamics in the neurons of bed nucleus of stria terminalis of the rat: a dynamic clamp study. *PLoS One* 5:e11920.

Takahashi LK, Nakashima BR, Hong H, Watanabe K (2005) The smell of danger: a behavioral and neural analysis of predator odor-induced fear. *Neurosci Biobehav Rev* 29:1157–1167.

Tepper JM, Bolam JP (2004) Functional diversity and specificity of neostriatal interneurons. *Curr Opin Neurobiol* 14:685–692.

Tepper JM, Sawyer SF, Groves PM (1987) Electrophysiologically identified nigral dopaminergic neurons intracellularly labeled with HRP: light-microscopic analysis. *J Neurosci* 7:2794–2806.

Tureson HK, Rodríguez-Sierra OE, Paré D (2013) Intrinsic connections in the anterior part of the bed nucleus of the stria terminalis. *J Neurophysiol* 109:2438–2450.

Uddin M, Aiello AE, Wildman DE, Koenen KC, Pawelec G, de Los Santos R, Goldmann E, Galea S (2010) Epigenetic and immune function profiles associated with posttraumatic stress disorder. *Proc Natl Acad Sci U S A* 107:9470–9475.

Ulrich-Lai YM, Herman JP (2009) Neural regulation of endocrine and autonomic stress responses. *Nat Rev Neurosci* 10:397–409.

Veening JG, Swanson LW, Sawchenko PE (1984) The organization of projections from the central nucleus of the amygdala to brainstem sites involved in central autonomic regulation: a combined retrograde transport-immunohistochemical study. *Brain Res* 303:337–357.

Vertes RP (1991) A PHA-L analysis of ascending projections of the dorsal raphe nucleus in the rat. *J Comp Neurol* 313:643–668.

Villarreal G, Hamilton DA, Petropoulos H, Driscoll I, Rowland LM, Griego JA, Koditwakku PW, Hart BL, Escalona R, Brooks WM (2002) Reduced hippocampal volume and total white matter volume in posttraumatic stress disorder. *Biol Psychiatry* 52:119–125.

Walker D, Yang Y, Ratti E, Corsi M, Trist D, Davis M (2009a) Differential effects of

the CRF-R1 antagonist GSK876008 on fear-potentiated, light- and CRF-enhanced startle suggest preferential involvement in sustained vs phasic threat responses. *Neuropsychopharmacology* 34:1533–1542.

Walker DL, Davis M (1997) Double dissociation between the involvement of the bed nucleus of the stria terminalis and the central nucleus of the amygdala in startle increases produced by conditioned versus unconditioned fear. *J Neurosci* 17:9375–9383.

Walker DL, Miles L a, Davis M (2009b) Selective participation of the bed nucleus of the stria terminalis and CRF in sustained anxiety-like versus phasic fear-like responses. *Prog Neuropsychopharmacol Biol Psychiatry* 33:1291–1308.

Walker DL, Toufexis DJ, Davis M (2003) Role of the bed nucleus of the stria terminalis versus the amygdala in fear, stress, and anxiety. *Eur J Pharmacol* 463:199–216.

Weaver ICG, Cervoni N, Champagne FA, D'Alessio AC, Sharma S, Seckl JR, Dymov S, Szyf M, Meaney MJ (2004) Epigenetic programming by maternal behavior. *Nat Neurosci* 7:847–854.

Weitlauf C, Honse Y, Auberson YP, Mishina M, Lovinger DM, Winder DG (2005) Activation of NR2A-containing NMDA receptors is not obligatory for NMDA receptor-dependent long-term potentiation. *J Neurosci* 25:8386–8390.

Willner P (1986) Validation criteria for animal models of human mental disorders: learned helplessness as a paradigm case. *Prog Neuropsychopharmacol Biol Psychiatry* 10:677–690.

Woodhams PL, Roberts GW, Polak JM, Crow TJ (1983) Distribution of neuropeptides in the limbic system of the rat: the bed nucleus of the stria terminalis, septum and preoptic area. *Neuroscience* 8:677–703.

Yehuda R (2002) Clinical relevance of biologic findings in PTSD. *Psychiatr Q* 73:123–133.

Yehuda R, Golier JA, Halligan SL, Meaney M, Bierer LM (2004) The ACTH response to dexamethasone in PTSD. *Am J Psychiatry* 161:1397–1403.

Yehuda R, Keefe RS, Harvey PD, Levengood RA, Gerber DK, Geni J, Siever LJ (1995) Learning and memory in combat veterans with posttraumatic stress disorder. *Am J Psychiatry* 152:137–139.

Yehuda R, Resnick HS, Schmeidler J, Yang RK, Pitman RK (1998) Predictors of cortisol and 3-methoxy-4-hydroxyphenylglycol responses in the acute aftermath of rape. *Biol Psychiatry* 43:855–859.

Yehuda R, Southwick S, Giller EL, Ma X, Mason JW (1992) Urinary catecholamine excretion and severity of PTSD symptoms in Vietnam combat veterans. *J Nerv Ment Dis* 180:321–325.

Yehuda R, Southwick SM, Nussbaum G, Wahby V, Giller EL, Mason JW (1990) Low urinary cortisol excretion in patients with posttraumatic stress disorder. *J Nerv Ment Dis* 178:366–369.

Yehuda R, Teicher M, Trestman R, Levengood R, Siever L (1996) Cortisol regulation in posttraumatic stress disorder and major depression: A chronobiological analysis. *Biol Psychiatry* 40:79–88.

Yehuda R, Teicher MH, Levengood RA, Trestman RL, Siever LJ (1994) Circadian regulation of basal cortisol levels in posttraumatic stress disorder. *Ann N Y Acad Sci* 746:378–380.

Young EA, Breslau N (2004a) Saliva cortisol in posttraumatic stress disorder: a community epidemiologic study. *Biol Psychiatry* 56:205–209.

Young EA, Breslau N (2004b) Cortisol and catecholamines in posttraumatic stress disorder: an epidemiologic community study. *Arch Gen Psychiatry* 61:394–401.

Zhang T-Y, Meaney MJ (2010) Epigenetics and the environmental regulation of the genome and its function. *Annu Rev Psychol* 61:439–66, C1–3.

Zucker RS, Regehr WG (2002) Short-term synaptic plasticity. *Annu Rev Physiol* 64:355–405.

## Vita

Olga E Rodríguez-Sierra

- 1978 Born May 30 in Mexico City, Mexico.
- 1997 Graduated from Instituto Técnico y Cultural (High school), Mexico City, Mexico.
- 1998-2002 Attended Psychology Faculty at the National Autonomous University of Mexico, Mexico City, Mexico.
- 2002 B.S., National Autonomous University of Mexico, Mexico City, Mexico.
- 2003-2005 M.Sc. Education at the International Max Planck Research School, Tübingen, Germany.
- 2006 M.Sc. in Neural and Behavioral Sciences, University of Tübingen, Germany.
- 2007-2013 Ph.D. Education in Neuroscience at Rutgers University, Newark, NJ.
- 2009 Merit Award, Executive Women of New Jersey, USA.
- 2010 Goswami S, Cascardi M, **Rodríguez-Sierra OE**, Duvarci S, Paré D (2010) Impact of predatory threat on fear extinction in Lewis rats. *Learning and Memory*, 17:494–501.
- 2012 Goswami S, Samuel S, **Sierra OR**, Cascardi M, Paré D (2012) A rat model of post-traumatic stress disorder reproduces the hippocampal deficits seen in the human syndrome. *Frontiers in Behavioral Neuroscience*, 6:26.
- 2013 Turesson HK, **Rodríguez-Sierra OE**, Paré D (2013) Intrinsic connections in the anterior part of the bed nucleus of the stria terminalis. *Journal of Neurophysiology*, 109:2438–2450.
- 2013 Goswami S, **Rodríguez-Sierra O**, Cascardi M, Paré D (2013) Animal models of post-traumatic stress disorder: face validity. *Frontiers in Neuroscience*, 7:89.
- 2013 **Rodríguez-Sierra OE**, Turesson HK, Paré D (2013) Contrasting distribution of physiological cell types in different regions of the bed nucleus of the stria terminalis. *Journal of Neurophysiology*, 110: 2017-2049.
- 2013 Gerdjikov TV, Haiss F, **Rodríguez-Sierra OE**, Schwarz C (2013) Rhythmic whisking area (RW) in rat primary motor cortex: an internal monitor of movement-related signals? *Journal of Neuroscience*, 33(55): 14193-14204.
- 2014 Ph.D. in Neuroscience.